University of Alberta

Flapwing Dephosphorylates Merlin and Moesin and

Regulates Epithelial Integrity in *Drosophila*

by

Yang Yang

A thesis submitted to the Faculty of Graduate Studies and Research
in partial fulfillment of the requirements for the degree of

Master of Science

Department of Cell Biology

Fall 2013
Edmonton, Alberta

Abstract

Merlin is a tumor suppressor protein whose inactivation is associated with familial Neurofibromatosis Type II (NF2) and other sporadic tumors (McClatchey & Giovannini, 2005; Rouleau et al, 1993; Trofatter et al, 1993). The growth-suppressive function of Merlin is modulated by reversible phosphorylation. Our previous finding showed the Sterile20 kinase Slik coordinately regulates the activity of Merlin and Moesin in *Drosophila melanogaster* (Hughes & Fehon, 2006). Here I report that the *Drosophila* protein phosphatase 1β flapwing (flw) is involved in the coordinate dephosphorylation of Merlin and Moesin. Flw forms a complex with Merlin and Moesin. Changes in *flw* expression level lead to corresponding changes in the phosphorylation pattern of Merlin and Moesin. Moreover, reducing *flw* expression in epithelial cells results in increased membrane-association of Merlin and Moesin and disruption of epithelial integrity. Taken together, flw plays a role in epithelial organization by regulating dephosphorylation of Merlin and Moesin.

Acknowledgement

This work is a result of the total endeavor of all the present and past members of the lab. Particularly, David Primrose and Albert Leung helped me greatly by conducting the biochemical experiments of the project (Figure 4). I appreciate the contribution from everyone to this project as well as the permission given to me for using their data in my thesis.

In particular, I would like to thank my supervisor, Sarah Hughes, who is a passionate, inspiring researcher and a wise, caring mentor both in my academic and personal life. It was her constant understanding and support that helped me through my down times, and this work is not possible without her guidance. Through her I learned that scientific research is a process of never ending pursuit of truth and is full of adventure, frustration, and ecstasy. It requires optimistic attitude, rigorous thinking and diligent work for one to make even the smallest progress on this road.

I would also like to thank my thesis committee member, Dr. Rosaline Godbout and Dr. Paul LaPointe, for their instructions and suggestions during my master program and the writing of the thesis. Special thank goes to Dr. Andrew Simmonds, for generously teaching me confocal microscopy techniques and giving me advice on life.

Lastly I would like to thank my mother, Liu, who has solely kept the family going and offered my important and indispensible care and support during

my study, and my husband, Carl, who is always proud of my work and gives me hope, comfort and support everyday from distance.

Thank you everyone for helping me achieve what I have done, and making me become who I am today.

Table of Contents

Chapter I - Introduction

Chapter II - Materials and Methods

Chapter III - Results

Chapter IV – Discussion

List of Tables

List of Figures

Chapter I

Chapter III

Chapter IV

List of Abbreviations

~	approximately
2D	two dimensional
AC	affinity chromatography
AJ	adherens junction
AKT	protein kinase B
APC	anaphase promoting complex
apt	*apterous*
Bcl-2	B-cell lymphoma 2
cdc20	cell division control protein 20
Cdc42	cell division control protein 42 homologue
Cdk1	cyclin-dependent kinase 1
CENPE	centromere protein E
CPI-17	C-kinase activated protein phosphatase 1 inhibitor of 17KDa
CRL4	cullin-ring E3 ligase 4
C-terminal	carboxyl terminal
C-termini	carboxyl termini
DAPI	4',6-diamidino-2-phenylindole
DCAF1	DDB1- and CUL4-associated protein 1
DDAB	dimethyl-dioctadecylammonium bromide
DIAP1	*Drosophila* Inhibitor of Apoptosis 1
DIGE	differential gel electrophoresis

Dm	*Drosophila melanogaster*
DNA	deoxyribonucleic acid
DTT	dithiothreitol
D-V boundary	dorsal-ventral boundary
EBP50	ERM binding protein 50
ECL	enhanced chemiluminescence
ECM	extracellular matrix
EDTA	ethylenediaminetetraacetic acid
EGFR	epidermal growth factor receptor
EGTA	ethyleneglycoltetraacetic acid
ERM	Ezrin-Radixin-Moesin
Ex	Expanded
F-actin	filamentous actin
FAK	focal adhesion kinase
FCP	TFIIF-associating component of RNA polyerase II CTD phosphatase
FERM	Four-point-one Ezrin-Radixin-Moesin
flw	flapwing
flw-IR	*flapwing*-RNAi
GFP	green fluorescent protein
GST	glutathione S-transferase
HA	hyaluronic acid
HEPES	hydroxyethyl piperazineethanesulfonic acid
HRS	hepatocyte growth factor regulated tyrosine kinase substrate
IEF	isoelectric focusing

IL-2	interleukin 2
IP	immunoprecipitation
JNK	Jun N-terminal kinase
knl1	kinetochore-null 1
LC20	myosin light chain 20
l-o-f	loss-of-function
LOK	lymphocyte-oriented kinase
MEF	mouse embryonic fibroblast
Mer	Merlin
miRNA	micro-RNA
MLCK	myosin light chain kinase
MLCK	myosin light chain kinase
MLCP	myosin light chain phosphatase
MLCP	myosin light chain phosphatase
Moe	Moesin
mRNA	messenger RNA
MT	microtubules
MYPT-1	myosin phosphtase targeting 1
MYPT-75D	myosin phosphatase targeting of 75KDa
NF2	Neurofibromatosis Type II
NF2	the neurofibromatosis type II gene
N-terminal	amino terminal
PAGE	polyacrylamide gel electrophoresis
PAK1/2	p21-activated kinase 1 and 2
PBD	polo-box domain
PBS	phosphate buffered saline

PCR	polymerase chain reaction
pERM	phosphorylated Ezrin-Radixin-Moesin
PIP2	phosphatidylinositol 4,5-bisphosphate
PKA	c-AMP dependent protein kinase A
Plk	Polo-like kinase
PP1	protein phosphatase 1
PP1c	protein phosphatase 1 catalytic subunit
PPM	metal-dependent protein phosphatase
PPP	phosphoprotein phosphatase
PSP	protein serine/threonine phosphatase
ptc	*patched*
R subunit	regulatory subunit
Rac	Ras-related C3 botulinum toxin substrate
RNA	ribonucleic acid
RNAi	RNA interference
RT	real time
RTK	receptor tyrosine kinase
S10	Serine 10
S19	Serine 19
S2	*Drosophila* Schneider S2
S315	Serine 315
S518	Serine 518
SAJ	subapical junction
Sav	Salvador
SCP	small CTD phosphatase
SE	standard error

SDS	sodium dodecyl sulfate
Sip1	SRY interacting protein 1
siRNA	small intefering RNA
siRNA	small intefering RNA
SJ	septate junction
Slik	Sterile20-like kinase
SMA	Somatic Mosaic Analysis
S-phase	synthesis phase
T230	Threonine 230
T558	Threonine 558
T559	Threonine 559
T567	Threonine 567
TJ	tight junction
UAS	upstream activating sequence
USVS	unilateral sporadic vestibular schwannoma
UV	ultraviolet
Wts	Warts
YAP	Yorkie associated protein
ZA	zonula adherens

Chapter One

Introduction

1. Merlin The Tumor Suppressor

1.1. Identification of Merlin

The tumor suppressor protein Merlin was first identified twenty years ago (Rouleau et al, 1993; Trofatter et al, 1993), when mutations in the human gene encoding Merlin, neurofibromatosis type II (*NF2*) located on chromosome 22q12, were found responsible for causing type II neurofibromatosis (NF2). NF2 is a multiple neoplasia syndrome with an incidence of 1 in 25000 live births and is inherited in an autosomal dominant manner (Evans et al, 1992b). Although considered a relatively rare disorder, NF2 has a nearly 100% penetrance by the age of 60 years old and is associated with high morbidity (Evans et al, 2005). NF2 patients develop multiple tumors in the central and peripheral nervous systems and are typically characterized with bilateral vestibular schwannomas (Evans et al, 1992a; Martuza & Eldridge, 1988; Mautner et al, 1996; Parry et al, 1994). Other common manifestations include spinal schwannomas, meningiomas, ependymomas, cutaneous neurofibromas and cutaneous schwannomas. In addition, loss of *NF2* is associated with the majority of spontaneous meningiomas and schwannomas (Sughrue et al, 2011). Contrary to other major human malignancies, these tumors not only occur in a specific and restricted spectrum of cell types, but also are benign, slow-growing and respond poorly to chemotherapeutic interventions. As a result, patients with NF2 are usually treated with repeated surgeries, which often result in damage to the structure of the nervous system (Evans et al, 1992a).

1.2. Structure of Merlin

Merlin is a member of the FERM (Four.1 Ezrin-Radixin-Moesin) superfamily, which are a large group of closely related proteins that are characterized by the presence of a highly conserved FERM domain at the amino terminal of the molecule.

Both Merlin and its closest ERM protein subfamily (Ezrin, Radixin, and Moesin) have an N-terminal tri-lobe globular FERM domain of high sequence identity important for interacting with other membrane associated proteins, an α-helical coiled-coil central linker domain, and a carboxyl terminal domain of high sequence divergence (Figure 1A). Merlin and ERMs can exist in either 'open' or 'closed' forms by undergoing intramolecular association between the C-terminal FERM domain and the N-terminal domain in a 'head-to-tail' manner (Gary & Bretscher, 1995; Magendantz et al, 1995; Sherman et al, 1997; Shimizu et al, 2002). This is achieved in part by reversible phosphorylation of serine (Merlin) or threonine (ERM) located at the C-terminal domain of the protein by the corresponding protein kinases and phosphatases (Merlin-S518, Ezrin-T567, Radixin-T564, Moesin-T558 (Bretscher et al, 2002)). The resulting conformational changes in turn modulate the activity of Merlin and ERM proteins and the subsequent cellular processes involved. All three ERM members contain a 'classic' filamentous (F)-actin binding site with high affinity at the last 34 residues of their C-termini (Turunen et al, 1994). However, this F-actin binding site is absent in Merlin. Instead, Merlin interacts with the cytoskeleton through two unconventional binding sites located at its N-terminal FERM domain (Brault et al, 2001; Xu & Gutmann,

1998). In addition, both Merlin and ERMs contain a conserved binding site for the membrane lipid, phosphatidylinositol 4,5-bisphosphate (PIP2) in their FERM domain. PIP2-binding is important for the membrane association of Merlin, and a recent study using the mammalian cultured cells suggests that this FERM domain-mediated PIP2 binding and membrane association are critical for the growth suppressive function of Merlin (Barret et al, 2000; Mani et al, 2011). A recent study on the differential role of PIP2-binding and phosphorylation of ERM proteins suggested that, in *Drosophila*, PIP2-binding is essential for the recruitment of Moesin to the membrane and for its subsequent phosphorylation (Roch et al, 2010). Thus, it is likely that PIP2 acts a dosing mechanism that locally regulates ERM membrane recruitment, whereas the phospho-regulation further modulates the activity of ERM proteins once they have become membrane-associated.

1.3. Disease-related Mutations in NF2

The human *NF2* gene contains 17 exons, which give rise to two Merlin isoforms due to alternative splicing. Isoform I of Merlin is encoded by exons 1-15 and 17 and contains 595 amino acids. On the other hand, Isoform II, which is encoded by exons 1-15 and 16, contains 590 residues and does not have an active tumor-suppressing role.

Published mutations of the *NF2* gene (both constitutional and somatic) from worldwide clinical case studies have been collected by the international *NF2* mutation database. These mutations were found in individuals and families

with the classic NF2, unilateral sporadic vestibular schwannoma (USVS) or sporadic meningioma. In all these types of *NF2*-related diseases, the most dominant influence on the spectrum of the mutations in the single base-pair substitution that causes the transition of an amino-acid coding codon such as arginine (CGA) to a stop codon (TGA) (Baser & Contributors to the International, 2006) (Figure 1C). Another predominant type of mutations is single base-pair deletion which leads to frameshift of the *NF2* open reading frame. In both cases, the resulting Merlin protein is either truncated or has a severely disrupted tertiary structure, unable to undergo the intra-molecular interaction between the N-terminal FERM domain and the C-terminal domain. Location wise, a large proportion of mutations leading to amino acid substitution occur at the N-terminal FERM domain, and the most parsimonious truncation mutants lack only the C-terminal segment (Ahronowitz et al, 2007; Baser & Contributors to the International, 2006) (Figure 1B). Again, these missense mutations supposedly have altered the critical properties of the FERM and C-terminal domains and their abilities of interaction. Taken together, the tumor-suppressor function of *NF2* is highly dependent upon the proper tertiary configuration of the protein.

1.4. Function of Merlin in Cell Adhesion and Motility

Similar to other ERM family members, Merlin serves as a linker between the plasma membrane and the actin cytoskeleton (Gusella et al, 1999). However, given the different structural features of Merlin compared to ERMs, it is not

surprising that Merlin plays a distinguishing role in regulating cytoskeletal organization and cell motility.

Studies on the subcellular localization of Merlin have shown that, in mammalian cells, endogenously expressed Merlin is primarily concentrated at the areas of dynamic cytoskeleton remodeling, such as ruffling edges and restructured cell membrane protrusions (Gonzalez-Agosti et al, 1996; Sainio et al, 1997). In *Drosophila* epithelial cells, prominent staining of endogenous Merlin is detected at the subapical junctional (SAJ) region, and partially co-localizes with the more apically localized Moesin (Hughes & Fehon, 2006; LaJeunesse et al, 2001). In addition, in confluent mammalian cells, Merlin is localized at the plasma membrane along the boundary of cell:cell contact and co-localized with components of adherens junctions (AJs) (Lallemand et al, 2003). Loss of Merlin at the sites of cell:cell contact leads to destabilization of AJs and cell transformation. In both *Drosophila* and mammalian cells of various types, Merlin is also detected as diffused or punctate structures in the cytoplasm of epithelial cells, probably representing the subset of proteins clustered in intracellular vesicles and lipid rafts (McCartney & Fehon, 1996; Stickney et al, 2004).

The enrichment of Merlin at F-actin-rich areas suggests that Merlin may play a role in regulating cytoskeleton remodeling-associated events such as cell migration. Indeed, several studies have shown that loss-of-function (l-o-f) of Merlin correlates with dysregulation of cell motility and migration, a process that requires driving forces generated and maintained by dynamic remodeling of the actin filaments (Rottner & Stradal, 2011). Primary *NF2*-

defiencent human schwannoma cells exhibit cytoskeletal defects such as increased membrane ruffling, disorganized stress fibers and altered spreading (Pelton et al, 1998). Moreover, re-expression of the wild-type, but not the NF2 patient-derived missense mutant Merlin (L64P) in *NF2*-deficient schwannoma and meningioma cell lines is able to rescue the abnormal cytoskeletal phenotypes (Bashour et al, 2002). Merlin may control cytoskeleton organization and inhibit cell invasion in part by suppressing Rac signaling. Schwannoma cells lacking Merlin showed an enhanced activation of Rac1 (Kaempchen et al, 2003), a Rho family of small GTPase that serves as the key regulator of actin cytoskeleton and has critical implications in the control of cell adhesions, migration and tumorigenesis (Mack et al, 2011). Furthermore, *NF2*-null cells exhibited up-regulated Rac activity manifested as excessive membrane ruffling, extensive lamellipodia and increased migratory rates (Shaw et al, 2001).

The complete understanding of how loss of *NF2* is causally related to tumor metastasis in a tissue-type specific manner still remains to be answered in further studies. Although Merlin-deficient primary schwannomas are benign and non-invasive, heterozygous *NF2* mutant mice developed a variety of malignant tumors of high metastatic properties (McClatchey et al, 1998). In addition, Merlin has been demonstrated to have an essential role in inhibiting the motility and invasiveness of several tumor cell lines (Lau et al, 2008; Poulikakos et al, 2006).

The role of Merlin in controlling cell adhesion and motility is not only important for suppressing tumor invasion but also ensuring morphological

processes during normal development. In developing mouse embryo, the expression of Merlin is spatially regulated and is critical for the establishment of cell-cell adhesion during tissue fusion, a morphogenic process by which epithelial sheets are drawn together and sealed to form a continuous layer (McLaughlin et al, 2007). Genetic mosaic *NF2* mouse embryo that harbored clones of homozygous *NF2*-null cells among the wild-type tissues due to somatic homologous recombination exhibit a global defect in tissue fusion such as ectopic detachment of the neuroepithelial cells and increased detachment-induced apoptosis resulting in a wide spectrum of neural tube defects as well as tissue fusion defects in the eye, cleft palate, cardiac ventricular septation. Regulated Merlin expression is also detected in the developing brain and the sites containing migrating cells such as neural tube closure during mouse embryonic development (Akhmametyeva et al, 2006). In addition, Schwann cells expressing dominant negative Merlin showed prominent defects in process elongation, axon alignment and myelination, compared to the cells expressing wild-type Merlin (Thaxton et al, 2011). Thus, Merlin-mediated regulation of cell adhesion and migration is important for the global development of the embryo as well as the differentiation of specific neural tissues.

1.5. Function of Merlin as A Negative Growth Regulator

The functional inactivation of the *NF2* gene in familial NF2 appears to be a two-hit mechanism, whereby the patients inherit a mutant *NF2* allele and lose

the remaining allele somatically during tumorigenesis (Gusella et al, 1996; Kley & Seizinger, 1995; Ueki et al, 1999). Somatic inactivation of both alleles of the *NF2* gene is also identified in most sporadically occurring schwannomas and a large fraction of sporadically occurring meningiomas (Lomas et al, 2005; Ruttledge et al, 1994; Stemmer-Rachamimov et al, 1997). In conditional mouse models, biallelic inactivation of *NF2* specifically in Schwann cells results in the development of schwannomas that resembles the phenotypes of tumors seen in NF2 patients (Giovannini et al, 1999), suggesting that loss of Merlin is directly responsible for the tumor growth in NF2-related schwannomas.

Loss of function of *NF2* is associated with tumor formation and progression not only limited to glial cells but also other non-neural tissues. Homozygous *NF2*-null mice fail to develop at the early embryonic stage due to defects in extra-embryonic structure (McClatchey et al, 1997). However, heterozygous *NF2*+/- mice develop a wide array of metastatic cancers including mesotheliomas, melanomas, hepatocellular carcinomas and colorectal cancers, indicating the growth suppressive activity of Merlin in a broader range of cell types (Bianchi et al, 1994; Lasota et al, 2001; Pineau et al, 2003; Sheikh et al, 2004). Mutations in Merlin also promote tumorigenesis and progression in cells simultaneously harboring other oncogenic lesions in a synergistic manner. In the *NF2*+/- mouse models, inactivation of p53, a 'classic' tumor suppressor, greatly accelerates the development of the tumor phenotypes of *NF2*-deficient cells (McClatchey et al, 1998; Robanus-Maandag et al, 2004). Thus, *NF2* behaves as a tumor suppressor gene in hereditary NF2

tumors, in their sporadic counterparts, and in malignant tumors unrelated to NF2 such as mesothelioma.

Consistent with its role as a tumor suppressor, overexpression of Merlin has been shown to inhibit cell proliferation in a variety of cell types. For example, overexpressing the wild-type, but not the mutant Merlin in MEFs was able to reverse Ras-induced growth and restore contact-dependent growth inhibition (Lutchman & Rouleau, 1995; Tikoo et al, 1994). Re-introduction of Merlin at a high density in NF2 patient-derived primary schwannoma cells led to growth suppression, G_0/G_1 arrest and apoptosis (Schulze et al, 2002). The mechanisms by which Merlin acts as a negative regulator of cell proliferation have been extensively studied in the past two decades. Some of the major cellular processes and signaling pathways Merlin is involved in will be discussed in Section 1.6.

1.6. Merlin in Model Organisms

Despite the unique and restricted set of tumor types in which *NF2* is directly involved, Merlin is expressed in all types of cells in multicellular organisms and well-conserved in vertebrates, fish, birds and invertebrates (e.g. *Drosophila melanogaster*, *Caenorhabditis elegans*, *Xenopus laevis* (Golovnina et al, 2005)). A *NF2* homolog, however, has not been identified in *Saccharomyces cerevisiae*, suggesting that the function of Merlin is specific to the evolutionary branching of metazoans (Bretscher et al, 2002), which require intricate and

well-organized cell:cell adhesion and inter-cellular communication to form various functional tissue types.

The functional conservation of Merlin across species has been well demonstrated by the experiment in which the introduction of a transgenic wild-type human *NF2* gene was able to rescue the lethality of the *Drosophila* Merlin mutant (Giovannini et al, 1999; LaJeunesse et al, 1998). Consistent to the role of *NF2* in vertebrates, *loss of function* of Merlin in *Drosophila* leads to over-proliferation. Using **s**omatic **m**osaic **a**nalysis (SMA), clones of homozygous *Merlin* mutant cells were created in the epithelial cells of the *Drosophila* eye (LaJeunesse et al, 2001). These cells showed a over-proliferation phenotype compared to the adjacent cells harboring two wild-type copies of *Merlin*. This suggests that the fundamental role of Merlin in negatively regulating cell proliferation is highly conserved in mammals and invertebrates.

The sequence and functional conservation of Merlin orthologues (~55% sequence identity between *Drosophila* and mammals) enables us to use animal models to study Merlin functions, which will later on facilitate the development of therapeutic strategies for *NF2*-related tumors. The animal models provide a powerful tool for investigating the effects of changes in Merlin activity in different intracellular and extracellular microenvironments. *Drosophila* is a particularly valuable model organism due to the availability of myriad molecular and genetic methodologies, which allows for convenient and extensive structural and functional analyses of Merlin.

A concern regarding using *Drosophila* to study functions of Merlin is whether findings based on the invertebrate model can shed light on tissue-specific pathology of the human NF2 disorder. A common notion is that the nervous system of vertebrate is developmentally and functionally distinct from their vertebrate counterparts. Such a conclusion is primarily a result of the apparent absence of conservation of initial cell-fate specification mechanisms. For example, the master regulator of fate determination of *Drosophila* glia, *glial cells missing* (*gcm*), has no *in vivo* role in glial specification in vertebrates (Hosoya et al, 1995; Jones et al, 1995; Kim et al, 1998; Vincent et al, 1996). Nevertheless, many aspects of later glial morphogenesis such as subtype diversity, migration, axon guidance and ensheathment and the ultimate function of glial cells in the mature CNS of glial cells are very similar between *Drosophila* and vertebrates at the molecular level (Freeman & Doherty, 2006). Even though *Drosophila* lacks Schwann cells, which are the major focus of the human disease, the peripheral glia of *Drosophila* is functionally equivalent to Schwann cells in many important aspects such as conducting nervous impulses, trophic support for neurons, and nerve development and regeneration. Striking similarities also exist in the morphological aspects of axon ensheathment. *Drosophila* peripheral glial cells wrap around axon bundles into a single nerve fascicle or individual axons by glial membranes, resembling the simplest form of ensheathment by Schwann cells in mammals (Leiserson et al, 2000). In addition, *Drosophila* glia are also capable of forming multi-layered membrane sheaths around neurons that are morphologically similar to the myelin sheaths of mammals important for high-speed salutatory conduction along lengthy nerves (Freeman & Doherty, 2006;

Salzer, 2003). In addition, *Drosophila* nervous system has been explored at molecular, genetic and morphological levels, due to the availability of a vast array of glial markers and genetic tools. Thus, it is both possible and advantageous that findings on functions of Merlin in normal development of *Drosophila* peripheral glial lead to a better understanding of loss of *NF2*-mediated tumor suppression contributes to the development of NF2 and *NF2*-related schwannomas.

1.7. The Mechanisms of Merlin Tumor Suppressive Function

In the conventional view, the marked difference between Merlin and other 'classic' tumor suppressors lies in its unique subcellular positioning as a cell membrane-cytoskeletal linker. Classic tumor suppressor proteins such as p53 function by regulating the cell cycle machinery in the nucleus (Giono & Manfredi, 2006; Mercer, 1992; Shaw, 1996), while other small signaling molecules such as *Neurofibromin 1* (*NF1*) directly inhibit the Ras-signaling pathway in response to extracellular cues (Harrisingh & Lloyd, 2004; Weiss et al, 1999). Therefore, it has been historically thought that, given the predominant localization of Merlin at the membrane-cytoskeletal interface, it is unlikely that Merlin plays a direct role in regulating mitotic cell cycle in the nucleus. However, recent studies have revealed the pleiotropic effects of Merlin on inhibiting mitogenic signaling pathways at the plasma membrane as well as promoting a growth-suppressive program of gene expression by migrating to the nucleus (Li et al, 2012b; Zhou & Hanemann, 2012). Studies of

various cell types in both *Drosophila* and mammals showed that Merlin functions as a negative growth regulator by intercepting a variety of mitogenic signaling pathways including Rac-PAK signaling (Kaempchen et al, 2003; Kissil et al, 2003; Okada et al, 2005; Shaw et al, 2001), PI3K-AKT pathway and FAK-Src signaling (Ammoun et al, 2008; Jin et al, 2006; Poulikakos et al, 2006) upon sensing the changes of cell:cell adhesion. Genetic analyses in *Drosophila* and subsequently in mice also suggest that Merlin is also involved in the activation of the Hippo tumor-suppressor pathway (Cho et al, 2006; Hamaratoglu et al, 2006; Zhang et al, 2010; Zhao et al, 2007).

1.7.1. Contact-dependent Growth Inhibition

For metazoans, controlled cell proliferation is crucial for establishing tissue organization. Regulated proliferation is in part achieved by contact-dependent growth inhibition, whereby normal cells cease to proliferate after coming into contact with one another and start assembling intercellular junction complexes. The loss of contact inhibition and the gain of anchorage-independent growth are hallmarks of cancer cells *in vitro* (Hanahan & Weinberg, 2000).

Studies showed that Merlin mediates contact-dependent inhibition of proliferation by stabilizing the adherens junctions (AJs) in association with the actin cytoskeleton (Lallemand et al, 2003). In confluent wild-type cells, Merlin co-localizes and interacts with AJ components (Shaw et al, 1998). *NF2*-deficient cells are unable to undergo contact-dependent growth arrest and to

form stable cadherin-containing cell:cell junctions. Alternatively, Merlin also exerts its tumor-suppressor function in cooperation with CD44, a cell surface receptor for hyaluronic acid (HA), an abundant component of extracellular matrix (ECM) (Morrison et al, 2001). As an important regulator of cell-to-cell and cell-to-matrix adhesion, cell motility and migration, CD44 is often up-regulated in malignant tumors (Stamenkovic & Yu, 2009). Studies demonstrated that increasing the expression level of wild-type Merlin in mouse Tr6BC1 schwannoma cells resulted in inhibition of CD44-HA binding and tumor growth, whereas overexpression of a mutant Merlin that lacks the CD44-HA binding domain was incapable of suppressing schwannoma proliferation (Bai et al, 2007).

1.7.2. Merlin Upstream of the Hippo Signaling Pathway

The highly conserved Hippo signaling pathway plays an essential role in regulating cell proliferation and survival (Edgar, 2006; Hergovich & Hemmings, 2009). Several core components and upstream regulators of the signaling pathways are either classified as tumor suppressors or oncogenes. The role of dysregulation of the Hippo pathway in cancer formation and development has been supported by extensive studies using various genomic and biochemical approaches on both human and mouse samples. In *Drosophila*, in which the Hippo pathway was originally defined, Merlin and a FERM family protein Expanded (Ex) is recruited to the plasma membrane by a membrane scaffolding protein Kibra, which results in subsequent activation

of the Hippo/Salvador (Sav) kinase complex (Baumgartner et al, 2010; Genevet et al, 2010; Pantalacci et al, 2003). The Hippo/Sav complex in turn phosphorylates and activates the Warts (Wts)/Mats kinase complex (Lai et al, 2005). Wts/Mats phosphorylates Yorkie, a transcriptional co-activator normally translocated into the nucleus to promote pro-proliferating and anti-apoptotic programs by up-regulating the expression of Cyclin E and *Drosophila* Inhibitor of Apoptosis 1 (DIAP1), respectively (Goulev et al, 2008; Zhang et al, 2008). Upon phosphorylation, Yorkie is sequestered in the cytoplasm, which leads to cell proliferation arrest and suppression of tissue growth (Huang et al, 2005; Oh et al, 2009).

Research using *Drosophila* as a model demonstrated that Merlin and Ex act in a partially redundant manner to inhibit cell growth by cooperatively regulating the Hippo signaling pathway (Hamaratoglu et al, 2006; McCartney et al, 2000; Pellock et al, 2007). Inactivation of both Merlin and Ex was shown to cause cell over-proliferation into tumorous outgrowth and reduction in apoptosis, suggesting that Merlin and Ex are the negative regulators upstream of the Hippo signaling pathway (Hamaratoglu et al, 2006; McCartney et al, 2000).

Recent studies shed light on the implication of the Hippo pathway in the *NF2*-associated cancers. For example, siRNA-mediated knockout of YAP (Yorkie-Associated Protein) in *NF2*-deficient meningioma cells inhibits cell proliferation by suppressing the S-phase entry (Striedinger et al, 2008), suggesting that the loss of growth-suppression in *NF2*-deficient cells is at least in part due to enhanced activity of YAP and likely the aberrant up-

regulation of the Hippo pathway. Interestingly, Merlin-mediated regulation of the Hippo pathway appears to play an important role in controlling the proliferation of *Drosophila* glial cells as well. The Merlin-Hippo pathway regulates glial cell numbers through Yorkie, and, when over-activated, Yorkie is sufficient to drive over-proliferation of *Drosophila* glia (Reddy & Irvine, 2011). The regulation of Yorkie-induced glial overgrowth is specific to Merlin, since other tested Hippo upstream regulators (*e.g.* Fat, Ex) have no detectable roles, indicating that dysregulation of the Hippo pathway by mis-expression of Merlin may be of particular significance in control of glial cell proliferation at least in invertebrates.

1.7.3. Merlin Regulating Membrane Receptors

The lipid rafts are subcellular structures required for receptor internalization from the plasma membrane and regulation of their downstream signaling (Di Guglielmo et al, 2003; Sigismund et al, 2008). Therefore, the enrichment of Merlin in lipid rafts implies that Merlin likely contributes to the regulation of the subcellular distribution and availability of the membrane receptor proteins. Results from several lines of research support this hypothesis (Curto & McClatchey, 2008; McClatchey & Fehon, 2009; McClatchey & Giovannini, 2005). For example, Merlin and Ex modulate receptor endocytosis and signaling. In *Drosophila* l-o-f of *Merlin* and *Ex* leads to defective endocytosis and degradation of a variety of receptor tyrosine kinases (RTKs) such as the epidermal growth factor receptor (EGFR) and a number of membrane

receptors such as Notch and Patched (Curto & McClatchey, 2008; Kissil et al, 2003; Maitra et al, 2006; Morrison et al, 2007; Poulikakos et al, 2006). As a result, the activity of the downstream signaling molecules such as JNK, Rac, Pak is up-regulated, leading to increased cell proliferation. Moreover, studies on mammalian cells also demonstrated the role of Merlin in intercepting EGFR-mediated cell proliferation by blocking the internalization of ligand-bound EGFR and sequestering the receptors into a non-signaling membrane compartment (Cole et al, 2008; Curto et al, 2007).

In addition, Merlin also physically interacts with hepatocyte growth factor-regulated tyrosine kinase substrate (HRS), an endosomal protein required for RTK trafficking and degradation (Le Roy & Wrana, 2005; Lloyd et al, 2002; Scoles et al, 2000). HRS is known to inhibit RTK signaling and studies showed its important role in suppressing growth of schwannoma cells (Sun et al, 2002). Over-expression of HRS in rat schwannomas produced the same functional consequences as regulated overexpression of Merlin. More critically, Merlin was incapable of suppressing cell proliferation of MEFs in HRS-null mouse models (Sun et al, 2002), indicating that the binding partner of Merlin, HRS, is required for the tumor-suppressive function of Merlin.

1.7.4. Merlin in the Nucleus

Recent advances on the tumor suppressor role of Merlin revealed that Merlin suppresses tumorigenesis by translocating to the nucleus, where it inhibits the activity of the E3 ubiquitin ligase $CRL4^{DCAF1}$ (Li et al, 2010).

Using an enhanced permeabilization technique and an antibody recognizing the C-terminus of Merlin, Merlin has been detected in the nucleus in multiple cells types such as HeLa squamous carcinoma cells, non-neoplastic HEI286 Schwann cells, LP9 mesothelial cells, and MCF-10A mammary epithelial cells. Moreover, the wild type, but not the NF2 tumor-derived Merlin with bona fide pathogenic missense mutations in the FERM domain, has a strong interacting affinity to $CRL4^{DCAF1}$, a cullin-ring E3 ligase family member involved in regulating chromatin remodeling, DNA replication and the response to DNA damage (Lee & Zhou, 2007; O'Connell & Harper, 2007). In addition, immunofluorescence studies illustrated that the dephosphoryated form of Merlin has the ability to translocate into the nucleus and binds $CRL4^{DCAF1}$. More importantly, siRNA-mediated silencing of $CRL4^{DCAF1}$in *NF2*-null human schwannoma cells suppressed cell cycle progression through G1 and S-phase entry in response to mitogens. Similar suppression of hyper-proliferation caused by loss of Merlin was also observed in human endothelial cells upon depletion of $CRL4^{DCAF1}$. Conversely, overexpression of a Merlin-insensitive mutant of $CRL4^{DCAF1}$ counteracted the anti-mitogenic effect of Merlin in human mesothelioma cells. Together, these data suggest that $CRL4^{DCAF1}$ plays a crucial role in mediating *NF2*-dependent hyper-proliferation and tumorigenesis in human schwannomas and *NF2*-related tumors.

2. Regulating Merlin and ERM Activities via Phosphorylation

2.1. Mechanism of Action

Merlin and other ERM members undergo activation-inactivation cycles via reversible phosphorylation by serine/threonine protein kinases and phosphatases. Inactive ERM proteins in a 'closed' conformation become activated when phosphorylation takes place at the C-terminal domain, which weakens the 'head-to-tail' intramolecular interaction (Figure 2A). On the other hand, Merlin retains its growth suppressive activity when the protein is phosphorylated/in an 'open' state, and becomes active upon dephosphorylation (Gutmann et al, 1999; Shaw et al, 2001; Sherman et al, 1997). Nevertheless, a recent crystallography study of Merlin suggested that the head-to-tail interaction provokes dimerization and dynamic moving and unfurling of the F2 motif of the FERM domain. Thus, the conventionally 'closed' Merlin conformer is in a more 'open' and active state for dimerization (Yogesha et al, 2011). The 'open-closed' switch model of Merlin conformation has been recently challenged by a study that assessed the tightness of self-association between the N- and C-terminal domain of various Merlin mutants and their corresponding efficiencies of growth suppression (Sher et al, 2012). The result of the study showed that, contrary to the previously proposed binary switch model, wild type Merlin is likely neither fully open nor closed, but may exist as a hierarchy of conformers with various degrees of 'openness' depending on the biological circumstances. Taken together, the marked contrast in the effect of phosphorylation on Merlin and other ERM activity may be in part due to the low sequence homology between Merlin and ERMs

particularly at the C-terminal domain, and may contribute to the unique role of Merlin in the hereditary neoplastic disorder.

2.2. Phosphorylation of Merlin

Early studies of Merlin post-translational modification revealed two to three major differentially phosphorylated isoforms of Merlin in both mammalian and *Drosophila* cells visualized using the standard SDS-PAGE with a . The difference in the mobility shift between the two phospho-isoforms was later found to be caused by phosphorylation at a single serine residue S518 at the C-terminus of Merlin which weakens protein self-association and inactivates the growth-suppressive function of Merlin (Kissil et al, 2002; Rong et al, 2004; Shaw et al, 2001; Xiao et al, 2002). Even though Merlin can also be phosphorylated at residues other than S518, the functional consequences and biological relevance of regulation of these residues largely remains unknown (McClatchey & Giovannini, 2005) (Figure 2B). In mammalian cells, Merlin phosphorylation at S518 is mediated by the p21-activated kinass-1 and 2 (PAK1/2), the major Rac/Cdc42-signaling effecter, in response to mitogenic stimuli (Kissil et al, 2002; Shaw et al, 2001; Xiao et al, 2002). S518 can also be phosphorylated by cAMP-dependent Protein Kinase A (PKA) in a PAK-independent manner (Alfthan et al, 2004). An additional player of Merlin phosphorylation in *Drosophila* is Slik kinase, a Sterile20-like kinase (Alfthan et al, 2004; Hughes & Fehon, 2006). In addition, Merlin inhibits PAK1 activity through a negative feedback loop by binding to and masking its PBD domain,

thus preventing PAK1 from being recruited to the focal adhesions (Kissil et al, 2003). Lastly, Protein Kinase B (AKT) phosphorylates Merlin at S10, T230 and S315, promoting the proteasome-mediated degradation of Merlin (Laulajainen et al, 2011; Tang et al, 2007).

The identification of more than one kinase responsible for Merlin phosphorylation suggests that multiple mitogenic signals may transduce to and converge on Merlin, where the growth-inhibitory activity of Merlin can be abrogated by regulated phosphorylation (see Table 1 for summary).

2.3. Dephosphorylation of Merlin

Tissue development and organization requires finely regulated switching between proliferative and adherent states. Therefore it is crucial that a negative growth regulator like Merlin can be effectively activated when required. Indeed, when cells are exposed to growth inhibitory signals such as contact inhibition, deprivation of growth factors and exposure to hyaluronic acid in the extracellular matrix (ECM), Merlin is dephosphorylated at S518, leading to a change from the 'open to the 'closed' conformation and subsequent activation (Morrison et al, 2001; Shaw et al, 1998). Mammalian studies have identified MYPT-1-PP1δ as the phosphatase that directly activates Merlin by dephosphorylating Merlin at S518 (Jin et al, 2006). In addition, expression of CPI-17 (C-kinase-activated PP1 inhibitor, Mr of 17kDa), a potent and specific endogenous MYPT1-PP1δ holoenzyme inhibitor, leads to increased Merlin phosphorylation, Ras activation and transformation.

The CPI-17-induced transformation can be reversed by constitutively active Merlin (S518A), indicating that Merlin is a substrate of MYPT-1-PP1 (Jin et al, 2006). Interestingly, the activity of CPI-17 is positively regulated by a considerable number of kinases such p21-activated kinase (Eto et al, 2001; Takizawa et al, 2002), which is also involved in the inactivating phosphorylation of Merlin as discussed above. Therefore, it is possible that CPI-17 acts as a signaling hub of multiple kinases and phosphatases to modulate Merlin activity effectively in an auto-regulatory circuit in response mitogenic stimuli (Figure 2A).

2.4. Phospho-regulation of ERM

The vertebrate ERM members, Ezrin, Radixin and Moesin, share a high degree of sequence and structural conservation likely due to a gene duplication event (Bretscher et al, 2002). ERM-mediated linkage between the actin-cytoskeleton and membrane-associated proteins is essential for the proper organization of apical membrane structures (Takeuchi et al, 1994). However, ERM proteins have partially overlapping functions, as the *Moesin* knockout mouse model exhibited virtually no discernible phenotype (Doi et al, 1999). This complicates the genetic analysis of the functions of ERMs in mammals. Nevertheless, studies on the sole *Drosophila* ERM orthologue, *Moesin*, revealed that the function of ERM-protein is essential for viability and epithelial integrity (Polesello et al, 2002; Speck et al, 2003). *Moesin* mutant

cells in the *Drosophila* wing imaginal disc have defective apical-basal polarity and are extruded from the basal surface of the epithelium (Speck et al, 2003).

Similar to Merlin, the regulation of ERM activity is primarily mediated by reversible phosphorylation. During platelet activation, Moesin was found phosphorylated at T558, accompanied by the reduction of the self-association of the protein (Nakamura et al, 1999). Phosphorylation of the corresponding residues of other ERM members was subsequently identified (Radixin-T564, Ezrin-T567). To date, three protein kinases have been found responsible for phosphorylation of Moesin at T558 in mammalian cells, Rho-kinase (Matsui et al, 1998), PKC-α (Ng et al, 2001), and PKC-θ (Pietromonaco et al, 1998). In *Drosophila*, the Merlin kinase Slik also phosphorylates and activates Moesin (Hughes & Fehon, 2006). Much like *Moesin* mutant, loss-of-function of Slik leads to mis-localization of Moesin, failed epithelial integrity and extrusion of cells from epithelium and subsequent apoptosis (Hipfner et al, 2004; Hughes & Fehon, 2006). The mammalian Slik and the related lymphocyte-oriented kinase (LOK) regulate phosphorylation and apical localization of Ezrin, which is required for the localization of microvilli to the apical membrane of the epithelial cells (Viswanatha et al, 2012).

Relatively less is known about the protein phosphatases required for Moesin dephosphorylation both in mammals and *Drosophila*. Beside the most analyzed Moesin phosphatase MYPT-1 (Adelstein et al, 1973), Sds22 is another phosphatase regulatory subunit implicated in the dephosphorylation and regulation of Moesin (Jiang et al, 2011) (see section 3.2.3 for further description). PP1-87B phosphatase has been shown to oppose the action of

Slik and restrict high Moesin activity at early mitosis and the regulated Moesin phosphorylation is required for cell elongation and cytokinesis in *Drosophila* Schneider 2 cells (Roubinet et al, 2011). In addition, a recent study showed that protein phosphatase 1α (PP-1α) mediates ceramide-induced ERM protein dephosphorylation (Canals et al, 2012).

3. ERMs and Epithelial Organization in Drosophila

Epithelial cells define the lining of metazoans and are crucial for delimiting the compartments of tissue architecture as well as maintaining homeostasis by allowing the exchange of molecules and ions within and between compartments. All epithelial cells are characterized with an asymmetric morphology, manifested in their cell shape, the uneven distribution of organelles and molecules, the oriented alignment of cytoskeletal networks, as well as the polarization of the plasma membrane (Knust & Bossinger, 2002). The polarized membrane is defined by elaborate cell-cell junctions and divided into two distinct regions: the apical domain, which faces the external environment or a lumen, and the basolateral domain, which is in contact with neighboring cells or a basal substratum (Knust & Bossinger, 2002). Epithelia of different species share a high degree of conservation in structure and molecular mechanisms, but also exhibit marked difference in regard to the composition and organization of the junction complexes. Epithelial cells of all species have an adhesive belt named zonula adherens (ZA) that encircles the cell below the apical surface. In vertebrate epithelial cells, a tight junction (TJ)

situated apically to the ZA, whereas in *Drosophila*, a distinct region apical to the ZA, the subapical region (SAR) is formed. In addition, *Drosophila* epithelium has a septate junction (SJ) positioned basally to the ZA (Figure 3).

The establishment and maintenance of epithelial organization has been extensively studied in the early developing embryo of *Drosophila*, in which the primary epithelium is formed from a syncytium by multiple invaginations of the plasma membrane during cellularization, leading to the formation of the cleavage furrows (Lecuit & Wieschaus, 2002). A transient basal adherens junction (BAJ) is subsequently formed just apically to the furrow canal (Lecuit & Wieschaus, 2002). BAJ is made of a protein complex containing DE-Cadherin, Armadillo (*Drosophila* β-catenin) PDZ-protein Disc lost (Dlt) and additional factors. Upon the completion of cellularization, the laterally dispersed spot adherens junctions coalesce apically and eventually form the ZA, which is linked to the apical membrane cytoskeleton by interactions between protein such as Crumbs, Moesin, Merlin and others positioned in the SAR (Bretscher et al, 2002; Medina et al, 2002).

The *Drosophila* apical polarity complex, the Bazooka (Baz)-Par6-atypical protein kinase (aPKC) complex, also plays a critical role in the proper development and differentiation of the primary epithelium (Ohno, 2001). Embryos devoid of Baz or aPKC show failed epithelial polarity and ZA formation (Bilder et al, 2000). The activity of the Baz-Par6-aPKC complex is mutually competitive, antagonistic to the Scribbled (Scrb)-Larval giant larvae (Lgl)-Disc large (Dlg) complex, which is the major junction component of the *Drosophila* SJ (Bilder et al, 2000). Thus, even though the full details of protein

interactions between distinct junction complexes needs to be further explored, it appears that *Drosophila* epithelial cells utilize elaborate and integrated regulatory mechanisms to establish and maintain apical-basal membrane identity.

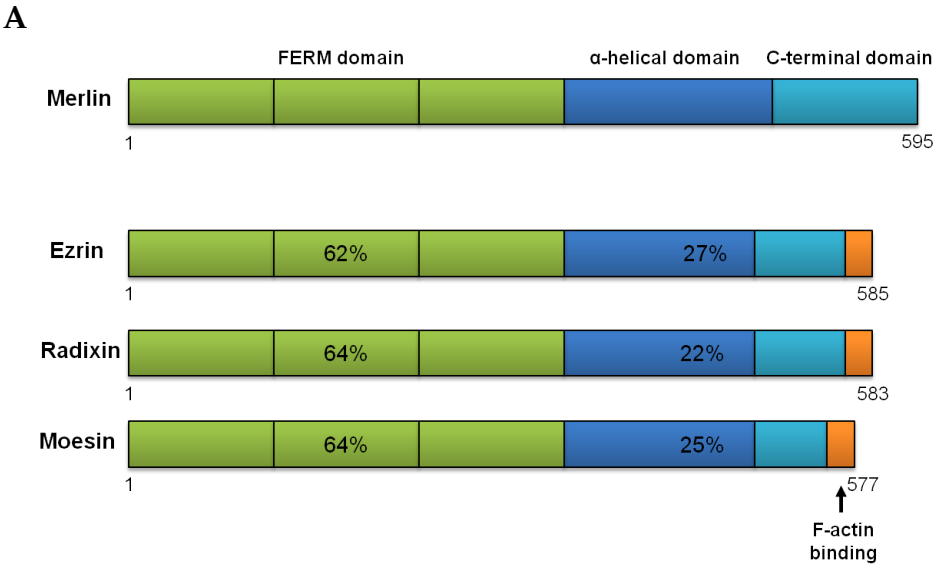
A
FERM domain
α-helical domain
C-terminal domain
Merlin
1
595
Ezrin
62%
27%
1
585
Radixin
64%
22%
1
583
Moesin
64%
25%
1
577
F-actin
binding

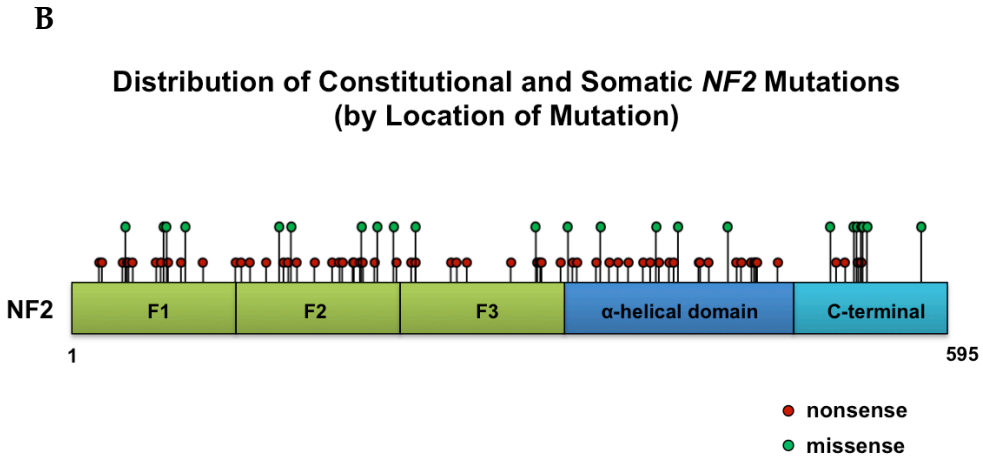
B
Distribution of Constitutional and Somatic NF2 Mutations
(by Location of Mutation)
NF2
F1
F2
F3
α-helical domain
C-terminal
1
595
nonsense
missense

C

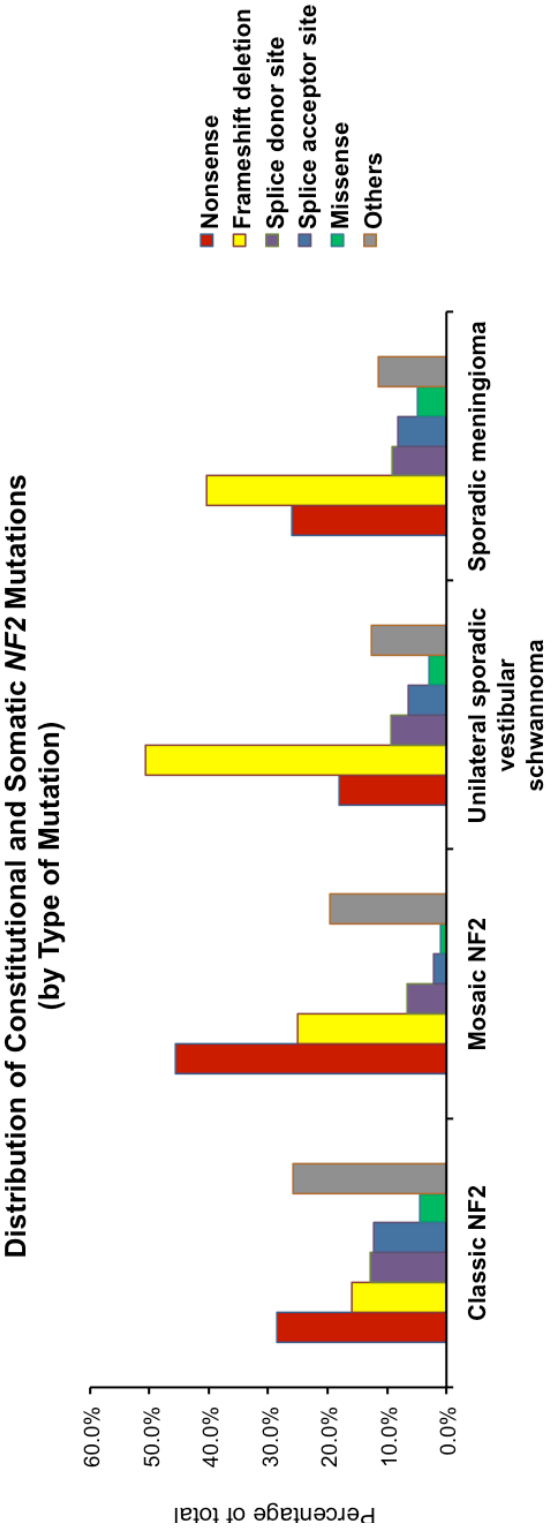
Distribution of Constitutional and Somatic NF2 Mutations
(by Type of Mutation)
Nonsense
Frameshift deletion
Splice donor site
Splice acceptor site
Missense
Others
Percentage of total
60.0%
50.0%
40.0%
30.0%
20.0%
10.0%
0.0%
Classic NF2
Mosaic NF2
Unilateral sporadic vestibular schwannoma
Sporadic meningioma

Figure 1 | Structural conservation of FERM proteins and disease-related mutations of *NF2*. (A) Structural conservation of FERM proteins. Both Merlin and the other ERM proteins (Ezrin, Radixin and Moesin) consist of a ~300 residue FERM domain of high sequence and structural conservation, a flexible α-helical coiled-coil domain, and a C-terminal domain. ERM proteins show very high sequence identify, whereas Merlin is more divergent. ERM proteins contain a conventional F-actin binding site at the end of C-terminal domain, which Merlin lacks. Sequence identity of ERMs to Merlin in mammals is shown as percentage. **(B)** Locations of point mutations (both constitutional and somatic) in the NF2 protein. **(C)** Major types of disease-associated mutations in the human *NF2* gene. Data were obtained from the international *NF2* mutation database.

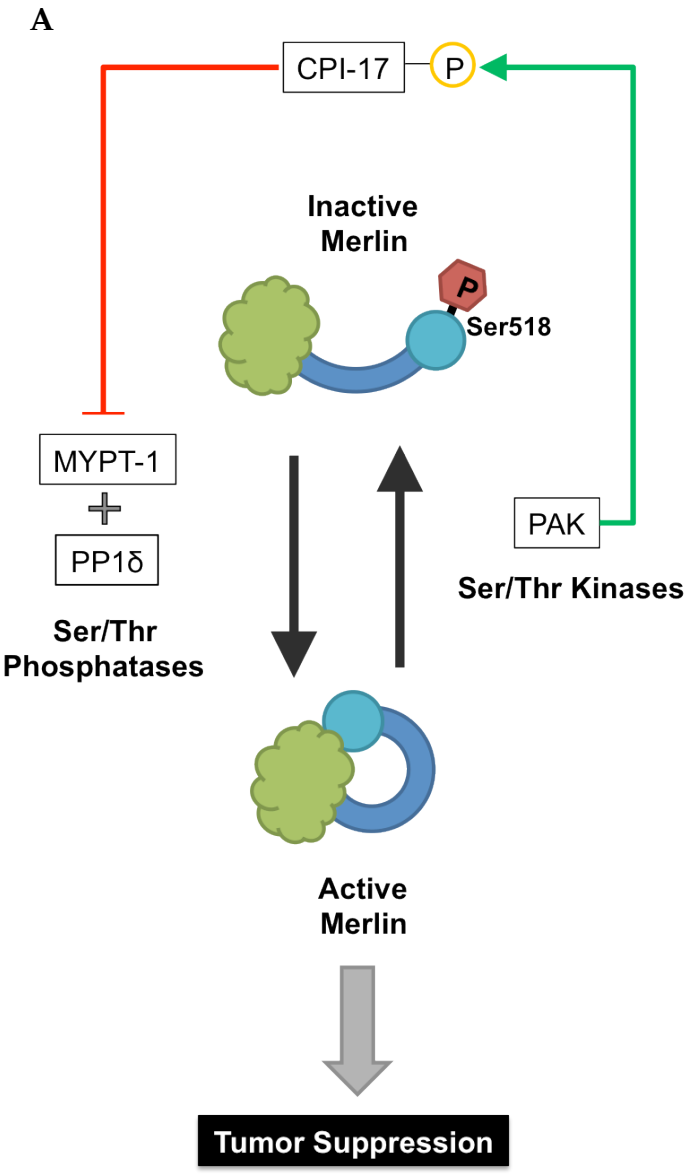
A
CPI-17
P
Inactive
Merlin
P
Ser518
MYPT-1
PP1δ
Ser/Thr
Phosphatases
PAK
Ser/Thr Kinases
Active
Merlin
Tumor Suppression

B

```
hMerlin         MAGAIASRMSFSSLKRKQPKTFTVRIVTMDAEMEFNCEMKWKGKDLFDLV 50
dMerlin         ----------MSPFGSKKNRSLSVRVSTFDSELEFKLEPRASGQDLFDLV 40
dMerlin         ----------------MSPKALNVRVTTMDAELEFAIQSTTTGKQLFDQV 34
                               . :::.**: *:*:*:**  :   .*::*** *

hMerlin         CRTLGLRETWFFGLQYT-IKDTVAWLKMDKKVLDHDVSKEEP---VTFHF 96
dMerlin         CRTIGLRESWYFGLQYVDTRSNVSWLKMEKRVRDQRVELHASNNVYVFSF 90
dMoesin         VKTIGLREVWFFGLQYTDSKGDSTWIKLYKKVMNQDVKKENP---LQFRF 81
                 :*:**** *:*****.  :.  :*:*: *:* :: *. . .     * *

hMerlin         LAKFYPENAEEELVQEITQHLFFLQVKKQILDEKIYCPPEASVLLASYAV 146
dMerlin         YAKFFPENVSEELIQEITQHLFFLQVKQSILSMDIYCRPEASVLLASYAV 140
dMoesin         RAKFYPEDVAEELIQDITLRLFYLQVKNAILTDEIYCPPETSVLLASYAV 131
                 ***:**:. ***:*:** :**:****: **  .*** **:*********

hMerlin         QAKYGDYDPSVHKRGFLAQEELLPKRVINLYQMTPEMWEERITAWYAEHR 196
dMerlin         HVQYGPYDYETYKDGMLAGGELLPKGVTDQYQMTPEMWEERIKTWYMDHE 190
dMoesin         QARHGDHNKTTHTAGFLANDRLLPQRVIDQHKMSKDEWEQSIMTWWQEHR 181
                :.::* ::  .:. *:**  .***: * : ::*: : **: * :*: :*.

hMerlin         GRARDEAEMEYLKIAQDLEMYGVNYFAIRNKKGTELLLGVDALGLHIYDP 246
dMerlin         PMTRDEVEMEYLKIAQDLDMYGVNYFPITNKNKTKLWLGVTSVGLNIYDE 240
dMoesin         SMLREDAMMEYLKIAQDLEMYGVNYFEIRNKKGTDLWLGVDALGLNIYEQ 231
                   *::. **********:******* * **: *.* *** ::**:**:

hMerlin         ENRLTPKISFPWNEIRNISYSDKEFTIKPLDKKIDVFKFNSSKLRVNKLI 296
dMerlin         RDKLTPKTTFQWNEIRHVSFDDKKFTIRLVDAKVSNFIFYSQDLHINKMI 290
dMoesin         DDRLTPKIGFPWSEIRNISFSEKKFIIKPIDKKAPDFMFFAPRVRINKRI 281
                 ::****  * *.***::*:.:*:* *: :* *   * * :  :::** *

hMerlin         LQLCIGNHDLFMRRRKADSLEVQQMKAQAREEKARKQMERQRLAREKQMR 346
dMerlin         LDLCKGNHDLYMRRRKPDTMEIQQMKAQAKEEKQRRQIERKKFIREKKLR 340
dMoesin         LALCMGNHELYMRRRKPDTIDVQQMKAQAREEKNAKQQEREKLQLALAAR 331
                * ** ***:*:*****.*::::*******:***  :* **:::      *

hMerlin         EEAERTRDELERRLLQMKEEATMANEALMRSEETADLLAEKAQITEEEAK 396
dMerlin         EKAEHERYELEKSMEHLQNEMRMANDALRRSEETKELYFEKSRVNEEQMQ 390
dMoesin         ERAEKKQQEYEDRLKQMQEDMERSQRDLLEAQDMIRRLEEQLKQLQAAKD 381
                *.**: : * *  : :::::   ::  * .:::      *: :  :   .

hMerlin         LLAQKAAEAEQEMQRIKATAIRTEEEKRLMEQKVLEAEVLALKMAEESER 446
dMerlin         LTECKANHFKTEMDRLRERQMKIEREKHDLEKKIRDADFYVHQLTVENDK 440
dMoesin         ELELRQKELQAMLQRLEEAKNMEAVEKLKLEEEIMAKQMEVQRIQDEVNA 431
                    :  . :  ::*:.        **  :*:::   :. . ::  * :

hMerlin         RAKEADQLKQDLQEAREAERRAKQKLLEIATKP----------------- 479
dMerlin         REAETEKLRKELICAKMAEREATARLLEFLNSGRKSSTDSLLTASSVSHA 490
dMoesin         KDEETKRLQDEVEDARRKQAEAAAALLAASTTP----------------- 464
                :  *:.:*:.::  *:  : .*   **   ..

hMerlin         --TYPPMNPIPAP------------------LPPDIPSFNLIGDSLS--- 506
dMerlin         ANTASSMAAISTPSLITSSSTNDLETAGGAELTTHSSHYLVQGDNSSGIS 540
dMoesin         -----QHHHVAED-------------------ENENEEELTNGDAGG--- 487
                         :.                        .      **  .

hMerlin         -------FDFKDTDMKRLSMEIEKEKVEYMEKSKHLQEQLNELKTEIEAL 549
dMerlin         DDFEPKEFILTDNEMEQITNEMERNHLDYLRNSKQVQSQLQTLRSEIAPH 590
dMoesin         -------DVSRDLDTDEHIKDPIEDRRTLAERNERLHDQLKALKQDLAQS 530
                          * : ..   :  .::    ...:::::.**: *: ::

hMerlin         KLKERETALDILHNENSDRGGSSKHNTIKKLTLQSAKSRVAFFEEL 595
dMerlin         KIEENQSNLDILS-EAQIKAGENKYSTLKKLKSGSTKARVAFFEEL 635
dMoesin         RDETKETANDKIHRENVRQ-GRDKYKTLREIRKGNTKRRVDQFENM 575
                : : .::  * :  *   : * .*:.*::::   .:* **  **::
```

Figure 2 | Regulation of Merlin and Moesin activities by reversible phosphorylation. (A) Activation-inactivation cycle of Merlin. Merlin switches between the active and inactive conformers by reversible phosphorylation at Ser518. Ser/Thr kinases add a phosphate group to Ser518, resulting in to intramolecular association between the N-terminal FERM domain and the C-terminal domain, inactivating Merlin tumor suppressor function. Dephosphorylation of S518 by Ser/Thr phosphatases such as MYPT-1-PP1δ weakens the head-to-tail interaction and activates Merlin. Merlin kinases such as PKC and PAK directly phosphorylate and activate CPI-17, which in turn inhibits the MYPT-1-PP1δ holoenzyme activity hence suppresses Merlin dephosphorylation, forming an auto-regulatory circuit of Merlin regulation. **(B)** Protein sequence alignment of human Merlin, *Drosophila* Merlin and *Drosophila* Moesin. Established residues of phosphorylation in human Merlin are shown in green. The homologous phosphorylation Threonine in *Drosophila* Merlin and Moesin used in this study are shown in cyan. Merlin orthologues, but not Moesin, contain the RVxF docking motif (framed residues) at the C-terminal end. The RVxF binding sequence is found in many PP1-interacting proteins and required for the formation of stable PP1 holoenzyme complexes.

Table 1. Kinases and Phosphatases of Merlin and ERMs in the Literature

	Merlin		ERM/Moesin	
	Name	***Residue***	***Name***	***Residue***
Protein kinase	PAK (Kissil et al, 2002)	S518	Rho-kinase (Matsui et al, 1998)	T558
	PKA (Alfthan et al, 2004)	S518	PKC-α (Ng et al, 2001)	T558
	Akt (Laulajainen et al, 2011; Tang et al, 2007)	S10,T230, S315	PKC-θ (Pietromonaco et al, 1998)	T558
	Slik (*Dm*) (Hughes & Fehon, 2006)	T616	Slik (Hipfner et al, 2004; Viswanatha et al, 2012)	T559 (*Dm*) T567 (Ezrin)
			LOK (Viswanatha et al, 2012)	T567 (Ezrin)
Protein phosphatase	MYPT-1* (Jin et al, 2006)		MYPT-1* (Adelstein et al, 1973)	
			Sds22 (*Dm*)* (Jiang et al, 2011)	
			PP1-87B (*Dm*) (Roubinet et al, 2011)	
	flapwing (*Dm*) (this study)		PP1-α (Canals et al, 2012)	
			flapwing (*Dm*) (this study)	

Dm: Drosophila melanogaster

** regulatory subunit of the phosphatase holoenzyme*

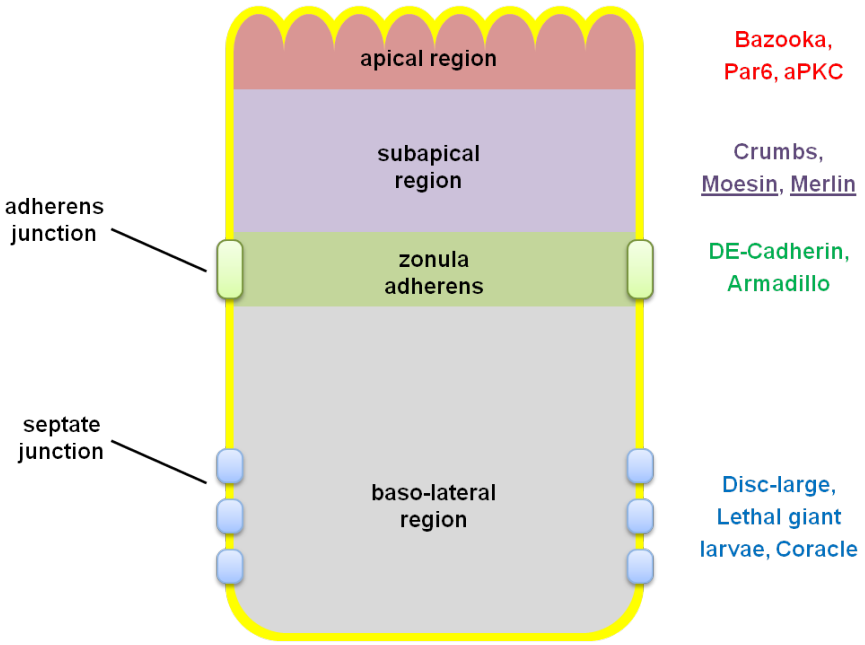

Figure 3 | Organization of polarized membrane domains in *Drosophila* differentiated epithelium. The zonula adherens (green) which is composed of adherens junctions divides the epithelial cell into the apical region (red and purple) and the baso-lateral region (grey). Some protein components of the junction complexes are selectively shown in colors accordingly.

4. Protein Phosphatases 1

4.1. Categorization

Quantitative phosphoproteomic studies showed that approximately 70% of all eukaryotic cellular proteins are regulated by reversible phosphorylation (Olsen et al, 2010), which is executed by the opposing activities of protein kinases and phosphatases on tyrosine, serine or threonine residues. 98.2% of all phosphorylation events are carried out by a plethora of serine/threonine kinases (86.4% pSer, 11.8% pThr), encoded by more than 420 genes in the human genome (Olsen et al, 2006).

In contrast to the hundreds of distinct Ser/Thr protein kinases, which have diversified during evolution by gene duplication and speciation, only about 40 Ser/Thr phosphatases (PSPs) have been identified up to date (International Human Genome Sequencing Consortium). The ratio of Ser/Thr phosphatases to Ser/Thr kinases in *Drosophila* is also low (1:6) (Morrison et al, 2000).

Ser/Thr phosphatases are categorized into three families: phosphoprotein phosphatases (PPPs), metal-dependent protein phosphatases (PPMs), and aspartate-based phosphatases such as FCP (TFIIF-associating component of RNA polymerase II CTD phosphatase) and SCP (small CTD phosphatase). Both PPPs and PPMs utilize a metal ion in their active site for the dephosphorylation reaction. As the largest family among the three, the PPP family consists of seven members in human (PP1, PP2A, PP2B/calcineurin,

PP4, PP5, PP6 and PP7) (Barton et al, 1994; Cohen, 1997), with PP1, PP2A and PP3 being the most extensively studied members.

Protein phosphatase 1 (PP1) is the most abundant enzyme in many eukaryotic cell types (Peti et al, 2013). In most eukaryotes, the catalytic subunit of PP1 (PP1c) is encoded by multiple genes, except for *Saccaromyces cerevisiae*, which has only one gene (*Glc7*) encoding PP1c (Stark, 1996). Through more than one billion years of eukaryotic evolution, PP1 has barely changed, since > 80% of PP1 sequence is identical between the yeast and human orthologues, and the human PP1 is able to rescue the lethality of a loss of PP1 in yeast (Gibbons et al, 2007).

4.2. Structure and Regulation of Activity

PP1 has a shallow active site and is capable of dephosphorylating a plethora of phospho-proteins *in vitro* (Heroes et al, 2013). Nevertheless, *in vivo* studies showed that PP1 acts in a highly substrate-specific and regulated manner. The remarkable *in vivo* specificity of PP1is achieved by its interaction with a large number of structurally unrelated proteins that modulate PP1 localization, activity and substrate specificity (Heroes et al, 2013). Together, the PP1 catalytic core subunit (PP1c) and its various binding partners/ regulatory subunits form a vast array of PP1 holoenzymes with distinct sets of substrates and mechanisms of regulation.

In mammalian genomes, there are four catalytic subunits of PP1: PP1c-α, PP1c-β/δ, and the splice variants PP1c-γ1 and PP1c-γ2 (Cohen, 1988; Sasaki et al, 1990), all of which have a similar enzymatic activity. In contrast, there are approximately 200 validated PP1 regulatory subunits to date (Bollen et al, 2010). Based on their main effects on PP1c, regulatory subunits can be divided into three groups. The first group is the activity-modulating proteins including PP1 true inhibitors such as Inhibitor-1 (Tamrakar & Ludlow, 2000) and CPI-17 (Koyama et al, 2000) as well as the substrate-specifiers including I_1^{PP2A}/PHAP-I, and I_2^{PP2A}/PHAP-II (Katayose et al, 2000), which functions as potent inhibitors of PP2A and promote dephosphorylation of PP1c substrates. The second group is called PP1 targeting-proteins, which typically bring PP1c in close proximity to the substrates or the substrate-containing subcellular structures (e.g. the glycogen-targeting G subunit (Liu & Brautigan, 2000)). This group also includes many 'scaffolding' proteins that mediate the formation of the multi-protein complexes that contain both the protein kinases and phosphatases. One of best characterized examples of the scaffolding proteins is MYPT1 (Fukata et al, 1998; Toth et al, 2000). The third group of PP1 regulatory subunits directly and tightly associates with PP1c and defines a subset of its substrates (Heroes et al, 2013).

Years of research has identified a considerable number of a PP1c-binding sequence in the PP1 regulatory subunits that is required for the formation of the stable PP1 holoenzyme complex. One of the well characterized PP1 docking motifs is the RVxF binding sequence, which is present in nearly 90% of all validated PP1 regulatory subunits (Egloff et al, 1997; Zhao & Lee, 1997).

The RVxF sequence is degenerate (the consensus sequence is K/R/H/N/S-V/I/L-x- F/W/Y) and specific for interactions with PP1, yet does not appear to cause important conformational changes of the catalytic subunit (Endo et al, 1996; Kwon et al, 1997). Instead, it is proposed that upon binding to a hydrophobic channel remote from the catalytic site of PP1c, the RVxF motif facilitates the regulatory subunit to make additional contacts with PP1 in an ordered or even cooperative manner (Yang et al, 2000).

4.3. Cellular Functions

Ubiquitously expressed in all eukaryotic cells, PP1 plays an essential role in a diverse variety of cellular processes such as cell cycle, apoptosis, cytoskeletal re-organization, muscle contraction, protein synthesis and RNA splicing (Lin et al, 1999; Shi, 2009). In the following text, I will briefly discuss part of the well-characterized cellular functions of PP1 relevant to the main focus of this project.

4.3.1. Spindle Checkpoint Silencing

Faithful cell division into two identical daughter cells during mitosis is crucial for the survival and functioning of eukaryotic organisms. This is in part accomplished by the spindle checkpoint, a surveillance mechanism that ensures each of the sister chromatids at the centromeric region be correctly attached to the plus end of the mitotic spindle microtubules (MTs) from the

opposite poles before the onset of the metaphase-anaphase transition (Musacchio & Salmon, 2007; Zich & Hardwick, 2010). In the absence of correct orientation of the chromosomes (*e.g.* unattached or mal-attached sister chromatids), the spindle checkpoint is activated, whereby the key components of the checkpoint machinery including protein kinases Aurora B and other non-kinase proteins collectively inhibit the activity of Cdc20, a specific activator of ubiquitin ligase anaphase promoting complex (APC) (Herzog et al, 2009; Kulukian et al, 2009; Nilsson et al, 2008; Pan & Chen, 2004). APC stimulates the onset of anaphase by marking securin and cyclin B for proteasome-mediated degradation (Hagting et al, 2002; Thornton & Toczyski, 2003). The function of securin is to liberate the protease separase, which subsequently cleaves the cohesion protein thus removing the cohesion between two sister chromatids and allowing their separation (Clift et al, 2009). Meanwhile, the degradation of cyclin E prevents the activation of cyclin-dependent kinase-1 (Cdk1), which promotes mitotic exit and cell cycle progression.

The essential role of PP1 in silencing the spindle checkpoint machinery first came from a study showing that suppression of PP1 activity led to persistence of mitosis in the absence of Cdk1 activity (Skoufias et al, 2007). Later studies revealed that PP1 functions antagonistically to Aurora B kinases to provide a safe passage to the mitotic exit (Emanuele et al, 2008; Hsu et al, 2000; Pinsky et al, 2006; Vanoosthuyse & Hardwick, 2009). Upon correct bipolar orientation of the chromosomes, PP1 is recruited to the kinetochore by its regulatory subunit Sds22 and directly binds to kinetochore protein KNL1 and

kinetochore motor CENPE (Kim et al, 2010; Liu et al, 2010; Posch et al, 2010). The ensuing kinetochore-localized PP1 then counteracts Aurora B kinases in substrate phosphorylation. In addition, Sds22-PP1c may be involved in modulating the activity of Aurora B kinases by suppressing the activating phosphorylation of Aurora B kinases (Posch et al, 2010). Conversely, the activity of PP1 can be inhibited when its binding partners, KNL1 and CENPE, are phosphorylated at their PP1-binding motifs by Aurora B kinases (Liu et al, 2010; Posch et al, 2010). Thus, the mutual regulation between PP1 and Aurora B kinases acts as a powerful and efficient switch-like mechanism to ensure the timely response of the diploid cell to errors in chromosome-spindle attachment.

The catalytic subunit of PP1 alone has broad substrate specificity, and it is the association of PP1c with its numerous regulatory subunits that specify the precise timing and subcellular localization of PP1. In addition to the well-conserved R subunit Sds22 mentioned above, another R subunit of PP1c involved in regulating spindle checkpoint silencing is myosin phosphatase targeting protein 1 (MYPT-1). Conserved in metazoan cells, MYPT-1-PP1c interacts directly with polo-like kinase (Plk) and antagonizes its activity to phosphorylate several checkpoint component proteins and to promote acute recruitment of Aurora B kinases to the unattached kinetochore (Salimian et al, 2011; Yamashiro et al, 2008). Thus, MYPT-1 facilitates checkpoint silencing by stabilizing kinetochore-spindle structure.

4.3.2. *Antagonizing Apoptosis*

Regulated cell death such as apoptosis is critical for the maintenance of tissue homeostasis and prevention of disease initiation and progression. Components and regulation of the apoptosis-initiating machinery for both intrinsic and extrinsic pathways have been well studied. In the extrinsic pathway, binding of death-receptor ligands to the death receptor triggers the cleavage of the pro-caspase 8 into its active form, which subsequently leads to the cleavage and activation of the effector caspase caspase-3, commencing the initiation of the apoptotic event (Song & Steller, 1999). In the intrinsic apoptotic pathway, cellular stresses including DNA damage, UV radiation, growth factor deprivation and oxidative stress result in the oligomerization of pro-apoptotic Bcl-2 family proteins such as Bak and Bax at the outer membrane of mitochondria (Adams & Cory, 2007). The resulting pore formation allows the release of cytochrome c from the mitochondrial intermembrane space to the cytoplasm. Cytosolic cytochrome c forms the apoptosome complex together with Apaf-1 and the activated caspase-9. Active casapse-9 cleaves and activates Casapase-3 to initiate apoptosis (Gogvadze et al, 2006).

The apoptotic signal transduction pathway is regulated at multiple steps and cross-talks occur between many signaling pathways that promote cell survival. For example, the serine/threonine kinase Akt, a key regulator of signal transduction in response to nutrients, growth factors and cytokines has been found to suppress apoptosis by serine phosphorylation of Bad (del Peso et al, 1997; Harada et al, 1999). Moreover, nuclear localized Akt counteracts

the actions of active caspase-3 by blocking the activity of caspase-3-activated DNase thereby preventing DNA fragmentation or inhibiting chromatin condensation by phosphorylating Acinus, a protein involved in chromatin condensation, and protecting it from casapase-3-mediated cleavage and activation (Ahn et al, 2006; Sahara et al, 1999).

Given the extensive cellular processes in which PP1 is involved, it is not surprising that PP1 is among the many regulators of apoptotic signaling pathways. PP1α and PP1β can directly dephosphorylate Akt and inhibit its full activation, thus negatively modulating cell survival and proliferation (Xiao et al, 2010). Furthermore, PP1α dephosphorylates caspase-9 at T125, resulting in its activation and subsequence IL-2 deprivation-induced apoptosis (Dessauge et al, 2006).

4.3.3. Muscle Contractibility and Cytoskeletal Reorganization

Reorganization of the cytoskeleton is an essential process for cell division, adhesion and motility. Dephosphorylation by PP1 occurs in many F-actin associated proteins to regulate their activity and properties (Ambach et al, 2000; Oleinik et al, 2010; Tsukada et al, 2006; Vereshchagina et al, 2004). One such example is MYPT1, the PP1 regulatory subunit that has recently been found to be involved in Merlin dephosphorylation as previously discussed. MYPT1 expression is most abundant in smooth muscle cells (Feng et al, 1999), where it binds to PP1cδ to form a heterodimeric complex myosin light chain phosphatase (MLCP) to regulate muscle contraction (Hartshorne, 1998; Ito et

al, 2004; Tanaka et al, 1998). Specifically, in response to increased cytosolic Ca^{2+} concentration, myosin light chain 20 (LC_{20}) is phosphorylated by myosin light chain kinase (MLCK) at S19, which leads to its interaction with actin and activation of the actin-activated ATPase of myosin (Chacko et al, 1977; Ikebe et al, 1986). Once [Ca^{2+}] returns to its basal level, LC_{20} is dephosphorylated by MLCP and dissociates from F-actin. The completion of the cross-bridge cycle generates contractile force or muscle shortening.

A study in *Drosophila* by Grusche et al suggested that Sds22 is involved in the dephosphorylation of two previously postulated PP1 targets, Spaghetti Squash (*Drosophila* non-muscle myosin II light chain) as well as Moesin (Grusche et al, 2009). Mutation of Sds22 causes change in cell shape and defective morphology of the columnar epithelia of imaginal discs and follicle cells. A more recent study by Kunda *et al* showed that dephosphorylation of Moesin by Sds22-PP1c is also important for cell cycle progression during mitotic cytokinesis (Kunda et al, 2012). At metaphase, phosphorylated Moesin constructs a rigid, rounded structure called the metaphase cortex. In order to progress through anaphase elongation, this pool of phospho-Moesin must be lost through inactivating dephosphorylation by Sds22 to allow for the disassembly of the cortex. RNAi-mediated depletion of *sds22* results in delayed clearance of the phospho-Moesin pool as well as defects in bipolar anaphase relaxation, a phenotype that was then re-capitulated by the expression of a constitutively active, phosphomimetic Moesin. Thus, Sds22 plays a dual role in both epithelial integrity and cell division by targeting the same substrate Moesin for dephosphorylation.

5. *Rationale of the Project*

Strong evidence from accumulating studies suggests that the tumor suppressor Merlin functions at the converging point of many mitogenic signal transduction pathways. Therefore, there is a great need to acquire a more complete understanding of the upstream regulators of activation-inactivation cycle of Merlin via reversible phosphorylation. We set out to identify and characterize the potential players of phospho-regulation of Merlin including both serine/threonine kinases and serine/threonine phosphatases. In our previous finding, a Sterile20 kinase, Slik, was found to control the phosphorylation of both Merlin and Moesin in a coordinate manner (Hughes & Fehon, 2006). This implies that the regulation of cell proliferation (*e.g.* by Merlin) and epithelial integrity (*e.g.* by Moesin) may also be coordinated to achieve the concerted, optimal outcome during tissue development.

Compared to the many protein kinases responsible for Merlin phosphorylation, the executors of the reverse reaction remain largely unknown. To date, the only known PP1 regulatory subunit involved in Merlin dephosphorylation is MYPT1, which binds to the mammalian PP1c δ and activates Merlin tumor suppressor function (Jin et al, 2006). However, the specific PP1 catalytic subunit for Merlin dephosphorylation has not been determined in *Drosophila*, and none is known for reversing the action of Slik by coordinately regulating the activity of both Merlin and Moesin.

The *Drosophila* PP1c-β9c, *flapwing* (*flw*) is homologous to the mammalian PP1c-β/δ and is the only *Drosophila* PP1β-encoding gene essential for viability. Contributing to 10% of the total phosphatase activity as tested in *Drosophila* larvae, *flw* was first characterized more than three decades ago as one of the five genes that affect the development and morphology of the indirect flight muscles of *Drosophila* (Axton et al, 1990; Dombradi et al, 1990; Dombradi & Cohen, 1992). Mutations in *flw* caused the complete loss of the indirect flight muscle fibers and hence produced 'flightless' flies (Deak, 1977; Raghavan et al, 2000). Moreover, loss-of-function of *flw* led to elevated level of phosphorylated myosin as well as disruption of actin organization in the *Drosophila* egg chamber (Vereshchagina et al, 2004). Based on the phenotypes resulted from *flw* mutations in relation to the cellular functions of FERM family proteins, it was proposed that *flw* is a good candidate that potentially controls phosphorylation of Merlin and Moesin.

In this project, the biochemical interactions of flw with Merlin (Mer) and with Moesin (Moe) were first tested *in vivo* and *in vitro*. Analyses were then conducted to assess how changing the expression level of *flw* in *Drosophila* tissues correlates with changes in the phosphorylation patterns of Mer and Moe. We also examined the effect of changing *flw* expression level on the subcellular localization of Mer and Moe. In the last step, the impact of loss of expression of *flw* on epithelial integrity was examined to determine the functions of flw-mediated phosphorylation of Mer and Moe in the whole organism.

Chapter Two

Materials and Methods

1. Drosophila stocks

y cho flw^{1}, UAS *Flw* HA was obtained from the Bloomington Drosophila Stock Center (stock #23703). The *flw* RNAi (*flw*-IR) line was obtained from the Vienna Drosophila RNA Center (stock #104677KK). Fly lines of *flw* over-expression and *flw* knockdown were produced by crossing MS1096-Gal4 (expressed in the dorsal surface of the wing imaginal disc), *patched*-Gal4, and *apterous*-Gal4 to the UAS transgenic line and the RNAi line, respectively. Flies were raised on the standard media currently used by the Bloomington Stock Center.

2. Transfection of Schneider 2 (S2) Cells

Two μg of Ubiquitin-Gal4, UAS HA Mer and UAS HA Flw plasmid DNA was added to 120 μl of 250 μg/ml DDAB (dimethyl dioctadecyl ammonium bromide; Sigma Aldrich) transfection reagent and 60 μl of Hyclone Serum free SFX insect cell culture medium for incubation at room temperature for 20 min. The transfection mix was added drop-wise into three ml of S2 cells (10^6 cells per ml) in a six well plate. Cells were then incubated at 25°C overnight.

3. Antibody preparation

An N-terminal GST-Merlin fusion protein was expressed and purified using the approach described in the previous study (Rebay & Fehon, 2009). The

GST protein was purified by column chromatography and, following elution with gluthathione, electroelution and then dialyzed into 1X PBS (phosphate-buffered saline). Polyclonal sera were raised in guinea pigs against the Merlin fusion protein (Pocono Rabbit Laboratory and Farms).

4. Co-immunoprecipitation and Immunoblotting

Cells were collected by centrifugation at 1000 Xg for 3 min. Cell pelletes was lysed and cross-linked into 1 ml of milk lysis buffer (50 mM HEPES ph 7.0, 50 mM NaCl, 1 mM EDTA, 0.5 mM EGTA, 10 mM DTT, 1% Triton X-100, 1 X Roche complete EDTA free inhibitor cocktail, 1 X Roche Phos STOP) + 0.1% formaldehyde for 10 min at 4°C. Cellular debris was cleared by centrifugation at 16000 Xg (relative centrifugal force) for 10 min at 4°C. For immunoprecipitation (IP) for flw, the supernatant was divided into two 1.5 ml tubes and incubated at 4°C overnight with mouse anti-HA (Sigma) dimethyl pimelimidate dihydrochloride crossed-linked protein G beads at a dilution of 1:500 v/v. For IP for Merlin, the supernatant was incubated 4°C overnight with guinea pig anti-Merlin dimethyl pimelimidate dihydrochloride crossed-linked protein A beads at 1:1000 or protein A beads alone as control. After incubation, the beads were pelleted by centrifugation at 1000 Xg for 30 s and washed four times in mild lysis buffer and eluted two times using 75 μl of Gentle Ag/Ab elution buffer (Thermo Scientific). The protein was precipitated in chloroform and methanol and resuspended in 50 μl of 1X SDS sample buffer. Protein samples were heated to 95°C for 5 min,

loaded and separated on a 10% SDS-PAGE gel, and transferred to nitrocellulose (Biorad). Western blots were visualized using an infrared imaging system (Odyssey; LI-COR).

For visualization of multiple phosphorylated forms of Merlin, wing imaginal discs (10 per genotype) were dissected in 1X PBS from wandering third instar larvae of the genotypes MS1096-Gal4 X UAS *flw*-IR, MS1096-Gal4 X UAS *flw* and MS1096-Gal4 X w^{1118} as *flw* knockdown, *flw* over-expression and the wild type control, respectively. For IP for Merlin, the supernatant of the tissue lysate was incubated with guinea pig anti-Merlin protein A beads as described. Protein samples were run on low-bis acrylamide gels as previously described. Merlin on the nitrocellulose blots was visualized using guinea pig anti-Mer antibody at 1:5000. To visualize phosphorylated Moesin isoforms, tissue lysates were obtained from wandering third-instar larvae of the genotype MS1096-Gal4 X UAS *flw*-IR, MS1096-Gal4 X UAS *flw* and MS1096-Gal4 X w^{1118}. A rabbit phospho specific anti-Moe antibody (Phospho-ERM; Cell Signaling) was used on blots at 1:500 and compared to a loading control of mouse anti-β-tubulin antibody at 1:5000 (E7; Developmental Studies Hybridoma Bank, DSHB, The University of Iowa, Iowa City, IO). Western blots were visualized and quantified using an infrared imaging system (Odyssey; LI-COR).

5. Quantitative Real-time PCR

Total RNA was extracted from five third-instar wing imaginal discs using Trizol Reagent (Invitrogen) according to manufacturer's instruction. cDNA was generated from 1 μg RNA for each sample using a mix of oligo (dT) and random primers (Quanta Biosciences), using qScript cDNA SuperMix (Invitrogen). Two-step qRT-PCR was performed on an Eppendorf realplex 2 PCR machine using 2 μl of cDNA mix and gene-specific primers with PerfeCTa SYBR Green FastMix (Quanta Biosciences). Threshold cycle values were normalized against *RP49* as an internal control. The $\Delta\Delta C_T$ (C_T threshold cycle) method was used to calculate relative concentrations of target mRNA. The following primers were used to detect their respective transcripts:

flw	forward 5′- GCCTACAAGATCAAATATCCGG -3′
flw	reverse 5′- AGCAATCTGTGAAAGTCTTCC -3′
RP49	forward 5′- TGTGATGGGAATTCGTGGC -3′
RP49	reverse 5′- ACTTTGGGCCTGTATGCTG -3′
Mer	forward 5′- GAGGAACGGATCAAGACATG -3′
Mer	reverse 5′- GGCGAATGGTGAACTTCT -3′

6. GST Pulldown Assays

The bait glutathione S-transferase (GST) fusion proteins were expressed in *Escherichia coli* BL21 DE3 cells and purified using Glutathione sepharose 4B beads (GE Healthcare). The proteins were labeled with ^{35}S *in vitro* using the

TNT-coupled *in vitro* transcription-translation system (IVT/T; Promega). For the *in vitr*o binding assay, 90 μl of ^{35}S-labeled probe proteins diluted to approximately 10,000 cpm/μl were incubated with approximately 100 μg of immobilized GST fusion proteins in 300 μl Affinity Chromatography (AC) buffer (20 mM Tris pH 7.6, 100 mM NaCl, 0.5 mM EDTA, 10% glycerol, and 0.1% Tween-20) at 4°C overnight. The beads were washed three times in 400 μl AC buffer. 4 X SDS sample buffer was added to the flow-through and elution fractions to a final concentration of 1X, and samples boiled for 5 min. Proteins were resolved by SDS-PAGE and exposed to X-ray film for 20-24 h.

7. 2-D and 2-D Differential in-gel Electrophoresis (DIGE)/Western Analysis

Wing imaginal discs of the wandering third-instar larvae of genotype MS1096-Gal4 X UAS *flw* and MS1096-Gal4 X w^{1118} were dissected in 1X PBS. A Merlin IP was performed as described above and analyzed by DIGE analysis (Applied Biomics, CA). Accurate volume measurements of differences in the amount of Mer proteins in the *flw* over-expressing tissue compared to in the wild type was determined using the DeCyder 2-D Differential Analysis software (GE). The differences of the volumes between the Mer spots from each tissue IP were expressed as a volume ratio. Guinea pig anti-Mer antibody was used for Western blot analysis at 1:5000. The experiment was repeated two times.

To confirm the altered pattern of Merlin isoforms identified by 2-D DIGE/Western analysis, half of the IP was treated with 5 μg lambda

phosphatase (NEB, 400 units/μl) at 30°C for 30 min, while the other half was mock treated. Each sample was resuspended in 140 μl isoelectric rehydration buffer (8 M urea, 2% Triton-X100, 2% ampholytes pH 4-7, 40 mM DTT, 1 X Complete EDTA-free protease inhibitors). Samples were then incubated at room temperature for 30 min and applied to Immobiline DryStrips (GE Healthcare; pH 4-7) and rehydrated for 13 h followed by IEF (100 V for 1.5 h, 500 V for 45 min, 1000 V for 45 min, 3000 V for 1 h, 5000 V for 2 h) using a Pharmacia Biotech IPGphor system. Strips were then removed and either used immediately or placed at - 80°C. Strips were incubated in equilibration buffer (2 ml per strip; 6 M urea, 75 mM Tris-HCl pH 8.8, 29.3% glycerol, 2% SDS, 1% bromophenol blue, 10 mg/ml DTT). The proteins were then run on 10% SDS-PAGE gels, transferred to nitrocellulose and probed with guinea pig anti-Merlin antibody (1:1000) and anti-guinea pig HRP (1:50,000) and developed using ECL (Pierce).

8. Immunofluorescence Microscopy

Wing imaginal discs from wandering third-instar larvae and early pupae prior to puparium formation of each genotype were dissected in 1X PBS and fixed in either 4% paraformaldehyde at room temperature for 20 min or in ice-cold 10% TCA for 1 h (phospho-Moesin staining). Primary and secondary antibodies used for immunofluorescence imaging are listed in Table 1. Images were collected on a Zeiss 700 confocal microscope (Carl Zeiss Canada) using a 63 X Plan-Apo NA 1.4 lens and compiled in Adobe Photoshop CS extended

Version 11.0. When required, images were smoothened using a Gaussian filter (0.5 pixels). Imaris (Andor AG) and Auto-deblur (media Cybernetics) were used for de-convolution and compilation for producing the maximum intensity projections shown in Figure 12 and 15. The gamma range of the activated caspase 3 channel was reduced from 1 to 0.5 in Figure 17.

Table 2. List of Antibodies and Reagents for Immunofluorescence Imaging

Name	Raised in	Dilution v/v	Source
anti-Merlin	guinea pig	1 : 2,000	this study
anti-phospho ERM	rabbit	1 : 500	Cell Signaling
anti-patched	mouse	1 : 200	DSHB
anti-DE-Cadherin	rat	1 : 200	DSHB
anti-Armadillo	mouse	1 : 500	DSHB
anti-Discs large	mouse	1 : 500	DSHB
anti-activated caspase 3	rabbit	1 : 100	Cell Signaling
anti-MYC	mouse	1 : 1,000	Cell Signaling
anti-pan Moesin	rabbit	1 : 20,000	D Kiehart, Duke University
anti-Coracle	guinea pig	1 : 10,000	R. Fehon, University of Chicago
Phalloidin A488/A546	/	1 : 1,000	Invitrogen
Alexa Fluor 488/546	various	1 : 2,000	Invitrogen
Cy3/Cy5	various	1 : 1,000	JacksonLabs Immunological

9. Wing Measurements

Flies were raised on standard Bloomington Stock Center food at 25 °C. Adult flies were incubated in 70% ethanol for 24 hr and the wings were dissected and mounted in Aquamount (Thermo Scientific) on a glass slide. Images of mounted wings were collected using an Orca ER Hamamatsu or Coolsnap HQ (Photometrics) camera mounted on a Zeiss Axioskop using a CP-Apocromat 5 X NA 0.12 Zeiss lens. Area measurements of each wing were obtained by outlining the appropriate wing area using the free hand draw tool in Image J (National Institutes of Health). Statistics were calculated using GraphPad software (GraphPad Software Inc.). The figures were compiled in Adobe Photoshop CS4 extended Version 11.0.

Chapter Three

Results

1. Flw Forms a Complex with Merlin and with Moesin

If Merlin (Mer) and Moesin (Moe) are substrates of flw for dephosphorylation, it is expected that Mer and Moe can interact with flw individually. In S2 cells transiently co-transfected with epitope tagged HA-*Mer* and HA-*flw*, we co-immunoprecipitated (co-IPed) endogenous Mer and detected the presence of HA-flw in the protein complex (Figure 4A), suggesting that flw interacted with Mer in a protein complex *in vivo*. Similarly, in the *Drosophila* Schneider S2 cells (a primary culture of late stage *Drosophila* embryos 20-24 hr old) transiently transfected with epitope tagged Myc-Moe and HA-flw, a significant amount of endogenous Moe was co-IPed with HA-flw (Figure 4B). This suggests that flw can form a protein complex with Mer and with Moe in S2 cells.

In the next step, we determined whether the interaction between flw and Mer/Moe was likely direct. Using *in vitro* GST pulldown assays, we found that the ^{35}S-radiolabeled bait protein flw was pulled down by the probe GST-Mer fusion protein, but not GST alone (Figure 4D), suggesting a direct physical interaction between flw and Mer. The same direct interaction was also detected between flw and Moe (Figure 4C). Interestingly, flw was also able to bind to Sip1 directly in the pull-down experiment (Figure 4C). Sip1 is a scaffolding protein required to facilitate the coordinate phosphorylation of Mer and Moe by the Slik kinase (Hughes et al, 2010). Taken together, flw can form a protein complex with Mer and with Moe *in vivo* and *in vitro*.

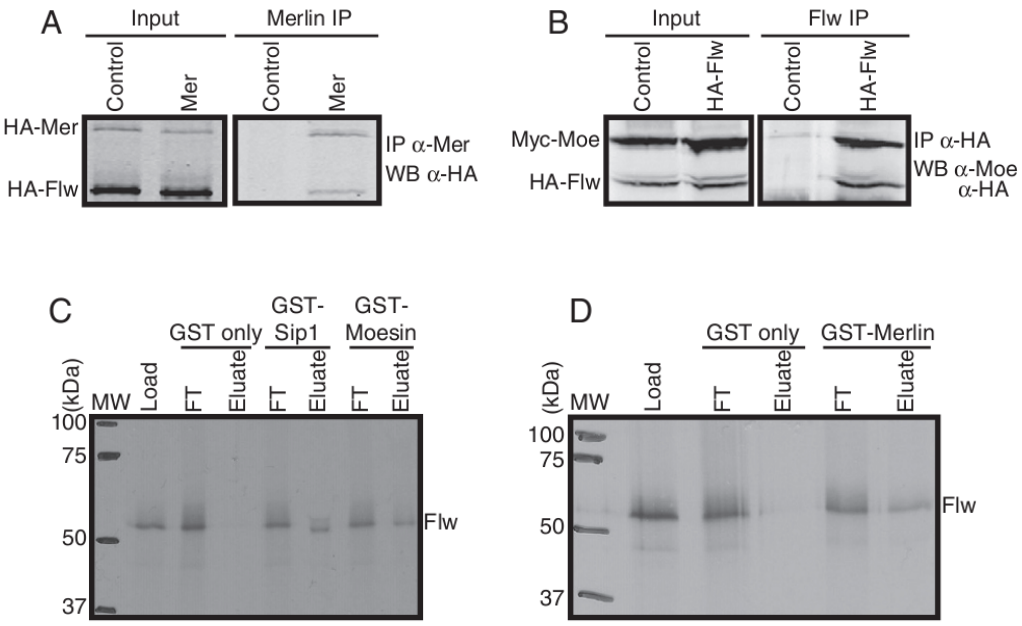

Figure 4 | Flw forms a complex with Mer and Moe. (A) Endogenous Mer was Co-IPed with HA-tagged flw in the transiently transfected S2 cells. Western blot was probed with anti-Mer and anti-HA antibody. No flw signal was detected in the control experiment, where no Mer antibody (protein A beads only) was used for the IP. **(B)** Co-IP of Myc-tagged Moe in S2 cells transiently transfected with Myc-Moe and HA-flw. The Myc-Moe signal identified by anti-Moe antibody was only present when IPing using anti-HA antibody on the protein G beads but not with the beads alone. **(C)** *in vitro* binding of GST-tagged Moe fusion protein to flw. Radiolabeled flw was selectively retained to the GST-tagged Moe eluate but not GST alone. GST-tagged Sip1 only retained flw in the eluate. **(D)** *in vitro* binding of GST-Mer to flw. Radiolabeled flw was selectively retained to the GST-tagged Mer eluate but not GST alone.

2. *Patterns of Mer and Moe Phosphorylation Isoforms Change in Response to flw Expression Level*

2.1. *Changes in flw Expression Level Lead to Corresponding Changes in Mer Phosphorylation Pattern*

If dephosphorylation of Mer and Moe is controlled by flw, it is expected that changes in the expression level of *flw* will lead to the corresponding changes in the ratios of cellular Mer and Moe phosphorylation isoforms. To test the hypothesis, we first examined the patterns of phospho-isoforms of Mer in the *Drosophila* larval wing imaginal disc tissue by Western blotting analysis. A phospho-Mer-specific anti-Mer antibody is not available in *Drosophila*. To circumvent this problem, we employed alternative detection methods based on the mobility shift of phospho-regulated proteins. In this case, the multi-site phosphorylation of Mer produces a specific pattern of Mer phospho-isoforms, which can be visualized on Western blots as two or three bands around the size of 75 kDa (Figure 5A, lane WT). Among the different phospho-isoforms, the hyper-phosphorylated isoforms migrate at a slower rate than the hypo-phosphorylated ones. Based on this principle, we measured the ratio of the two slower migrating hyper-phosphorylated Mer isoform bands to the faster migrating hypo-phosphorylated band using quantitative Western blot. The ratio obtained from the wild-type tissue was then compared to that of *flw* knockdown and *flw* overexpression.

To manipulate the expression level of *flw* in specific cells or and regions of the tissue, the UAS-Gal4 gene expression technique was used (Brand & Perrimon, 1993). In principle, the yeast transcription factor *Gal4* gene is placed under the

control of a *Drosophila* native gene promoter (*e.g.* gene A), while the Gal4 cognate *cis*-acting regulatory sequence UAS (upstream activating sequence) is fused to the target gene (*e.g.* gene B) (Duffy, 2002). In the organism, the Gal4 protein is only present in the gene A-expressing cells, where it binds to UAS and activates the transcription of gene B. Alternatively, micro-RNA (miRNA) or small interfering RNA (siRNA) specifically targeting gene B can be used to reduce or knockout the expression of gene B, respectively. This way, the expression level of gene B (*flw* in this case) can be up- or down-regulated in the desired cell types or tissues.

In the wing imaginal disc tissue where *flw* expression was reduced via RNAi-mediated knockdown (MS1096-Gal4 X UAS *flw*-IR), the ratio of hyper-phosphorylated versus hypo-phosphorylated isoform of Mer was significantly increased compared to that in the wild-type tissue (1.70 ± 0.12 standard error), indicating an elevated level of phosphorylation of cellular Merlin protein pool (Figure 5A, UAS-FlwIR). Conversely, when *flw* was over-expressed (MS1096-Gal4 X UAS *flw*) in the tissue, the ratio of hyper- to hypo-phospho Mer isoforms was decreased in relative to the wild type (0.73 ± 0.07 standard error), indicating a reduction of phosphorylation of Mer protein pool (Figure 5A, UAS-Flw). Therefore, the change in the pattern of Mer phospho-isoforms is in accordance with the change in the level of phosphatase activity of flw, as regulated by manipulating its cellular gene expression level.

In order to acquire the pattern of phospho-Mer isoforms with a higher resolution, and to confirm Mer phosphorylation in response to changing flw

expression level, we also carried out 2-D DIGE followed by Western blotting analysis. The spots representing phospho-Mer isoforms on the blot of Mer IPed using the wild-type tissue lysate were compared to that using the *flw*-overexpressing tissue lysate (Figure 5B). These spots were verified as Merlin-specific isoforms by determining the protein size as well as by immunoblotting using the Mer-specific antibody.

In total, four Mer-specific isoforms were detected using this approach, separated according to their distinct isoelectric points supposedly resulted from the difference in their phosphorylation state (Figure 5B). The spot volume of each Mer-isoform signal was quantified and the volume was compared for each of the four spots between the wild type tissue sample and the tissue where *flw* was over-expressed (Figure 5C). A volume ratio was then calculated to represent the difference in the volume of Mer-isoform spots in the two genotypes. The volume ratios of the most hyper-phosphorylated Mer isoform (Figure 5C and D, spot a) were similar between the two genotypes. However, the relative volumes of the other three more hypo-phosphorylated Mer isoforms (Figure 5C and D, spots b, c and d) were greater in the tissue where *flw* was over-expressed compared to the wild type. Therefore, *flw* overexpression led to a reduction in the level of Mer phosphorylation.

To confirm the changes in gene expression of *flw* in the different genotypes, quantitative RT-PCR was used to determine the relative amount of *flw* mRNA level. Compared to the wild-type control, the mRNA level of *flw* in MS1096-Gal4 X UAS *flw*-IR was reduced by 92.9% (± 0.0017 standard error), whereas

in the tissue over-expressing *flw*, the level was increased by 150.4 fold (± 0.5213 standard error).

To confirm that the observed change in the pattern of Mer isoforms was a direct reflection of the change in their phosphorylation state, half of the Mer IP lysate was treated with the lambda phosphatase, a bacterial phosphatase with activity towards phospho-serine, threonine and tyrosine residues. Compared to the mock treated lysate, the phosphatase-treated sample exhibited on the immunoblot a significant increase in the signal representing the least phosphorylated Mer isoform, and a decrease in the remaining signals of the more phosphorylated isoforms (Figure 5E). Thus, addition of the lambda phosphatase caused an overall shift in the Mer isoforms toward the more hypo-phosphorylated state, a result similar to that shown in the tissue of *flw* overexpression as described above. This indicates that the four Mer-specific spots indeed represented different phospho-specific isoforms. Altogether, the data suggest that over-expressing *flw* was responsible for causing increased hypo-phosphorylation of Mer.

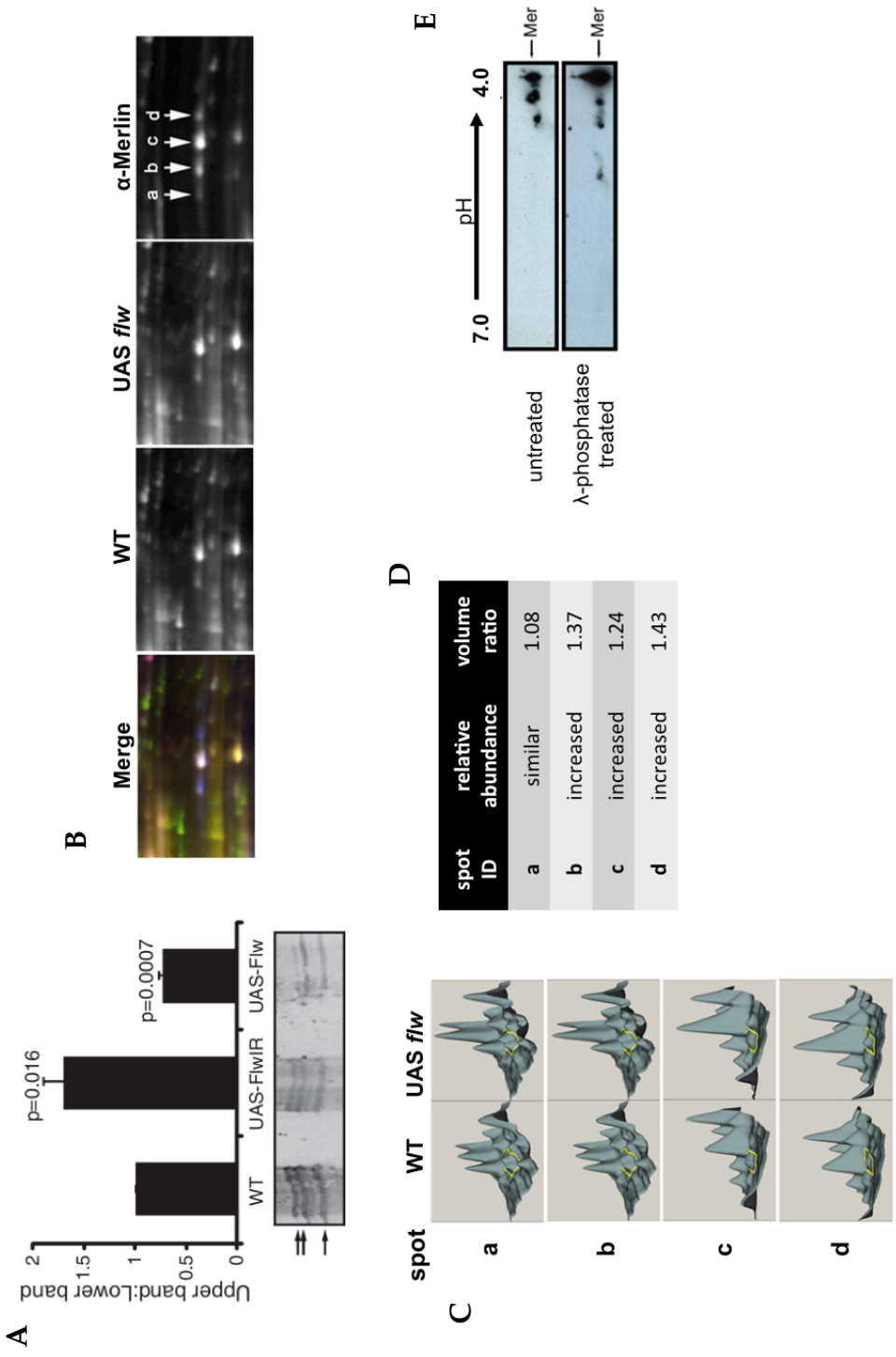
A
Upper band:Lower band
2
1.5
1
0.5
0
p=0.016
p=0.0007
WT
UAS-FlwIR
UAS-Flw
B
Merge
WT
UAS fiw
α-Merlin
a b c d
C
spot
WT
UAS fiw
a
b
c
d
D
spot ID
relative abundance
volume ratio
a
similar
1.08
b
increased
1.37
c
increased
1.24
d
increased
1.43
E
7.0
pH
4.0
Mer
Mer
untreated
λ-phosphatase treated

Figure 5 | Changes in phosphorylation of Mer in response to changing *flw* expression level. (A) Fly crosses in which the expression level of *flw* was either reduced by *ds*mRNA-mediated knockdown (UAS-*Flw*IR) or enhanced (UAS-Flw) in the wing, using the MS1096-Gal4 driver. Lysates of the third-instar wing imaginal disc tissue were used for the IP and anti-Mer antibody was used for detecting different isoforms of Mer on the Western blots. The ratio of the relative intensity of the two upper (hyper-phosphorylated) Mer-isoform bands to the (hypo-phosphoryalted) lower bands was calculated and normalized to the wild type tissue. Reduced flw expression resulted in an increase in the proportion of the hyper-phosphorylated Mer isoforms (1.70 ± 0.12 *SD*), whereas *flw* overexpression corresponded to a decrease in the ratio of hyper-phosphorylated isoforms (0.73 ± 0.07 *SD*). **(B)** Four Mer isoforms were detected in total by 2D DIGE/Western blot using the wild-type (WT) and *flw* overexpressing (UAS Flw) imaginal wing disc tissues. These four signals (spot a, b, c and d) were verified as Mer-specific by Western blotting using anti-Mer antibody. **(C)** 3-dimensional graphic representation of the volume of the Mer isoform signals a-d in the *flw* overexpressing tissue as compared to that in the wild type. **(D)** Comparison of the volume ratio of signals a-d in the two genotypes. Compared to the wild type, the three less phosphorylated isoforms (spots b, c and d) showed increased abundance when *flw* was overexpressed. **(E)** Changes in the pattern of Mer isoforms were due to change in the phosphorylation state of Mer. Half of Mer-IP lysate was treated with lambda phosphatase. After the treatment, there was an increase in the relative abundance of the most phosphorylated Mer isoform, compared to the untreated sample.

2.2. *Changes in flw Expression Level Lead to Corresponding Changes in Moe Phosphorylation Pattern*

In the next step, we determined whether changing the expression level of flw also led to changes in phosphorylation of Moe. The relative amount of total and phosphorylated Moe from the tissue lysate, in which *flw* expression was either reduced or enhanced, was compared to that of the wild type (Figure 6). The total Moe protein level, as detected by using a pan-Moe antibody, was unchanged when *flw* expression is reduced (Figure 6 panel A, UAS-flwIR, 1.03 ± 0.01 SE; $p = 0.29$) or enhanced (UAS-flw, 1.04 ± 0.03 SE; $p = 0.90$) as compared to the wild type (WT), indicating that the effect of changing flw expression on Moe is most likely at the post-translational level. In contrast, the relative amount of phospho-specific Moe was significantly decreased in the tissue sample where *flw* expression was reduced (Figure 6 panel B, 0.65 ± 0.04 standard error). When over-expressing *flw*, there was a significant increase in the relative amount of phospho-specific Moe compared to the wild type (1.43 ± 0.03 SE). Therefore, changing flw expression level resulted in the corresponding changes in the level of phosphorylated Moe, suggesting that, similar to the effect of *flw* on Mer phosphorylation, *flw* is one of the phosphatases responsible for phosphorylation of Moe.

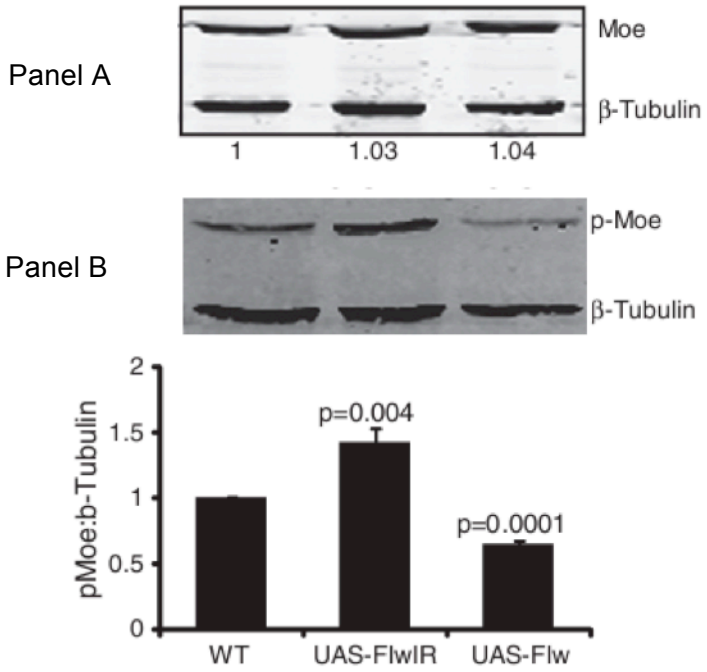

Figure 6 | Changes in phosphorylation of Moe in response to changing *flw* expression level. Genetic crosses in which the expression level of flw was either reduced by *ds*mRNA-mediated knockdown (UAS-*Flw*IR) or enhanced (UAS-*Flw*) in the wing, using the MS1096-Gal4 driver. Lysates of the third-instar wing imaginal disc tissue were used for the IP. A pan-Moe and a phospho-Moe antibody were used to detect the total level and the phospho-specific form of Moe on the Western blots, respectively. Neither up- or down-regulation of flw expression caused a significant change in the amount of total (both phosphorylated and non-phosphoryated) Moe, compared to the wild type. The changes were normalized to the loading control beta-Tubulin and displayed as numbers directly below the Western blot. Reduced *flw* expression led to an increase in level of the phosphor-specific Moe, whereas *flw* overexpression resulted in a decrease in the level of the phosphorylated Moe. The changes in the ratio compared to the wild type were graphed below the Western blots.

3. Reduced flw Expression Caused Altered Mer and Moe Subcellular Localization in Epithelia

3.1. Reduced flw Expression Led to Increased Plasma membrane Localization of Mer

A previous study suggested that in *Drosophila*, the phosphorylated form of Mer was more tightly associated with the plasma membrane of the cell (Hughes & Fehon, 2006). Therefore, if *flw* regulates dephosphorylation of Mer, changing *flw* expression level would cause a corresponding change in the plasma membrane localization of Mer.

To test this idea, epithelial cells of the *Drosophila* imaginal discs were used to determine the change of subcellular localization of Mer and Moe upon changing *flw* expression level. The *Drosophila* imaginal discs are small groups of cells set aside during embryogenesis. These cells proliferate during larval development to form folded, single-layered epithelial sacs. Upon pupal formation, the imaginal disc cells cease dividing and begin to differentiate into structures that give rise to wings, legs, antennae, and other corresponding parts of the adult animal. The wing imaginal disc, which is composed of a monolayer of tall, columnar epithelium and a membrane of large, squamous peripodial cells situated apically to the epithelium, is an excellent model for studying the maintenance of cell adhesion, polarity and organization in the mature, differentiated epithelial cells (Figure 7B). Morphogenetically, a wing disc is divided into the anterior (A) and posterior (P) compartments by the A-P boundary and the dorsal (D) and ventral (V) compartments by the D-V boundary (Figure 7A). Although there is no apparent morphological structure associated with the boundaries, each

compartment at the larval stage defines a restricted area of cells destined to become a specific part of the adult wing. For example, the D-V boundary correlates with the wing margin between the dorsal and ventral surfaces of the adult wing, whereas the A-P boundary runs as a straight line between the vein L3 and L4.

We used a *patched*-Gal4 driver to knock down and overexpress *flw* specifically in a vertical strip of 8 – 10 columnar epithelial cells at the anterior-posterior boundary of the developing larval wing disc (Figure 7D, Figure 8). The efficacies of changing *flw* expression were assessed by real-time quantitative PCR. When the double-stranded RNA targeting *flw* was expressed in the *ptc*-expressing tissue, there was an average reduction in the *flw* transcript level by 81.1% (± 0.03 standard error) compared to the wild-type control (data not shown). In contrast, over-expressing *flw* in the *ptc*-expressing domain led to an elevated level of *flw* transcripts 50.8 folds of the wild type (± 0.18 standard error).

In the cells where *flw* expression was enhanced, no significant change in the subcellular localization of Mer was observed and the epithelial tissue morphology of the affected region was indistinguishable from the remaining regions where cells expressed normal level of endogenous *flw* (Figure 9). However, when *flw* expression was reduced, the region of affected tissue exhibited prominent epithelial deformation as the strip of apically located epithelial cells were pulled basally, resulting in the formation of a 'ripped hole' phenotype along the anterior-posterior boundary of the wing disc, as

outlined by the apical cell-membrane markers Mer and DE-Cadherin (Figure 10, A'-L').

To determine whether the subcellular localization of Mer was different from the wild-type in the epithelial cells with reduced *flw* expression, a stack of single confocal sections of the whole wing disc was acquired to obtain a complete orthogonal view of the cells surrounding the epithelial deformation. Comparison of the orthogonal views of the epithelial cells was made between the site of deformation where *flw* expression was knocked down using the *patched*-Gal4 driver (Figure 10, orthogonal 3), the natural folding of two opposing epithelial surfaces of the wild-type *patched*-expressing wing disc (Figure 10, orthogonal 1), and the natural folding of non-*patched* expressing cells (Figure 10, orthogonal 3). Compared to the two latter cases where in both endogenous *flw* expression level remained unaffected, the cells where *flw* expression was reduced showed a brighter intensity of immunostaining of both Mer as well as DE-Cadherin, particularly at the apical plasma membrane forming the pit of deformation (Figure 10, 3a and 3b). Thus, reducing *flw* expression led to the increased plasma membrane localization of Mer.

Because knocking down *flw* expression in the narrow strip of *patched*-expressing cells resulted in such a drastic deformation phenotype that caused the affected epithelial cells to be pulled toward the basal wing surface and organize more tightly in the local disc region, a concern was that the brighter than wild-type staining intensity of Mer might be due to the tighter organization of the cells at the site of deformation, since the signals of immunofluorescence microscopy cannot be quantified without the presence

of an appropriate reference signal. In order to eliminate the possibility of potential artefacts, as well as to confirm the previously observed phenotype of changes in Mer immunostaning, *flw* was knocked down using another driver, *apterous*-Gal4, which is expressed in the dorsal surface of the larval wing imaginal disc (Figure 7C). When *flw* expression was reduced in the epithelial cells of the disc dorsal surface, a similar deformation phenotype was observed particularly in close proximity to the dorsal-ventral (D-V) boundary of the wing disc, albeit the formation of a larger and shallower 'pit' (Figure 11, E-H). More importantly, in the cells located on the dorsal side of the D-V boundary, there was an apparent increase in the plasma membrane localization of Mer in response to the reduced *flw* expression (Figure 11J), as compared to the cells on the ventral side where *flw* expression was unaffected (Figure 11K), or to the cells on the dorsal side of the wild-type wing disc (Figure 11I). Taken together, this suggests that reduction in *flw* expression result in an increase in the recruitment of Mer to the plasma membrane.

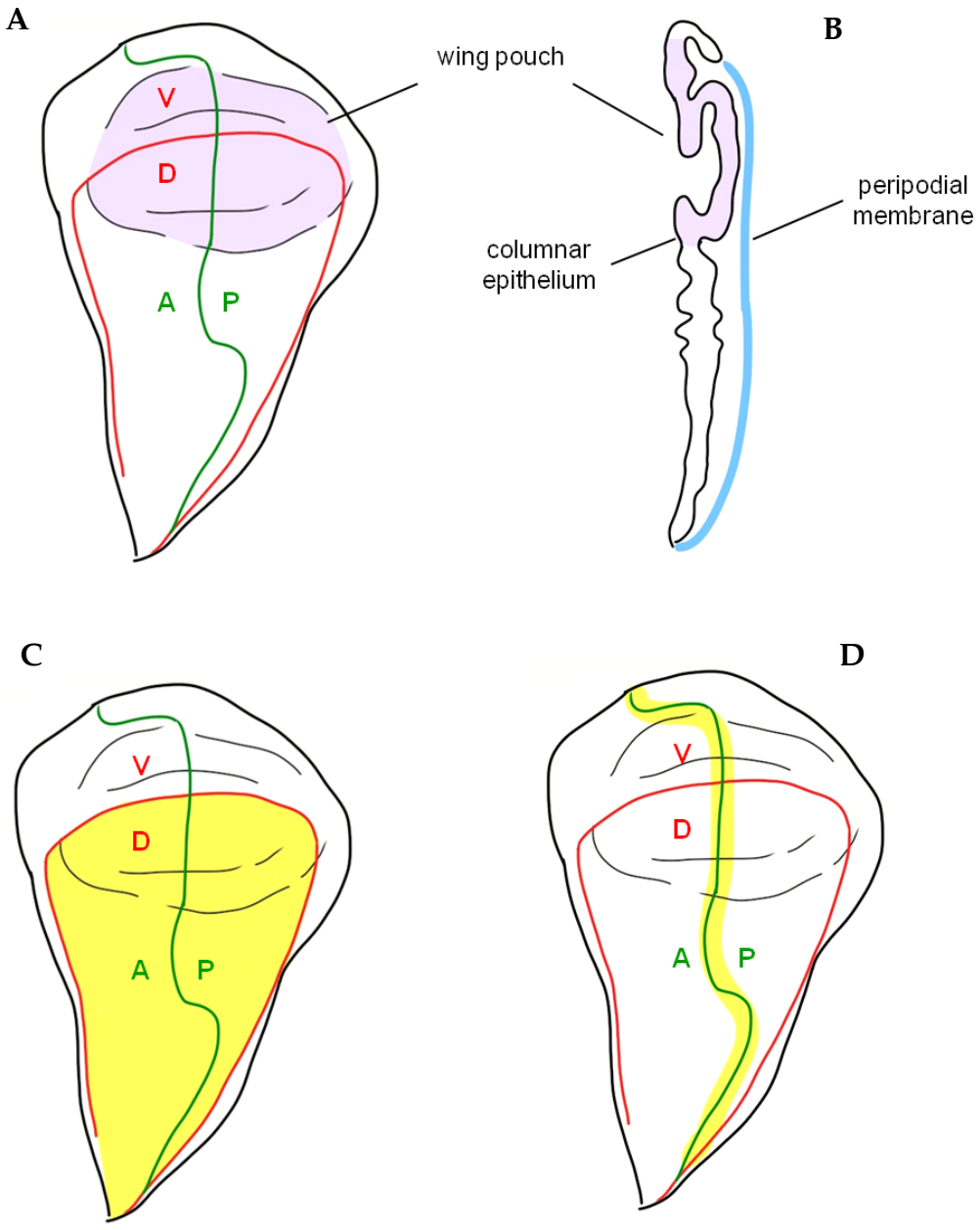
A
V
D
A
P
wing pouch
B
peripodial
membrane
columnar
epithelium
C
V
D
A
P
D
V
D
A
P

Figure 7 | Composition of *Drosophila* wing imaginal disc and expression of Gal4-drivers in the larval wing disc. (A) Fate map of the *Drosophila* third instar larval wing imaginal disc showing the anterior-posterior (A-P) and dorsal-ventral (D-V) compartment boundaries. The wing pouch (pink) gives rise to the wing blade in the adult. **(B)** Two cell layers of the wing disc: the squamous peripodial membrane (blue) and the tall columnar epithelium. **(C)** Expression domain of *apterous*-Gal4 (yellow). **(D)** Expression domain of *patched*-Gal4 (yellow).

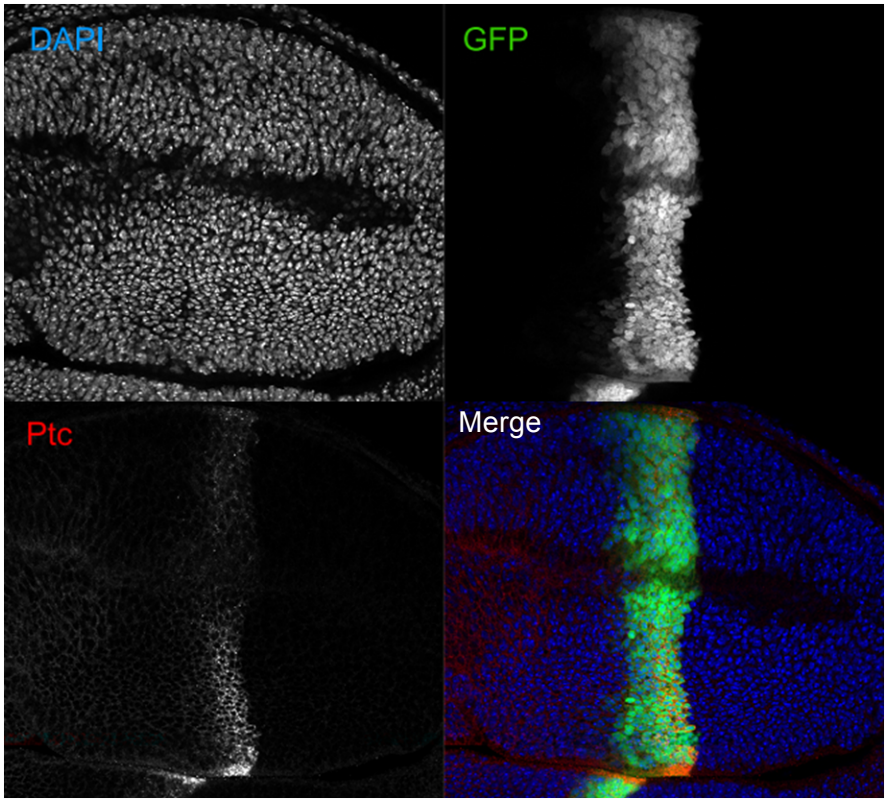

Figure 8 | Expression of *ptc*-Gal4 in the wild-type larval wing disc. Imaginal wing discs of the wandering third instar larvae of *patched*-Gal4 X UAS-GFP were dissected and examined for the pattern of endogenous *patched* expression by anti-Patched antibody and GFP-positive cells. GFP was expressed in a strip of epithelial cells along the anterior-posterior boundary of the wing disc. DAPI was used for the nuclear staining. Except indicated otherwise, all discs are oriented with the anterior compartment to the left and the ventral compartment to the top.

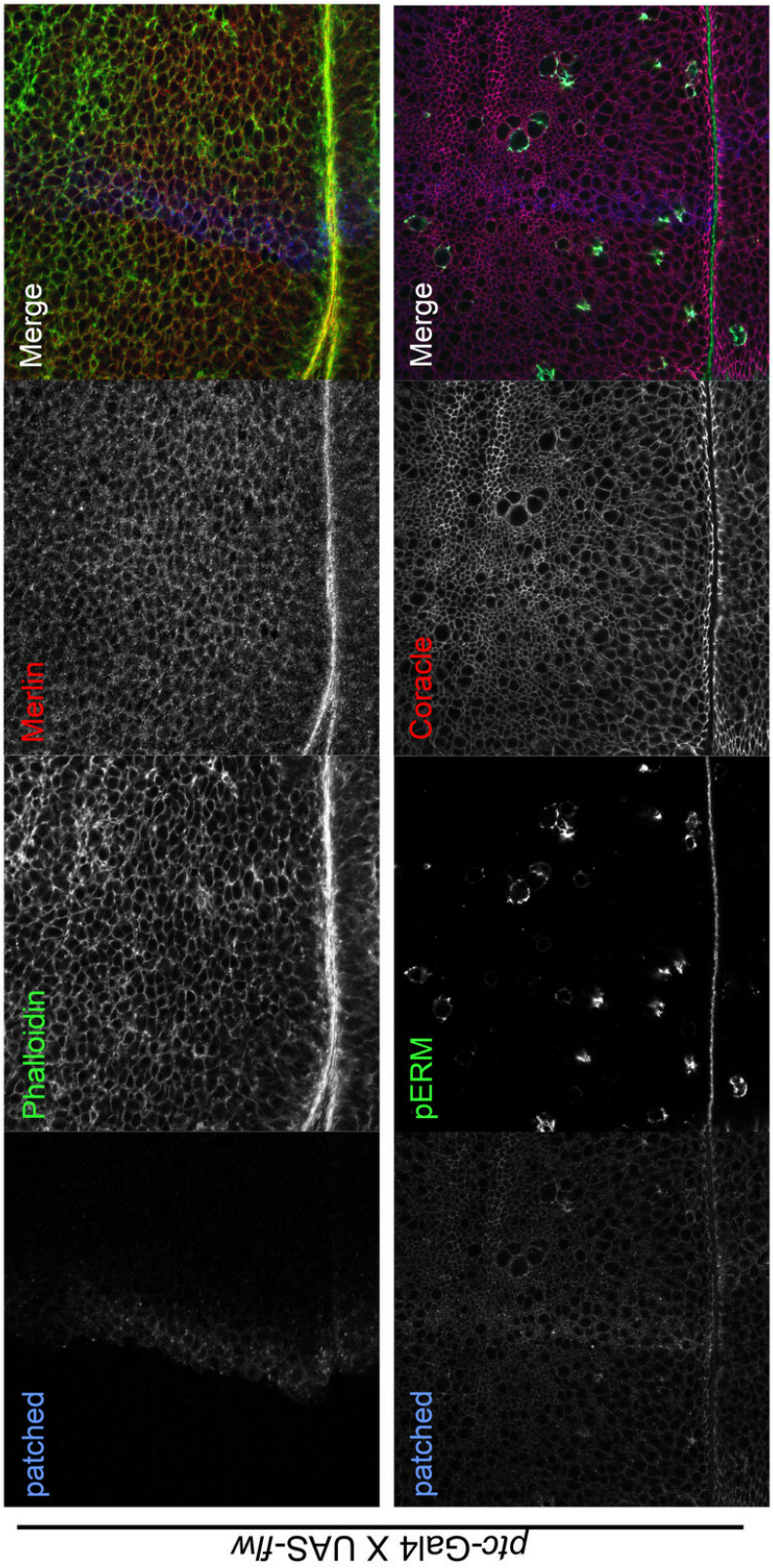
Merge
Merge
Merlin
Coracle
Phalloidin
pERM
patched
patched
ptc-Gal4 X UAS-flw

Figure 9 | Over-expression of wild-type *flw* caused no discernible phenotype in the wing disc epithelial morphology. Wing imaginal discs of the wandering third instar larvae were examined for change of localization of components of junction complexes and epithelial integrity. Over-expressing *flw* in cells within the *ptc*-expressing domain (blue) did not lead to any detectable changes in the subcellular localization of Mer (red) or pERM (green). Cells overexpressing *flw* looked morphologically similar to the remaining area where *flw* expression level was unaffected, as visualized by apical membrane marker F-actin (Phalloidin, green) and baso-lateral membrane marker Coracle (red).

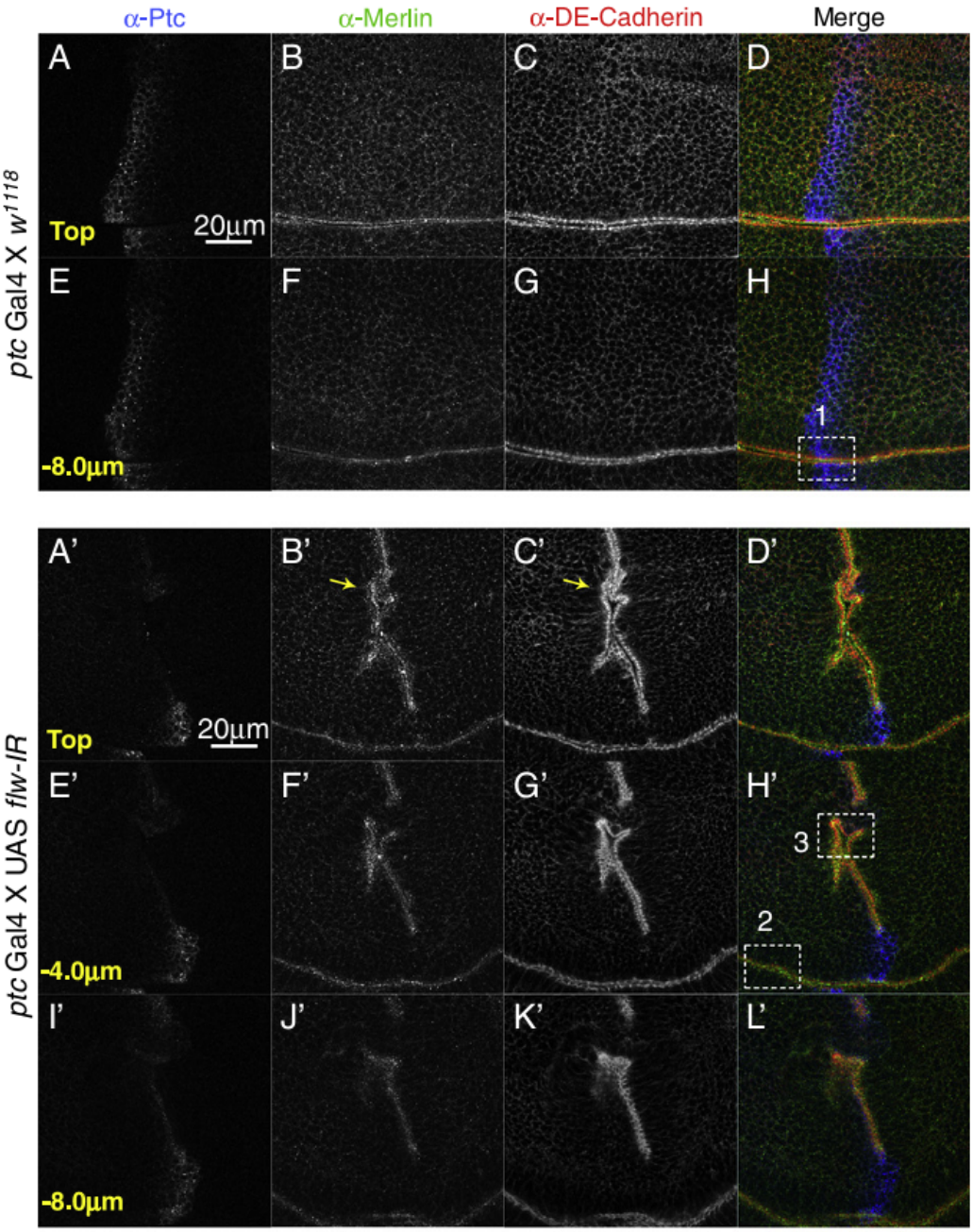
α-Ptc
α-Merlin
α-DE-Cadherin
Merge
ptc Gal4 X w1118
ptc Gal4 X UAS flw-IR
A
B
C
D
Top
20µm
E
F
G
H
-8.0µm
1
A'
B'
C'
D'
Top
20µm
E'
F'
G'
H'
3
2
-4.0µm
I'
J'
K'
L'
-8.0µm

Figure 10 A-L′

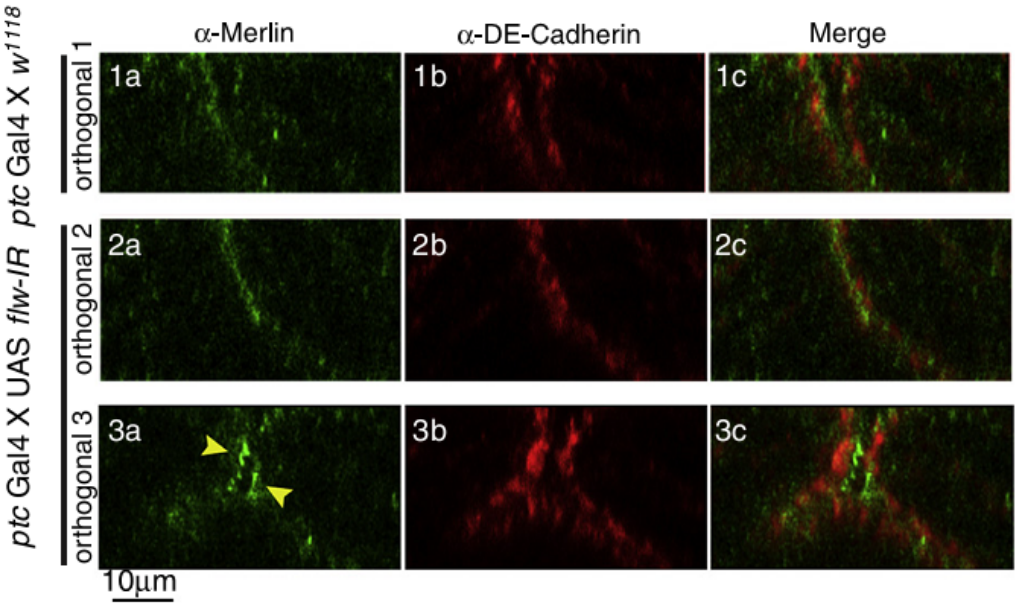

Figure 10 1a-3c

Figure 10 | Reduction in *flw* expression resulted in increased Mer localization at the apical plasma membrane and epithelial deformation of the wing disc. (A-H) Wing imaginal discs of the wandering third instar larvae where *flw* expression was unaffected (*ptc*-Gal4 X w^{1118}) were dissected and immunostained for patched (blue), Merlin (green) and DE-Cadherin (red). Images of the top and 8.0 μm below apical surface (8.0 μm) were shown to visualize the epithelial organization of various depths of the wing disc. Staining of Mer (B, F) and DE-Cadherin (C, G) of the strip of cells expressing patched (A, E) was similar to that in surrounding tissue both at the apical surface and 8 μm below surface. (A'-L') Wing discs where *flw* expression was reduced (*ptc*-Gal4 X UAS *flw*-IR) were examined at various depths (top, -0.4 μm, -0.8 μm). The epithelium at the *ptc*-expressing strip (A', E', L') was severely deformed (arrow). There was a marked increase in the signal intensity of the Mer (B', F', J') and DE-Cadherin (C', G', K') staining in these cells where *flw* was knocked down. **(1a-3c)** Orthogonal sections obtained at box 1 in H, or box 2 in H' are through a natural fold in the wing disc where two apical surfaces come apposed. Orthogonal section at box 3 in H' showed deformed epithelium where *flw* expression was reduced. Both Mer and DE-Cadherin staining intensity was increased at the apical plasma membrane in these cells.

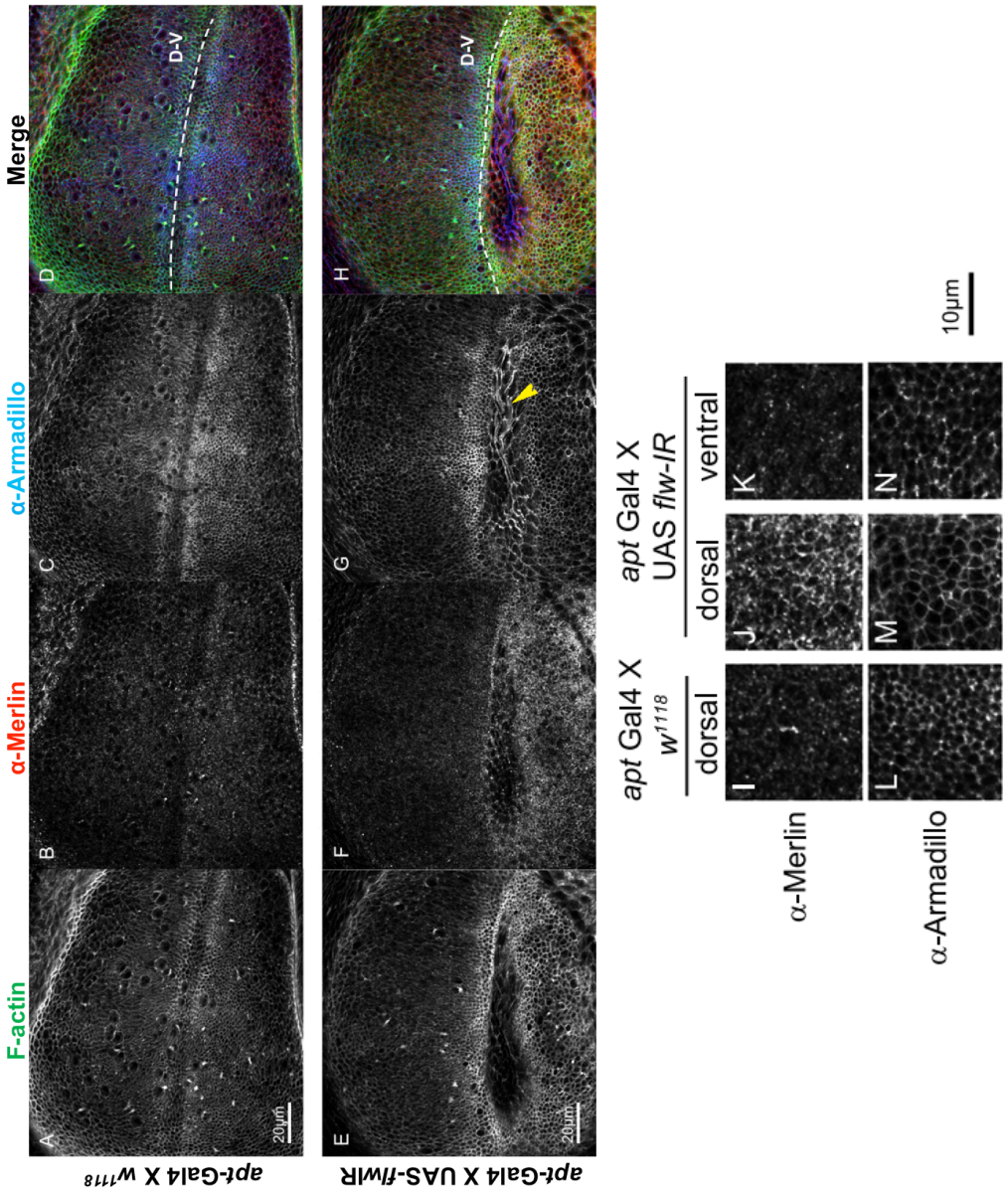
F-actin
α-Merlin
α-Armadillo
Merge
A
B
C
D
D-V
20µm
apt-Gal4 X w1118
E
F
G
H
D-V
20µm
apt-Gal4 X UAS-flwIR
apt Gal4 X w1118
apt Gal4 X UAS flw-IR
dorsal
dorsal
ventral
I
J
K
L
M
N
α-Merlin
α-Armadillo
10µm

Figure 11| Reduction in *flw* expression resulted in increased Mer localization at the plasma membrane. (A-D) Wing imaginal discs of the wandering third instar larvae where *flw* expression was unaffected (*apt*-Gal4 X w^{1118}) were dissected and labeled for membrane markers F-actin by Phalloidin (green), Merlin (red) and Armadillo (blue). Epithelial cells on the two sides of the anterior-posterior (D-V) boundary showed comparable shape, structure and staining intensity for all three markers. **(E-H)** In the wing discs of the animal where *flw* expression was reduced, deformation was observed in the dorsal epithelial cells in close proximity to the DV-boundary. Large, squamous peripodial cells, outlined by the Armadillo staining, (G, arrowhead) were pulled into the disc tissue. **(I-N)** In the cells of the dorsal side, there was a marked increase in the localization of Mer to the plasma membrane, as compared to the ventral side of the same wing disc or to the dorsal side of the wild-type disc. The membrane localization of the other marker, Armadillo, remained largely unchanged between the dorsal and ventral side of the D-V boundary and compared to the wild-type tissue.

3.2. Reduced flw Expression Led to Increased Plasma membrane Localization of Moe

Previously, studies using mammalian cells demonstrated that dephosphorylated ERM proteins (mammalian orthologues of *Drosophila* Moesin) were less associated with the plasma membrane, whereas a phosphomimetic form of Moesin or its related protein Ezrin were more membrane-associated (Hao et al, 2009). Thus, similar to the membrane-localization of phospho-Mer, it was postulated that *flw* knockdown would result in the increased membrane-localized phosphorylated Moe in the cell.

As expected, in cells where *flw* expression was reduced in the larval wing disc, a bright staining of phosphorylated Moe (pERM) (Figure 12E) was observed on the cell membrane along the strip of *ptc*-expressing cells (Figure 12D). The fold formed by the two opposing apical surfaces of the epithelial cells along the strip was stained for phosphorylated Moesin (pERM) at a much brighter overall maximum projection intensity (Figure 12F, yellow arrow), as compared to the natural fold at the region with unaffected level of *flw* expression (Figure 12F, white arrow) or in the wild-type wing disc (Figure 12C). This indicates that reduced *flw* expression caused increased level of phosphorylated Moe and its recruitment to the plasma membrane.

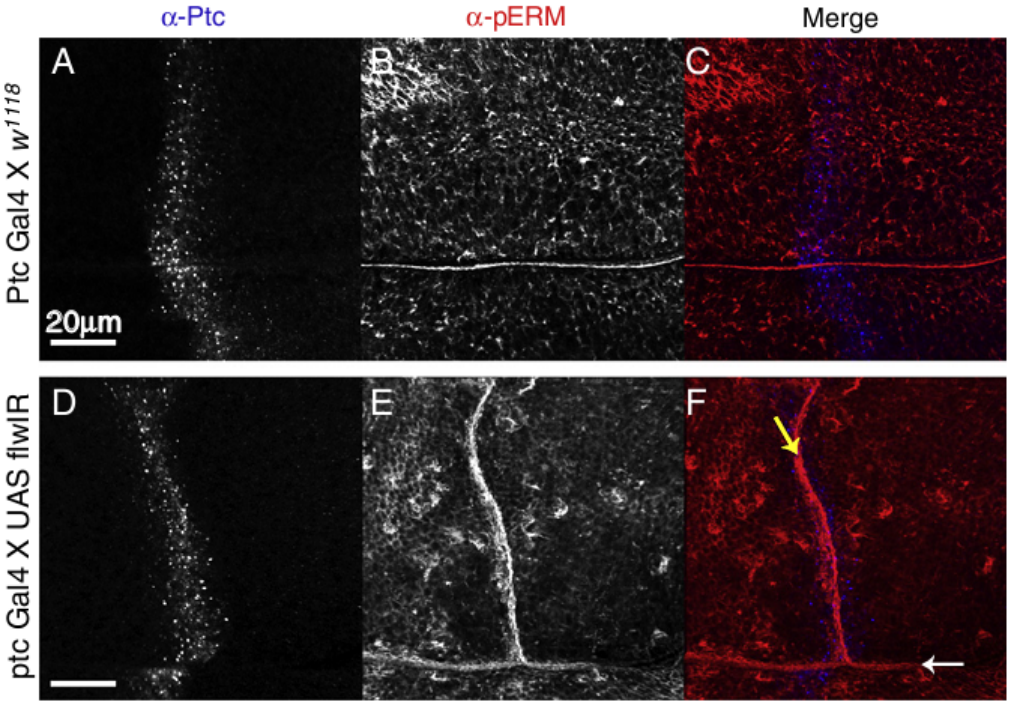

Figure 12 | Reduction of *flw* expression caused increased phosphorylated Moe and its localization to the plasma membrane. (A-C) A maximum intensity projection of the wing disc of a *ptc*-Gal4 X w^{1118} larva. The disc was immunostained for patched (blue) and phosphorylated-Moesin (pERM, red). (D-F) A maximum intensity projection of the wing disc of a *ptc*-Gal4 X UAS *flw*-IR larvae. The pERM staining of the folding resulted from epithelial deformation of the apical surface was brighter (F, yellow arrow) compared to the nature folding where *flw* expression was unaffected (F, white arrow).

4. *Reduction in flw Expression Results in Disruption of Epithelial Integrity and Polarity*

The prominent deformation of the disc epithelia resulting from reduced *flw* expression was intriguing, and I was interested in finding out whether the epithelial defects became more severe at a later developmental stage. In the wing imaginal disc during the transition from the larval to pupal stage, the epithelial integrity was further deteriorated, leading to the formation of large holes in the apical surface of the disc within the area of cells where *flw* expression was reduced. In the prepupal wing disc where *flw* was knocked down using the *ptc*-Gal4 driver, the disc epithelium was devoid of cells on the top section of the apical surface, as illustrated by the lack cell nuclei indicated by DAPI staining (Figure 13Q', dashed line) and cell membrane markers (Figure 13A'-D', dashed line). However, sections taken deeper below the top revealed the presence of clustered cells with increased brightness of staining for F-actin and Armadillo on the cell membrane (Figure 13 E' and F'), as compared to the adjacent cells, where *flw* expression remained unaffected (Figure 13 E and F). The cluster of cells, particularly those of which F-actin and Armadillo staining was accumulated on the cell membrane (Figure 13E' and F'), exhibited a round cell shape as compared to their columnar wild-type control counterpart (Figure 13 E and F). In addition, merged images of staining for membrane markers showed that the alternation in the cell shape upon *flw* expression knockdown was accompanied with partial co-localization of apical membrane markers (F-actin, Armadillo) and the septate junction marker (Coracle) (Figure 13L', arrowheads), suggesting the typical

polarity of the epithelial cells was drastically disrupted. Thus, reduced *flw* expression resulted in more severe epithelial defects in the developing tissue including altered cell shape and loss of epithelial cell polarity.

The similar phenotype of altered cell shape and loss of cell polarity was also observed in the larval wing discs where *flw* expression was reduced on the entire dorsal side of the D-V boundary using the *apt*-Gal4 driver (expressed in the dorsal region of the wing disc, Figure 7C). In the wild-type tissue, the phosphorylated, active Moe (anti-pERM) is normally found as a component of the apical junctions of the epithelial cell membrane (Hipfner et al, 2004; Hughes & Fehon, 2006). Accordingly, in the wing disc where *flw* expression was unaffected, the staining of phospho-Moe was only detected in the image showing the apical section of the epithelial layer (Figure 14A), but absent in the more basolateral section of the epithelium, except for the small subset of actively dividing cells (Figure 14D). In contrast, in the wing disc with reduced *flw* expression, abnormally large, round epithelial cells with occasional blebbing were found to cover the dorsal side of the disc at deeper sections below the apical surface, as illustrated by staining the cell membrane using anti-pERM (Figure 14D' and G') and anti-Coracle antibodies (Figure 14 E' and H'). On the ventral side of the boundary, round cells with positive phospho-Moe staining were also detected but with a much lower density. The majority of phospho-Moe positive cells were concentrated to close proximity in the D-V boundary, possibly representing the dorsally originated epithelial cells that had dispersed across the boundary due to altered motility. Again, phospho-Moe and Coracle, the two components of junction complexes which typically

have distinct subcellular localizations were found to partially co-localize, and accumulated as brightly stained puncta on the cell membrane in some of the cells on the dorsal side of the wing (Figure 14 F′ and I′ arrowheads), indicating the loss of epithelial cell polarity associated with a change in cell shape and adhesive properties.

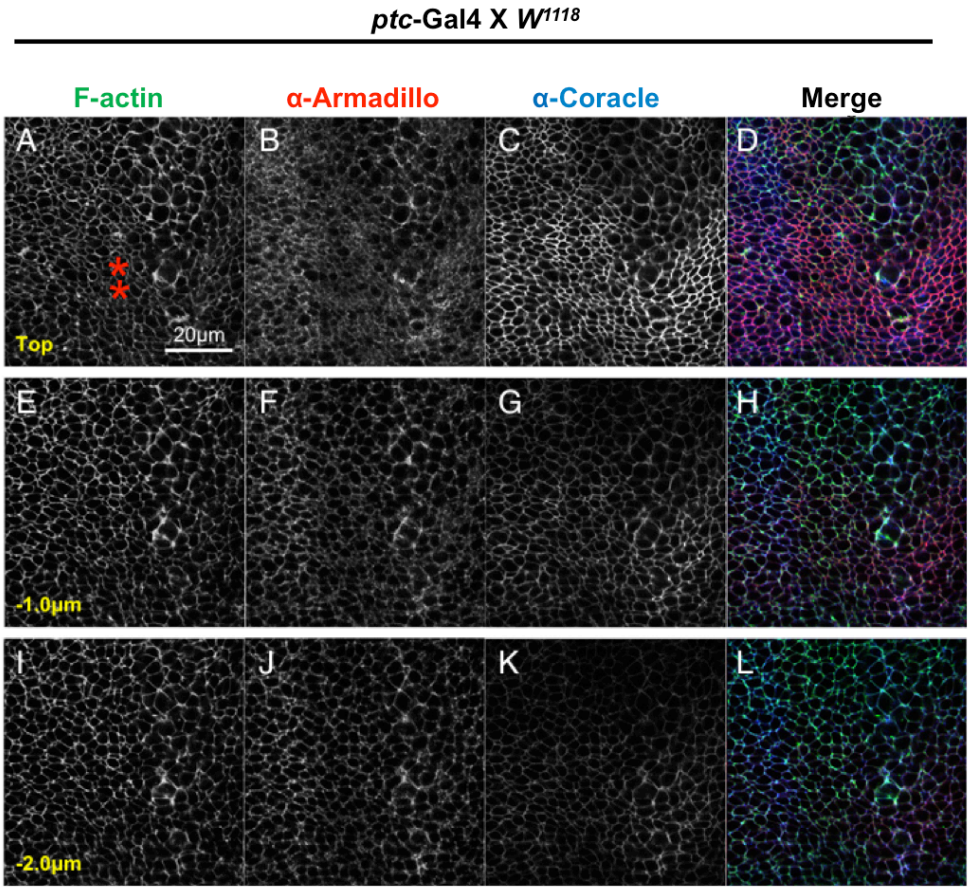
ptc-Gal4 X W1118
F-actin
α-Armadillo
α-Coracle
Merge
A
B
C
D
Top
20μm
E
F
G
H
-1.0μm
I
J
K
L
-2.0μm

Figure 13 (A-L)

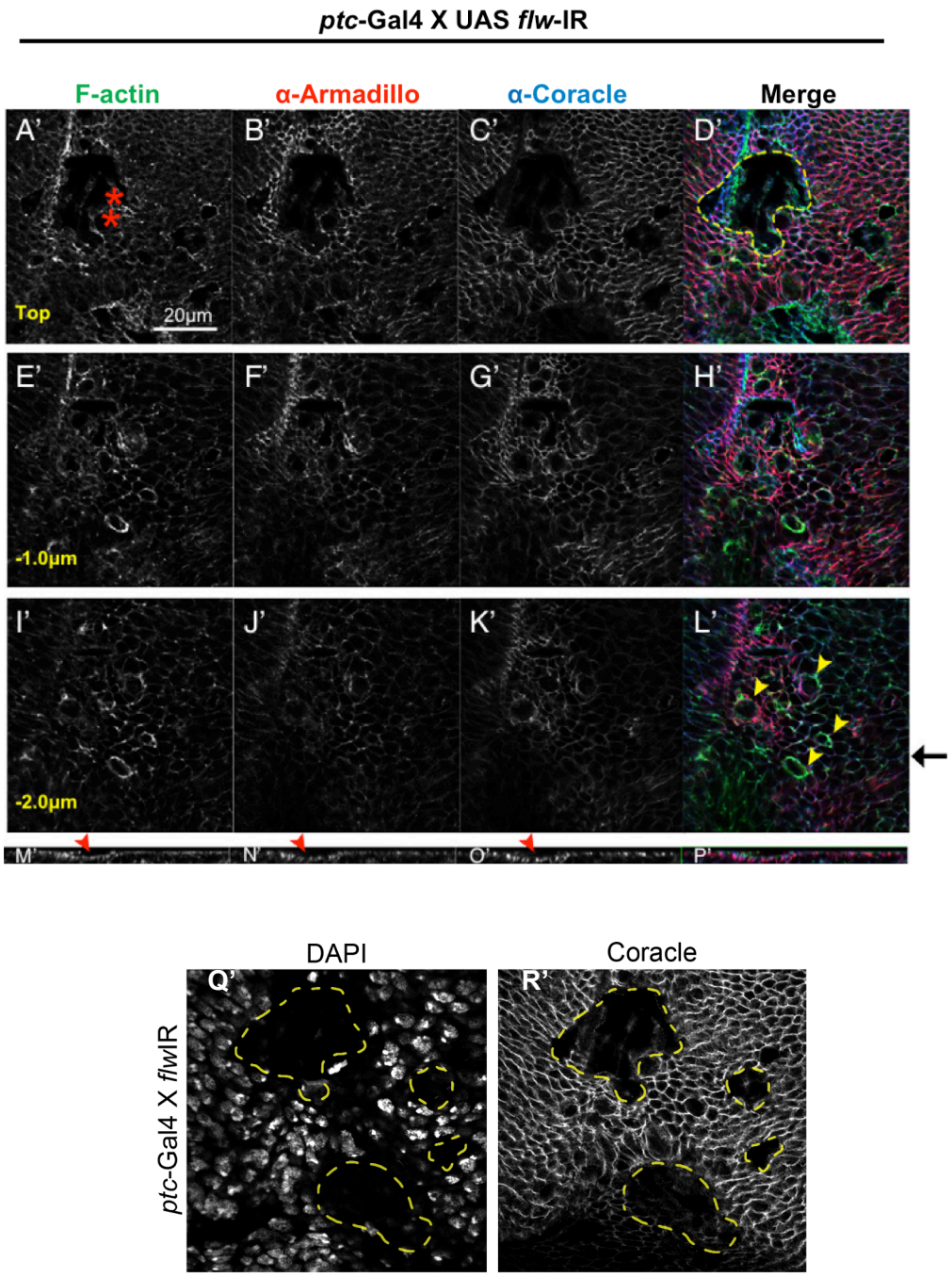
ptc-Gal4 X UAS flw-IR
F-actin
α-Armadillo
α-Coracle
Merge
A'
B'
C'
D'
Top
20μm
E'
F'
G'
H'
-1.0μm
I'
J'
K'
L'
-2.0μm
M'
N'
O'
P'
DAPI
Coracle
Q'
R'
ptc-Gal4 X flwIR

Figure 13 (A′-R′)

Figure 13 | Reduced *flw* expression led to formation of holes on the apical surface of pre-pupal wing disc and loss of epithelial polarity. (A-L) Imaginal wing discs from 10h pupae of the control wild type (*ptc*-Gal4 X w^{1118}) were dissected and examined for staining of F-actin (green), Armadillo (red) and Coracle (blue). The domain of *ptc*-expressing cells was labeled with asterisks. Single confocal sections of the apical surface of the disc (A-D), 1 μm (E-H) and 2 μm below the apical surface showed even intensity of staining of all examined markers. **(A'-L')** In the 10h pupal wing disc with reduced *flw* expression in the *ptc*-expressing cells (*ptc*-Gal4 X UAS *flw*-IR), the apical surface on the top (top) was devoid of cells (D', dashed line). Cells in the deeper confocal sections taken 1 μm and 2 μm below the top had brighter staining F-actin (E', I') and Armadillo (F'). Some cells exhibited a round shape, with mis-localized F-actin and Armadillo staining that partially over-lapped with Coracle on the cell membrane (L', arrowheads). **(M'-P')** Orthogonal sections taken perpendicular to the *ptc* expression domain at the designated point (black arrow) showed deformation of the epithelium on the apical surface (arrowheads). **(Q'-R')** Regions of disc epithelium at the apical surface which lack baso-lateral membrane marker Coracle are also devoid of nuclear staining by DAPI staining (dashed line).

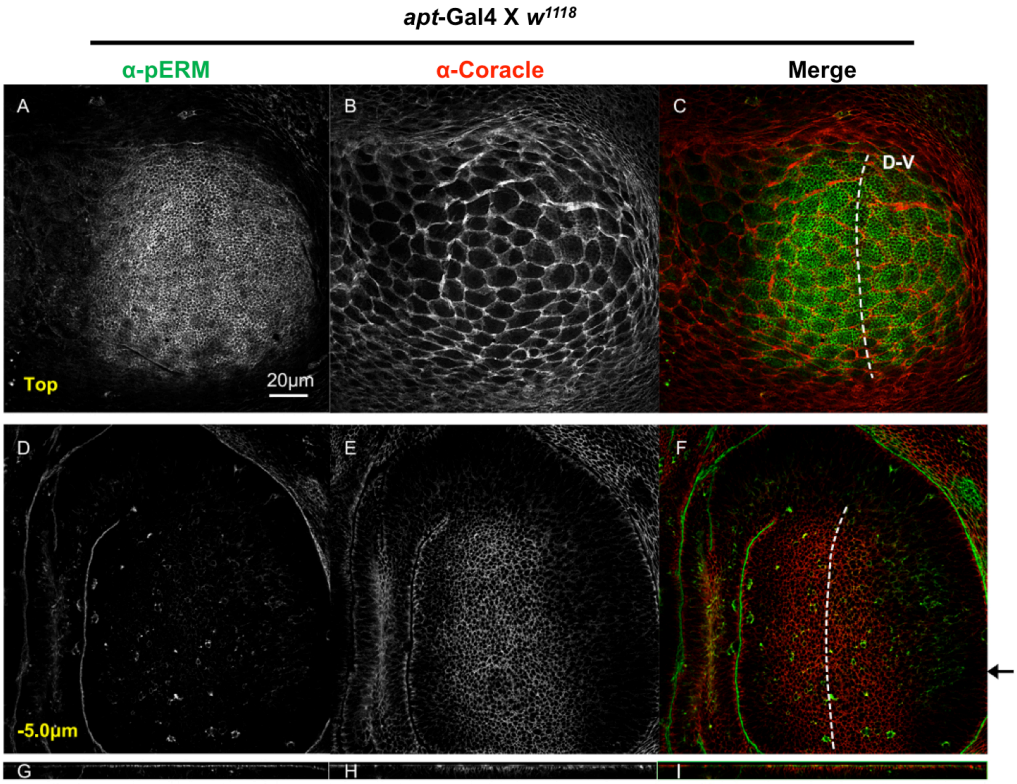
apt-Gal4 X w1118
α-pERM
α-Coracle
Merge
A
B
C
D-V
Top
20μm
D
E
F
-5.0μm
G
H
I

Figure 14 (A-F)

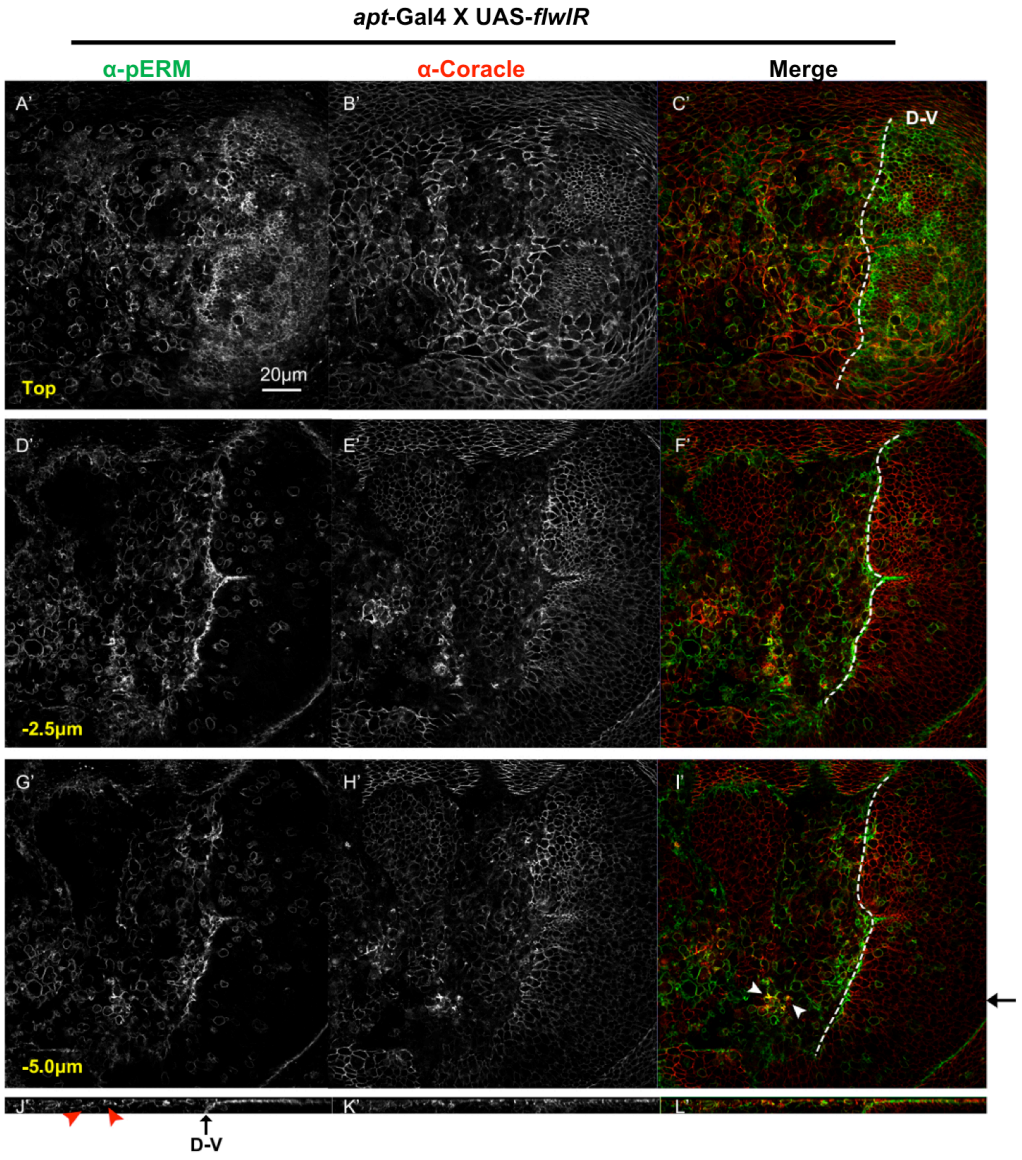
apt-Gal4 X UAS-flwIR
α-pERM
α-Coracle
Merge
A'
B'
C'
D-V
20μm
Top
D'
E'
F'
-2.5μm
G'
H'
I'
-5.0μm
J'
K'
L'
D-V

Figure 14 (A′-L′)

Figure 14 | Reduced *flw* expression in the dorsal side of the larval wing disc caused drastic disruption of cell polarity and alteration in cell shape. (A-I) Wandering third instar larval discs of wild-type control (*apt*-Gal4 X w^{1118}) were dissected and analyzed for staining of the apical membrane marker phospho-Moe (pERM, green) and the basolateral membrane marker Coracle (red). Discs are turned 90 degree clockwise, with dorsal compartment to the left and anterior to the top. (A) Single confocal section taken at the top of the apical surface of the disc showed enriched localization of phosphorylated, active Moe on the apical membrane of the epithelial cells. (B) anti-Coracle staining visualized the basal membrane of the large peripodial cells situated directly above the epithelium. (D) A deeper section taken 5 μm below the top showed little phospho-Moe staining, except for the scattered pattern of actively dividing cells. (E) anti-Coracle staining of the columnar epithelial cells. (C, F) The staining of pERM and Coracle are consistent in cells on both sides of the D-V boundary (dashed line). (G-I) An orthogonal view of the disc indicated a normal intact epithelial, with the phospho-Moe staining situated apically to the Coracle staining on both sides of the D-V boundary. **(A'-L')** Larval wing disc in which *flw* expression was reduced at the dorsal side of the D-V boundary (*apt*-Gal4 X UAS *flw*-IR). Confocal sections taken 2.5 μm and 5 μm below the top of the disc apical surface showed bright membrane staining of phospho-Moe in many basally situated epithelial cells on the dorsal side of the D-V boundary (D', G'). These cells exhibited a round shape, in which staining of phospho-Moe and Coracle partially co-localized as bright spots on the cell membrane (F, I, arrowheads). (J'-L') An orthogonal view of the wing disc with large deformation of the epithelia of the apical surface (J', arrowheads). phospho-Moe was mis-localized in relation to the Coracle staining on the dorsal side of the D-V boundary (L').

5. *The Alterations of Other Junction Complex Components by Reduced flw Expression*

So far the data suggest that reduction in *flw* expression resulted in increased plasma membrane association of Mer and Moe and led to disrupted epithelial integrity. The next question I asked was whether reduced *flw* expression also affected other proteins in the junction complexes, since the activities of many junction complex components have been known to cause defects in cell adhesion and integrity (Bhat et al, 1999; Cox et al, 1996; Lamb et al, 1998; Muller & Wieschaus, 1996; Tanentzapf & Tepass, 2003; Wodarz et al, 2000). A caveat in answering this question is that the severe epithelial deformation and the altered localization of junction complexes in the rounded-up cells could potentially render cells more or less brightly stained for membrane markers, when examined only at a *single* section, resulting in production of artefacts. Therefore, maximum intensity projections were produced based on a stack of single confocal image sections through the depth of the entire apical surface of the imaginal disc, in order to visualize the *overall* staining intensity of the junction complex protein of interest of the whole apical epithelia. In the larval wing disc where *flw* expression was reduced using the *apt*-Gal4 driver, there was an apparent increase in the overall staining intensity of F-actin within the *ptc*-expressing domain (Figure 15F) particularly on the cell membrane, compared to the wild type control (Figure 15B). The staining intensity for Coracle, a septate junction protein, remained largely unchanged (Figure 15 C and G). Staining for Armadillo, a component of the apical junction complex, showed a moderate increase in intensity (Figure 15 A and

E). Thus, reduced *flw* expression was associated with an increased cell membrane-association of F-actin, but did not affect the localization of Coracle.

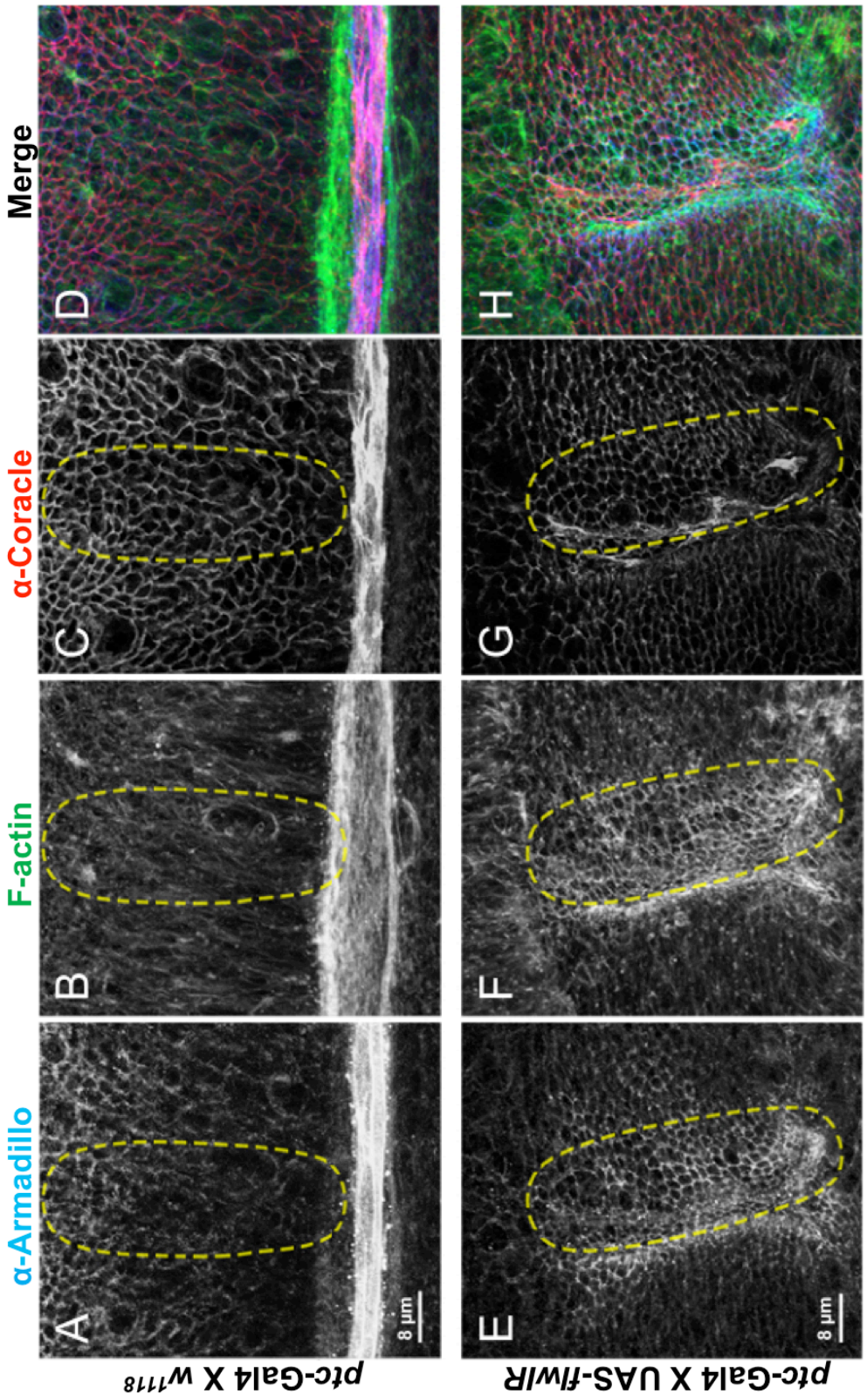
Merge
α-Coracle
F-actin
α-Armadillo
A
B
C
D
E
F
G
H
8 µm
8 µm
ptc-Gal4 X w1118
ptc-Gal4 X UAS-flwIR

Figure 15 | Reduction in *flw* expression led to increased membrane-localization of F-actin and Armadillo, but did not affect the localization of Coracle. Wandering third instar larval wing discs of either the wild type control (*ptc*-Gal4 X w^{1118}) or with reduced *flw* expression (*ptc*-Gal4 X UAS *flw*-IR) were dissected and analyzed for the staining of Armadillo (blue), F-actin (green) and Coracle (red). Maximum projection intensity for each of the membrane markers was acquired by summing up a stack of multiple confocal sections taken from the top of the most apically situated epithelial layer to the bottom of the most basally situated layer of cells through the whole apical surface of the wing disc. The domain of cells in which *ptc* was expressed was outlined (dashed line). **(A-D)** In the wild type, the overall intensity of staining for all three markers in the *ptc*-expression domain was similar to that of the adjacent non *ptc*-expressing cells. **(E-H)** In the *ptc*-expressing cells where *flw* expression was reduced, the overall staining intensity of Armadillo and F-actin was increased compared to the surrounding epithelial cells, or the same domain in the wild type control (E, F). Armadillo and F-actin both showed increased localization to the cell membrane. The staining intensity of Coracle in the *ptc*-expressing epithelial cells was not affected (G) and the increased staining at the left edge of the domain was of the peripodial cells pulled in basally due to epithelial deformation.

6. Reduction of flw Expression Is Associated with Increased Apoptosis

The drastic deformation of the larval and prepupal wing disc epithelia led me to investigate further how reduced *flw* expression may affect the formation of the adult wing disc. Adult flies in which *flw* expression was reduced in the dorsal surface of the wing exhibited a prominent 'curled-up' wing phenotype (data not shown), likely resulting from the decrease in the size of the dorsal wing area compared to the ventral side. Furthermore, *flw* knockdown using the *ptc*-Gal4 driver resulted in a significant (~25%) decrease in the wing size in the area between the *ptc* expression-corresponding L3 and L4 veins (Figure 16A, middle). The region of the wing between L3 and L4 was slightly deformed and did not lie on the same focal surface when examined under the microscopy (Figure 16A, middle, dashed line). In addition, counting of numbers of wing bristles per area between the L3 and L4 veins showed no significant increase compared to that of the remaining wing area (data not shown), suggesting that the decrease in the wing size caused by reducing *flw* expression was not due to smaller cell size but the reduction in the overall cell numbers.

To determine if the decrease in the corresponding wing area upon *flw* knockdown was at least in part caused by increased cell death, e.g. apoptosis, immunostaining of larval wing discs was carried out using the anti-active Caspase 3 antibody, which marks the cells actively undergoing apoptosis. In the wild type control cells on the larval wing disc, active-Caspase 3 positive cells were primarily detected in the squamous peripodial cells and the disc notum (data not shown), where regulated tissue growth and differentiation

was to take place at the later developmental stages, and were absent from the distal part of the disc epithelia (Figure 17C). In contrast, along the strip of *ptc*-expressing cells where *flw* was knocked down, a significantly increased proportion of cells were stained positive for active Caspase 3 (Figure 17G), compared to the same region in the wild type control (Figure 17C). This suggests that reduction in *flw* expression was associated with increased apoptosis, which may contribute to the decreased wing size observed in the adult fly.

A

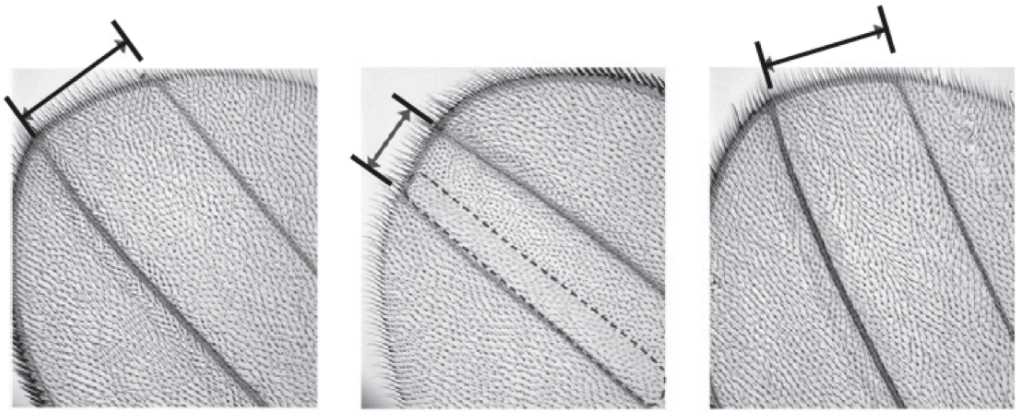
ptc-Gal4 X w1118
ptc-Gal4 X UAS flw-IR
ptc-Gal4 X UAS flw

B

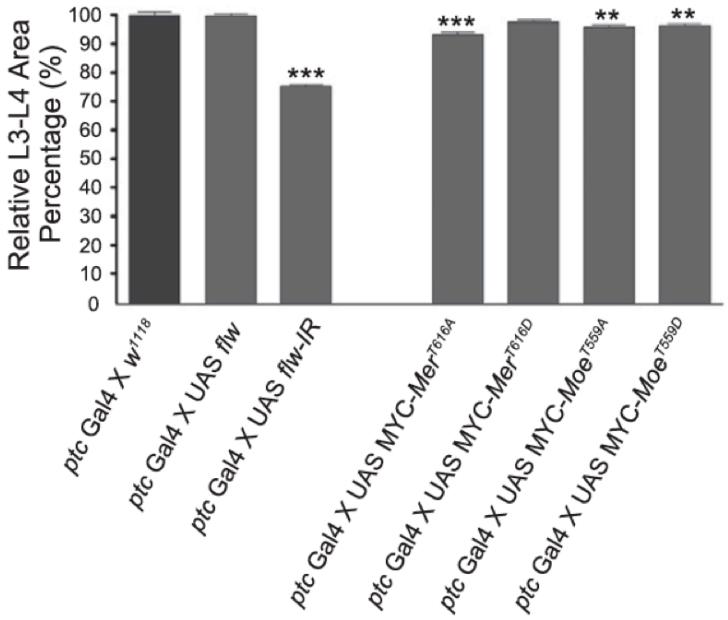
Relative L3-L4 Area Percentage (%)
100
90
80
70
60
50
40
30
20
10
0
***
***
**
**
ptc Gal4 X w1118
ptc Gal4 X UAS flw
ptc Gal4 X UAS flw-IR
ptc Gal4 X UAS MYC-Mer T616A
ptc Gal4 X UAS MYC-Mer T616D
ptc Gal4 X UAS MYC-Moe T559A
ptc Gal4 X UAS MYC-Moe T559D

Figure 16 | Reduced *flw* expression in the *ptc*-expressing domain resulted in a reduction in the adult wing size in the corresponding area between the L3 and L4 veins. (A) Adult fly wings of the wild type control (*ptc*-Gal4 X w^{1118}), the reduced *flw* expression (*ptc*-Gal4 X UAS *flw*-IR) and the *flw* overexpression (*ptc*-Gal4 X UAS *flw*) were dissected. The relative area of the wing between the L3 and L4 veins (area in bracket) was measured, which corresponds to the domain where *ptc* is expressed in the wing imaginal disc. Reduced *flw* expression resulted in a reduction in the L3-L4 area by ~25%, whereas *flw* overexpression did not significantly affect the wing size compared to the wild type control. Part of the wing between L3-L4 with reduced *flw* expression also showed slight deformation as visible by the inability to focus completely on the same focal plane. **(B)** Overexpression of the non-phosphorylatable *Mer* transgene (Mer^{T616A}), the non-phoshporylatable *Moe* (Moe^{T559A}) and the phosphomimetic *Moe* (Moe^{T559D}) all partially recapitulated the reduced wing size phenotype by the loss of *flw* expression. The reduction in the wing size between the L3-L4 veins was small but significant compared to the wild type control, except for overexpression of the phosphomimetic *Mer* (Mer^{T616D}). ** $p < 0.01$. *** $p < 0.001$.

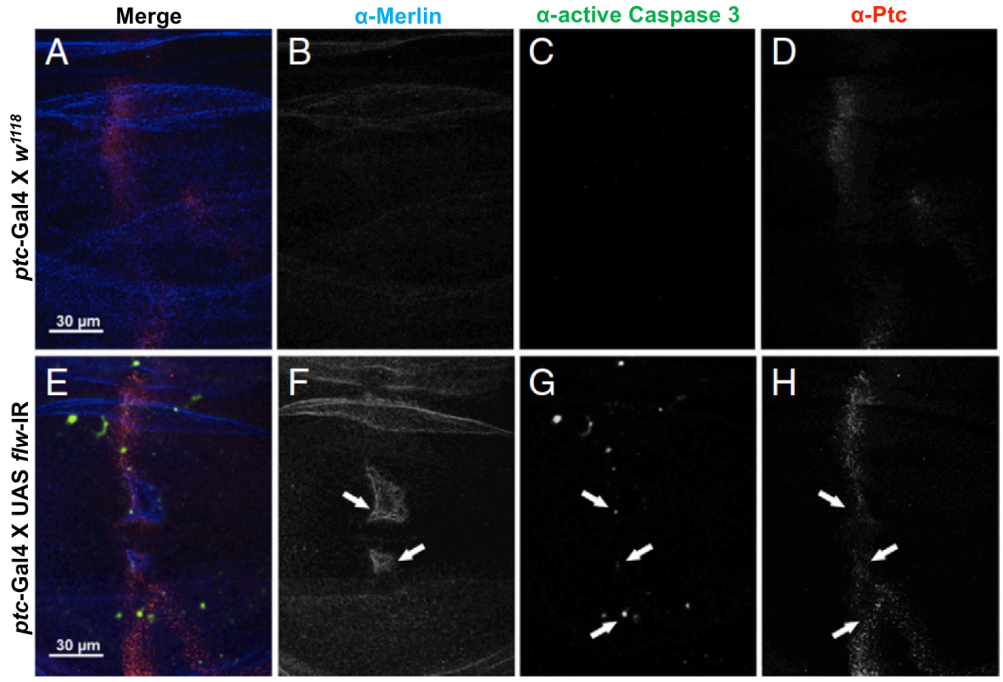

Figure 17 | Reduced *flw* expression correlated with an increase in the number of apoptotic cells. Wandering third instar larval wing imaginal discs of either the wild type control (*ptc*-Gal4 X w^{1118}) or with reduced *flw* expression (*ptc*-Gal4 X UAS *flw*-IR) were dissected and immunostained for Merlin (blue), active Caspase 3 (green), and Patched (red). **(A-D)** Maximum projection of the apical epithelia of the wing disc showed a minimal number of apoptotic cells marked by the anti-active Caspase 3 staining. **(E-H)** Maximum projections of all confocal sections of the disc showed more cells undergoing apoptosis, as marked by the positive anti-active Caspase 3 staining. Apoptotic cells were particularly concentrated at the edges of the *ptc*-expressing region where cells had reduced level of *flw* expression (G, H, arrowheads).

7. *Recapitulation of Phenotype by Alternate Epitopic Mer and Moe Mutant Expression*

If the defect in epithelial arrangement and cell adhesion and polarity upon reducing flw expression was mediated by alterations in the phosphorylation state and hence activities of Mer and Moe, it was predicted that directly manipulating Mer and Moe phosphorylation would result in a phenotype in the epithelial tissue similar to that of *flw* knockdown. To test the prediction, epitope-tagged transgenic wild type *Mer* and *Moe* as well as both the non-phosphorylatable (UAS-MYC-Mer^{T616A}, UAS-MYC-Moe^{T559A}) and phosphomimetic forms (UAS-MYC-Mer^{616D}, UAS-MYC-Moe^{T559D}) mutants were over-expressed in the third instar larval wing disc using the *ptc*-Gal4 driver. Thr616 of *Drosophila* Mer is homologous to Thr559 of *Drosophila* Moesin and but *not* homologous to Ser518 of the mammalian Mer.

Overexpression of the wild type *Mer* (UAS-MYC-Mer^{WT}) and both the constitutively active, non-phosphorylatable (UAS-MYC-Mer^{T616A}), and the inactive, phosphomimetic form (UAS-MYC-Mer^{T616D}) of *Mer* all produced an epithelial phenotype of the wing imaginal disc similar to what was observed in the *flw* knockdown mutant, albeit a much less degree of severity (Figure 18 L, P, T). There was a range of phenotypes showing various extents of the defect. In some case, epithelial cells showed a brighter than wild-type staining of Mer and F-actin on the cell membrane and were relatively more compact in cell size (Figure 18 R, S). Orthogonal views of the disc apical epithelia revealed a 'deep dent' formed on the apical surface (Figure 18 R-T', arrowheads). Alternatively, apparent epithelial deformation was observed in

other cases within the domain where *ptc* expression was reduced, as the large squamous peripodial cells on the apical surface were pulled in basally into the disc tissue (Figure 18K, N, O). Thus, overexpression of all three *Mer* transgenes partially recapitulated the loss of *flw* expression phenotype.

When the wild type (UAS-MYC-Moe^{WT}), the inactive, non-phosphorylatable (UAS-MYC-Moe^{T559A}) and the constitutively active, phosphomimetic (UAS-MYC-Moe^{T559D}) form of Moe were each overexpressed in the wing disc using the *ptc*-Gal4 driver, the epithelial defect phenotype seen in loss of *flw* expression strain was also reproduced to a lesser degree of severity (Figure 19 L, P, T). Subtle defects in the epithelial cells on the apical surface were observed, manifested by the tight organization of small cells with plasma membrane concentrated F-actin and Moe of a bright staining intensity compared to the adjacent unaffected cells (Figure 19K, L, R, S, arrowheads). More apparent deformation such as epithelial folding was also detected for the more severe cases (Figure 19N, O, arrowheads). Therefore, the loss of *flw* expression phenotype was partially recapitulated by the overexpression of all three *Moe* transgenes.

Overexpression of the non-phosphorylatable and phosphomimetic mutants in the *ptc*-expressing cells also resulted in a small but statistically significant decrease in the adult fly wing size between the L3 and L4 veins, except for overexpressing the phosphomimetic Mer (Mer^{T616D}), which caused no significant change in the wing size (Figure 16B). Compared to the wild type control where *flw* expression was unaffected, overexpression of Mer^{T616A} resulted in a decrease in wing size by 6.8%, while overexpression of Moe^{T559A}

and Moe^{T559D} caused reduction in the wing size of 4.2% and 3.7%, respectively. Taken together, these data suggested that the phenotype of epithelial defects caused by reduction in *flw* expression can be partially recapitulated by altering the phosphorylation states of Mer and Moe.

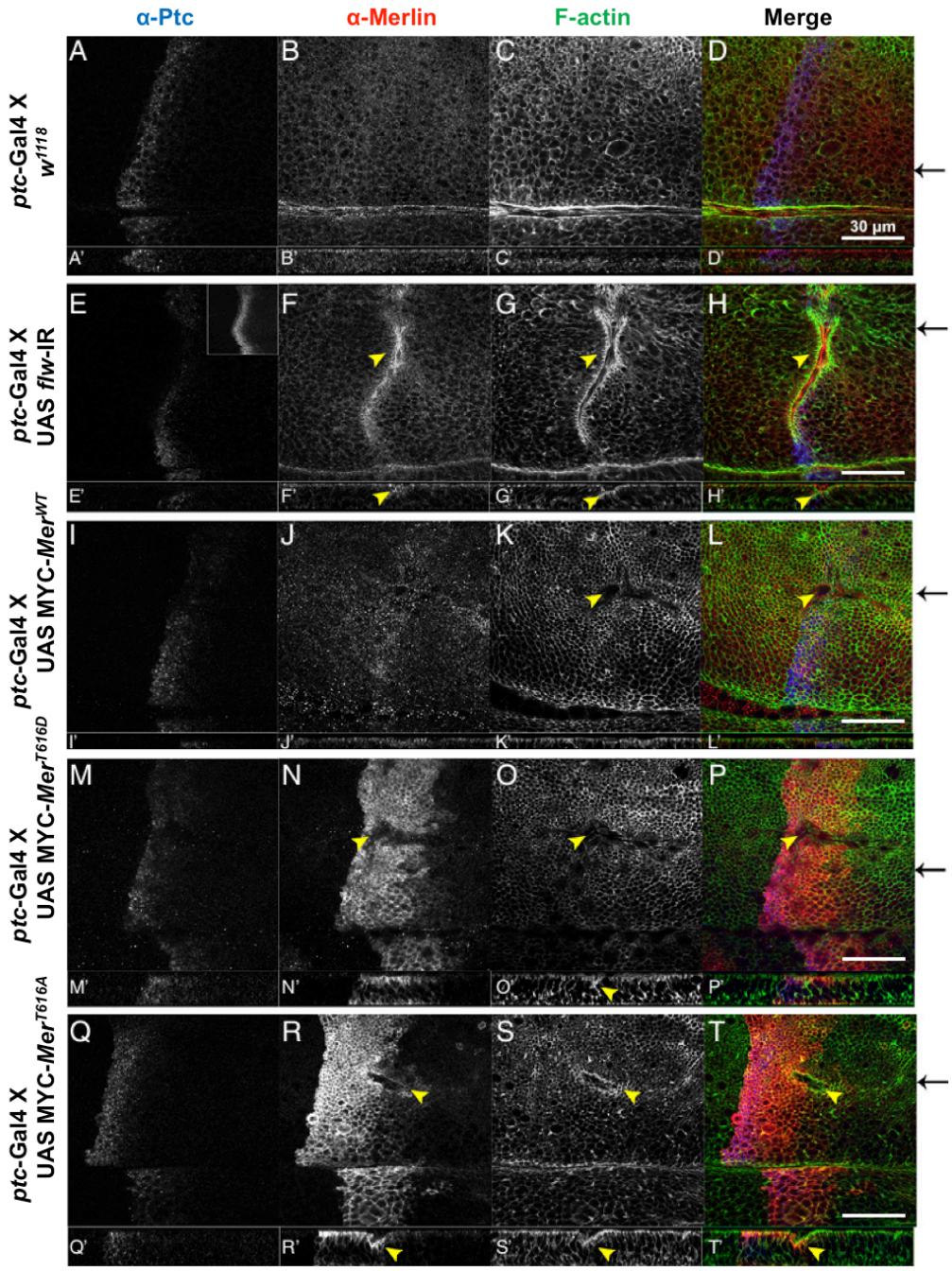
α-Ptc
α-Merlin
F-actin
Merge
ptc-Gal4 X w1118
ptc-Gal4 X UAS flw-IR
ptc-Gal4 X UAS MYC-MerWT
ptc-Gal4 X UAS MYC-MerT616D
ptc-Gal4 X UAS MYC-MerT616A
A
B
C
D
A'
B'
C'
D'
30 µm
E
F
G
H
E'
F'
G'
H'
I
J
K
L
I'
J'
K'
L'
M
N
O
P
M'
N'
O'
P'
Q
R
S
T
Q'
R'
S'
T'

Figure 18 | Overexpression of the wild type, constitutively active and inactive *Mer* transgenes partially recapitulated the loss of *flw* expression phenotype. (A-D) A wild type control wing disc (ptc-Gal4 w1118) showing no significant changes in epithelial organization. **(E-H)** Within the domain where *flw* expression was reduced (*ptc*-Gal4 X UAS *flw*-IR) there was a prominent defect in the apical surface of the wing disc marked by the bright staining of Mer and F-actin along the region of deformation (F, G, arrowheads). Inset in E showed a maximum projection of all the cells expressing *ptc*-Gal4. An orthogonal view revealed the deformed epithelium at the apical surface (F'-H', arrowheads). **(I-L)** Overexpression of wild type *Mer* (*ptc*-Gal4 X UAS MYC-Mer^{WT}) caused minor disorganization of the epithelium, as indicated by the large peripodial cells being pulled into the disc tissue (K, L, arrowheads) **(M-P)** Subtle epithelial deformation in the wing disc where the inactive, phosphomimetic *Mer* transgene (*ptc*-Gal4 X UAS MYC-Mer^{T616D}) was overexpressed (O, P, arrowheads). **(Q-T)** Overexpression of the constitutively active, non-phosphorylatable *Mer* (*ptc*-Gal4 X UAS MYC-Mer^{T616A}) resulted in an apparent epithelial defect in a small area of the apical disc surface, marked by the brighter local staining of Merlin and F-actin at the site of deformation (R-T, arrowheads). The deep dent at the edge of the *ptc*-expressing domain was easily seen in the orthogonal view of the disc epithelia (R'-T', arrowheads).

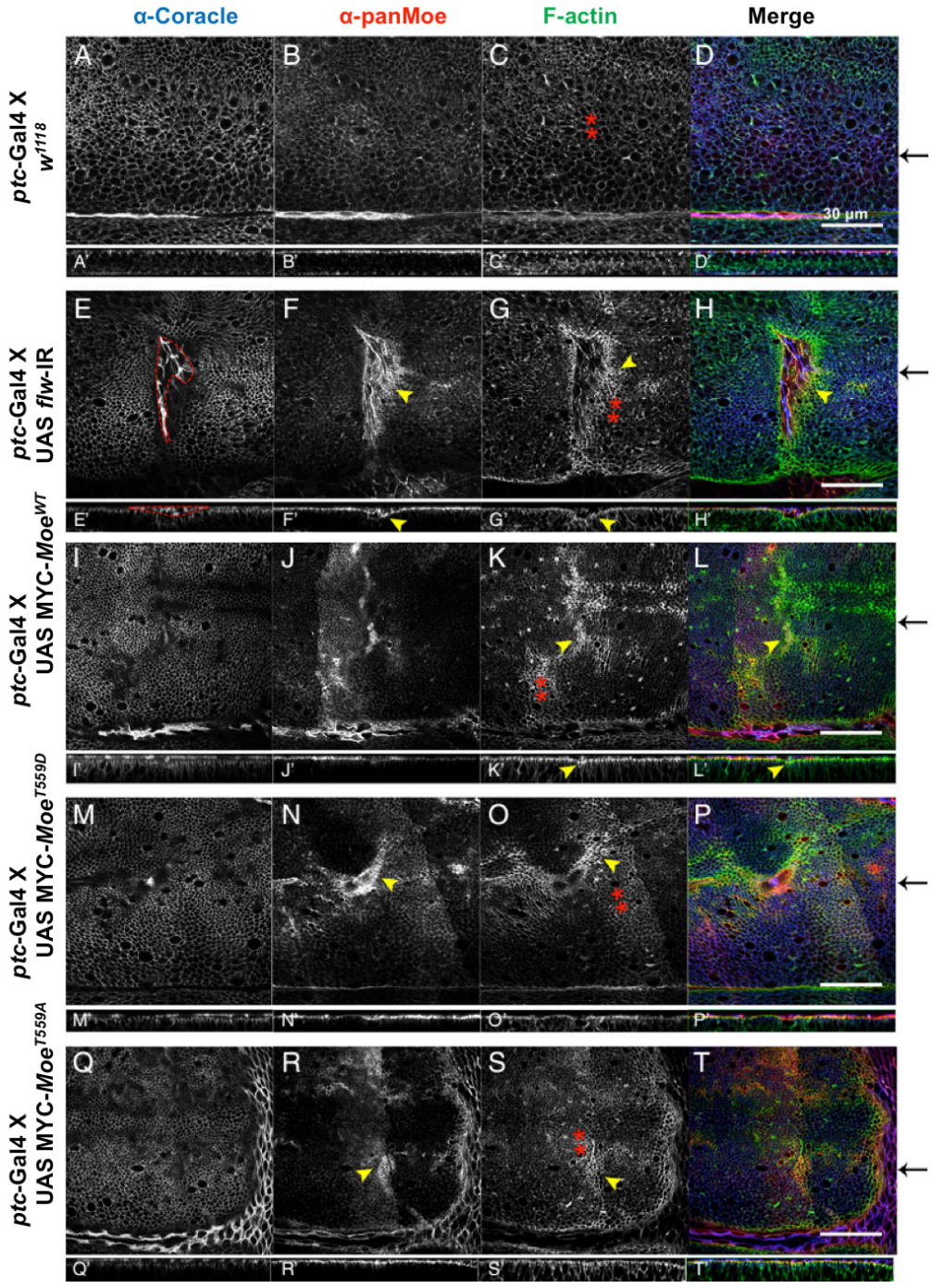
α-Coracle
α-panMoe
F-actin
Merge
ptc-Gal4 X w1118
ptc-Gal4 X UAS flw-IR
ptc-Gal4 X UAS MYC-MoeWT
ptc-Gal4 X UAS MYC-MoeT559D
ptc-Gal4 X UAS MYC-MoeT559A
30 µm

Figure 19 | Overexpression of the wild type, constitutively active and inactive *Moe* transgenes partially recapitulated the phenotype of loss of *flw* expression. (A-D) A wild type control third instar wing disc showing no significant changes in the epithelial organization, as marked by the staining of pan-Moe and F-actin. **(E-H)** Reduced *flw* expression (*ptc*-Gal4 X UAS *flw*-IR) resulted in prominent epithelial defects where cells showed brighter staining of pan-Moe and F-actin (F, G, arrowheads). Peripodial cells with bright Coracle staining were pulled in the disc tissue (E, dashed line). The large depression of the apical disc surface was easily seen in the orthogonal view (F', G', arrowheads) **(I-L)** Overexpression of the wild type *Moe* (*ptc*-Gal4 X UAS-Moe^{WT}) caused minor disorganization of the epithelial cells, as marked by the increased signal intensity of the pan-Moe and F-actin staining (J, K, L). The cells stained brightly for F-actin had constricted cell size and more compact organization compared to the wild type control (K, arrowhead). **(M-P)** Formation of a fold in the wing disc with overexpression of a constitutively active, phosphomimetic *Moe* (*ptc*-Gal4 X UAS MYC-Moe^{T559D}), as marked by the brighter staining of pan-Moe and F-actin in the cells surrounding the deformed region. **(Q-T)** Epithelial cells where an inactive, non-phosphorylatable *Moe* transgene was overexpressed (*ptc*-Gal4 X UAS MYC-Moe^{T559A}) had brighter staining of pan-Moe and F-actin and were smaller in size compared to the wild type control (R, S, arrowheads).

8. Summary of Results

The *Drosophila* phosphatase PP1 flw forms a Sip1-containing protein complex with Mer and with Moe. Changes in *flw* expression level resulted in corresponding changes in the dephosphorylation states of Mer and Moe. Loss of *flw* expression led to increased localization of Mer and Moe on the plasma membrane. In the epithelial tissues, reducing *flw* expression caused changes in cell adhesion and polarity, as well as disruption of epithelial integrity. The phenotype of loss of *flw* expression was partially recapitulated by overexpression of the wild type, non-phosphorylatable and phosphomimetic forms of *Mer* and *Moe* transgenes.

Chapter Four

Discussion

1. flw and Phosphorylation of Merlin and Moesin

The molecular activity of the tumor suppressor Merlin and its closely related ERM proteins is primarily governed by reversible phosphorylation by Ser/Thr kinases and Ser/Thr phosphatases. Phosphorylation results in the 'open' conformation of the protein, activating ERMs while deactivating Merlin. Among the many characterized kinases of Merlin and Moesin the *Drosophila* ERM orthologue, the sterile-20 kinase Slik has been recently found to coordinate the phosphorylation of Merlin and Moesin (Hughes & Fehon, 2006). The result of this project showed that, the *Drosophila* PP1β-9c, flapwing, acts antagonistically to Slik by coordinately regulating the dephosphorylation and cellular activities of Merlin and Moesin (Figure 20).

Firstly, flw was found in a protein complex with Merlin and with Moesin, and associated with a scaffolding protein Sip1 (Figure 4), which was previously demonstrated to be required for Slik-mediated phosphorylation of Merlin and Moesin (Hughes et al, 2010). In the follicle cells of *Drosophila* developing oocytes, loss of *Sip1* expression resulted in complete loss of phospho-Moesin on the apical plasma membrane and marked reduction in the membrane-associated DE-Cadherin. Second, changing the expression level of *flw* in *Drosophila* disc tissue by either overexpression or RNAi-mediated knockdown caused the corresponding changes in the cellular level of hypo-phosphorylated Mer/Moe isoforms in relative to the hyper-phosphorylated isoforms. When the phosphatase *flw* was overexpressed, an increase in the ratio of hypo-phosphorylated Merlin isoforms was detected (Figure 5C, D). In addition, 2D-DIGE/Western analysis revealed the presence

of four phospho-specific Merlin isoforms (Figure 5B), as compared to the two to three Mer isoform reported in the previous studies (Hughes & Fehon, 2006; Kissil et al, 2002), indicating that Merlin is phosphorylated at multiple sites in *Drosophila* and that this may contribute to the differential regulation of Merlin and its participation in multiple signal transduction pathways.

The similar effect of changing *flw* expression on Moesin phosphorylation was also observed. Overexpression of *flw* correlated with an increase in the amount of phosphorylated Moesin in the tissue, but did not affect the total Moe level (Figure 6), suggesting that the activity of Moesin was modulated by *flw* at the post-translational level only. Therefore, the dephosphorylation of Merlin and Moesin appear to be both controlled by the PP1 flw.

Is binding to flw by Merlin and Moesin competitive or even mutually exclusive? Although experiments in this study did not give an explicit answer to the question, it is noteworthy and intriguing that Merlin contains a PP1-binding RVxF motif at its C-terminus (Figure 2B). This gives rise to several speculations, which all need to be tested in further experiments. Firstly, the Merlin::flw interaction may occur at the C-terminal domain of Merlin, mediated by the RVxF motif (Figure 21). Second, the RVxF motif is conserved in *Drosophila* Merlin and human NF2 orthologue, but not present in ERM proteins. This implies that Merlin likely has a distinct affinity for binding to flw compared to Moesin, and that the phosphorylation of Merlin and Moesin may be differentially regulated by flw even under the same enzymatic condition. Moreover, since the RVxF motif is present in a large number of PP1 regulatory subunits and required for the formation of the stable PP1

holoenzyme complexes, it is likely that Merlin acts *both* as a substrate and a regulatory subunit of flw. Binding of Merlin to flw may alter the substrate specificity and/or subcellular localization of flw, facilitating dephosphorylation of other flw substrates such as Moesin. In this case, Merlin would act synergistically with flw to stimulate Moesin dephosphorylation. Conversely, Merlin may act as an inhibitor of flw, blocking the catalytic site of flw and suppressing flw-mediated Moesin inactivation. Thirdly, many PP1 regulatory subunits such as MYPT-1 and CPI-17 are inhibitory only when phosphorylated by the corresponding kinases of which actions oppose that of PP1. Thus, if Merlin binds to flw in its phosphorylated, inactive form, and stimulates/inhibits Moesin dephosphorylation, a coordinate regulation between Merlin and Moesin activity would be possible through the mediation of flw. Lastly, the RVxF motif is specific to the regulatory subunit of PP1 but not PP2A or PP2B, which may indicate that flw the *Drosophila* PP1 is the only Ser/Thr phosphatase subclass involved in Merlin dephosphorylation.

2. *flw, Mer/Moe Localization and Epithelial Integrity*

Moesin plays an important role in maintaining cell polarity, epithelial integrity and motility, whereas Merlin has additional functions such as contact-dependent growth inhibition that are not ascribed to the ERM members (Carreno et al, 2008; Curto et al, 2007; Kunda et al, 2012; Morrison et al, 2001; Okada et al, 2005; Polesello et al, 2002; Speck et al, 2003). Therefore, it

was postulated that if Merlin and Moesin are substrates of flw, changing *flw* expression level in epithelial tissue would cause a defect in epithelial cell morphology and tissue integrity. As expected, when *flw* expression was reduced in the larval wing disc in a strip of *ptc*-expressing cells, epithelial deformation was detected within the *ptc*-expression domain and at the boundary between the *ptc*-expression domain and the surrounding 'wild-type' cells where *flw* expression remained unaffected (Figure 10 A'-L'). The defects caused by *flw* expression knockdown were prominent as in some cases, large, squamous peripodial cells typically situated apically to the epithelia were pulled basally into the disc tissue due to the dramatic apical surface deformation (Figure 19E).

In the epithelial cells where *flw* expression was reduced by using the *ptc*-Gal4 driver, there was an increase in the signal intensity of immunostaining for Merlin particularly at the apical membrane of the cell (Figure 10, orthogonal 3a), as well as increased phospho-Moesin staining on the plasma membrane, as visualized by the maximum intensity projections of a stack of multiple single sections through the disc epithelia (Figure 12F). The phenotype of *loss of flw* expression was confirmed by reducing *flw* expression using another driver, *apt*-Gal4, which resulted in similar epithelial defects and increased membrane-localized Merlin staining in the dorsal disc epithelia (Figure 11J). In contrast to the orthogonal view of the epithelial deformation at the *ptc*-expressing domain, which allowed the enriched localization of Merlin at the *apical* membrane to be visualized, the single confocal image of the disc epithelia in *apt*-Gal4 X *flw*IR failed to indicate whether the membrane-

enriched Merlin was more apically or basolaterally located. However, the less deformed apical surface of the dorsal wing disc allowed for a more clear visualization of increased membrane-associated Merlin in *individual* cells as opposed to a stack of locally tightly packed epithelial layers, thus diminishing the possibility that the membrane-enrichment of Merlin upon *loss of flw* expression was due to potential artefacts induced by microscope resolution. Furthermore, it is noteworthy that the deformation was most severe in the cells with reduced *flw* expression that were situated along the boundary to the wild-type cells (e.g. the D-V boundary, Figure 11G, arrowhead). This implies that the drastic difference in the cellular level of phosphorylated Mer and Moe at the two sides of the boundary may contribute to the disruption of intercellular junction stabilization and hence cell-cell adhesive properties, leading to the formation of the subsequent epithelial defects observed.

The data suggest that flw is responsible for Mer and Moe dephosphorylation and that hyper-phosphorylated Mer and Moe caused by *loss of flw* expression are more tightly associated with the plasma membrane. This is in accordance to the previous finding on the alteration of subcellular localization of Mer and Moe by Slik-mediated phosphorylation (Hipfner et al, 2004; Hughes & Fehon, 2006). In the mitotic clones of *slik* mutant cells in *Drosophila* wing disc, phospho-Moe staining on the membrane was greatly reduced, while Merlin staining at the apical surface of the epithelium was also decreased. A similar mutant phenotype was also observed in Jeg-3 mammalian epithelial cells, in which unregulated Slik activity caused mis-localization of Ezrin from the apical membrane to the basolateral membrane (Viswanatha et al, 2012).

Therefore, loss of *flw* expression produces an effect on the membrane-localization of Mer and Moe in epithelium exactly opposite to that of *loss of function* of *slik*, indicating the opposing regulatory roles of flw and Slik in phosphorylation and localization of Mer and Moe.

3. flw in A Protein Complex - A Signaling Module?

In stark contrast to the dramatic epithelial phenotype of *loss of flw* expression, overexpression of *flw* produced a phenotype that was virtually indiscernible from the wild type control (Figure 9). Because *flw* overexpression in the wing tissue did lead to increased hypo-phosphorylation of Merlin and Moesin (Figure 4A, Figure 5), this means that the presence of an excessive amount of hypo-phosphorylated Mer and Moe is causally unlinked from the potential downstream effects on epithelial integrity and cell adhesion. This part of the result seemed puzzling at first but may be explained by a saturation mechanism, where additional protein components of the flw-Mer and flw-Moe complexes are required to mediate the cellular functions of Mer and Moe in epithelial organization. Thus, when the level of flw is minimal (*e.g.* RNAi-mediated *flw* knockdown), less than sufficient cellular level of phosphorylated Mer and Moe is present in the membrane-localized protein complex, resulting in the formation of epithelial defects as described in the UAS-*flw*IR genotype. On the other hand, when *flw* is overexpressed in the cells, the excessive portion of under-phosphorylated Mer and Moe cannot be incorporated into the actively functioning protein complex due to the limited

pool of other critical components, thereby causing no detectable changes to the epithelial organization.

Based on the many studies of interacting proteins of PP1, it has been proposed that one of the three groups of PP1-binding partners is the so-called 'scaffolding' proteins, which not only mediate the formation of the protein complexes and bring the substrate protein into close proximity to the enzymes, but, more importantly, function by rendering the complex a signaling module containing both protein kinases and phosphatases for the downstream event cascades (Bollen, 2001). The scaffolding protein Sip1, the *Drosophila* orthologue of mammalian EBP50/NHERF1 is a membrane-cytoskeletal linking protein localized to the apical surface of the epithelial cells and can interact with ERM proteins (Fouassier et al, 2001; Kreimann et al, 2007; Morales et al, 2004; Reczek et al, 1997). Moreover, Sip1 was previously found in the protein complex containing the kinase Slik and its substrates Moesin (Hughes et al, 2010), and was detected in a complex with the phosphatase flw in this project. It is hence very likely that Sip1 is one of the key components of this signaling module and is required to mediate the effects of Mer and Moe on epithelial integrity and adhesion upon phospho-regulation.

4. flw and Change of Cell Polarity

In addition to altering membrane localization of Mer and Moe, reducing *flw* expression also correlated to change in cell shape and polarity. Knocking

down *flw* expression in the *ptc*-expressing domain caused the cells to adopt a smaller than wild-type shape and more compact intercellular organization (Figure 10 A'-L'). Interestingly, in the wing disc where *flw* expression was reduced using *apt*-Gal4, the affected cells were instead round and large in size, as illustrated by the staining of phospho-Moe (Figure 14, A'-I'). These cells showed positive phospho-Moe staining at various confocal sections even below the apical surface (Figure 14 D' and G'), as opposed to the wild type epithelial cells, in which the phosphorylated, active Moe was most abundant only in the apical domain of the cell membrane (Figure 14 A and D). Thus, *loss of flw* expression caused mislocalization of Moesin and rounding up of the tall, columnar epithelial cells.

The difference in cell morphology observed upon using the *ptc*-Gal4 and *apt*-Gal4 drivers is likely due to the differential efficacy of knockdown and the ensuing different stages of phenotype representation. When the *early pupal* discs of *ptc*-Gal4 UAS *flw*IR were examined, large holes devoid of cells were formed on the apical surface of the disc within the *ptc*-expression domain (Figure 13 D'). In addition, large, round cells with mislocalized junction complex proteins were detected underneath the apical surface (Figure 13 E' and I'), resembling the phenotype of *loss of flw* expression seen using the *apt*-Gal4 driver. Most importantly, in the knockdowns using both drivers, the mislocalized apical membrane markers phospho-Moe partially colocalized with the baso-lateral membrane marker Coracle (Figure 13L' arrowheads, Figure 14I' arrowheads), indicating the loss of apical-basal polarity in these cells. Therefore, the alteration in the activity of Mer and Moe in response to

reduced *flw* expression likely caused a progressive change in cell shape and gradual disruption of epithelial cell polarity during the process of tissue development.

5. flw and Apical Junction Complexes

Moesin is required for the stabilization of adherens junctions, and previous studies showed that the *loss of function* of *Drosophila Moe* mutant led to loss of apical junctional markers and disruption of the disc epithelial integrity (Hipfner et al, 2004; Speck et al, 2003). In accordance with this finding, reduced *flw* expression led to an elevated level of phosphorylated, active Moe, with increased staining intensity of several apical junction markers including F-actin, Armadillo and DE-Cadherin (Figure 15 E and F; Figure10-3b), but not the septate junction marker Coracle (Figure 15G), as determined by the maximum projection of the disc epithelia. Therefore, reducing *flw* expression affected the membrane-localization of other members of the apical membrane junction complex. This is reminiscent of the phenotype of *l-o-f* of *flw* in the *Drosophila* oocyte, which led to increased membrane levels of the apical proteins including aPKC, Bazooka, PatJ, and the AJ components Armadillo and DE-Cadherin, whereas the distribution and the protein level of the basolateral protein Disc large remained similar to the wild type (Sun et al, 2011). Thus, the potential alteration in the activities of these apical membrane proteins, along with the over-phosphorylated Mer and Moe, may

together exert an impact on the apical-basal polarity and the adhesive properties of the epithelial cells.

6. flw and Cell Motility

The observation of occasional round epithelial cells on the *ventral* side of the disc tissues upon reducing *flw* expression using *apt*-Gal4 was intriguing (Figure14 D' and G'). Based on the similarity in the cell shape to the dorsal counterparts and their close proximity to the D-V boundary, it is speculated that these cells possibly originated from the dorsal epithelial compartment and dispersed across the boundary to the ventral side due to enhanced cell motility and invasiveness. However, whether this is true requires further confirmation by tracking the dorsally originating cells with a live cell fluorescence marker. In *Drosophila* epithelium, loss of function of Moe has been shown to induce invasive migratory cellular behavior (Speck et al, 2003). Mounting evidence from studies of tumor progression also suggested that the closely related protein of Moesin, Ezrin, correlated with increased cell migration and metastasis in several cancer cell lines (Li et al, 2012a; Ou-Yang et al, 2011; Ren et al, 2009; Shang et al, 2012). Thus, it is possible that flw plays a role in controlling epithelial cell motility by regulating the activity of Moesin.

7. Other Cellular Processes Potentially Affected by flw Knockdown

The large, round cells with bright overall membrane staining of phospho-Moe (Figure 14 D' and G') may alternatively represent mitotic cells that were unable to proceed to cytokinesis due to impaired cortical Moesin activity upon *flw* knockdown. A recent study on the role of Moesin during mitosis demonstrated that, in *Drosophila* S2 cells, upon activating phosphorylation by Slik, Moesin is recruited to the cell cortex at mitosis entry and functions to increase cortical rigidity (Roubinet et al, 2011). Over-activation of Moe triggers excessive stiffness and blocks cell elongation. Interestingly, depletion of another phosphatase of Moe, PP1-87B, was shown to cause over-phosphorylation of Moe and cytokinesis failure. Therefore, even though *Drosophila* S2 cells and epithelial cells are two different systems, the possibility cannot be excluded that the round, occasionally blebbing epithelial cells with reduced *flw* expression may be a result of aberrant phospho-Moe activity and defects in cytokinesis during the early rapid-proliferating stage of the imaginal disc tissue.

8. Recapitulation of loss of flw Expression by Mer and Moe Overexpression

To confirm that the effects of loss of *flw* expression on epithelial integrity was at least in part due to abnormal cellular level of phosphorylated Mer and Moe, wild type, non-phosphorylatable and phosphomimetic transgenes of Mer and Moe were overexpressed using the *ptc*-Gal4 driver. As expected, overexpression of all forms of Mer and Moe transgenes indeed produced a

spectrum of defective epithelial phenotypes similar to, but in general less severe than that of loss of *flw* expression (Figure 18, 19). The severity of the defects varied considerably, from formation of deep local dents in the disc epithelia (Figure 18 T and T') to the large yet shallow surface deformation (Figure 19 N-P).

Despite the successful recapitulation of the phenotype, what remained puzzling was that similar epithelial defects were detected in the mutants over-expressing the phospho-mimetic as well as the non-phosphorylatable forms of Merlin and Moesin transgenes. This observation is unexpected and seems contradictive to the previous results that loss of expression, but *not* overexpression of the phosphatase *flw* in the wing discs caused epithelial defects. We came up with two explanations possible for the similar phenotypes caused by expressing transgenes with opposite activities. Firstly, the majority of the epithelial defects in the transgene mutants were located at the boundary region between the cells with reduced *flw* expression and those with unaffected, wild-type *flw* expression level. It is hence possible that the defects were *not* a direct result of the absolute level of active Merlin or Moesin in individual cells, but rather caused by the steep changes in the relative level of Merlin/Moesin activity from the mutant epithelial cells to the adjacent wild-type cells. Since both Merlin and Moesin function as part of the intercellular junction complexes, changing the activities of Merlin/Moesin in a subset of epithelia but not the neighboring cells would likely alter the adhesive properties of the affected epithelial cells and disrupt their proper cell-cell contact to the surrounding tissue. Secondly, overexpressing Merlin

and Moesin transgenes may not faithfully dictate the cellular circumstances of *flw* knockdown. When examined with the anti-MYC antibody which labels the Merlin and Moesin transgenes but not the endogenous proteins, it was found that prominent MYC staining localized in close proximity to the plasma membrane (data not shown), even in the epithelial cells overexpressing non-phosphorylatable, 'closed' Merlin and Moesin, which are supposed to be dissociated from cell membrane. Therefore, the drastic increase in the total cellular level of Merlin and Moesin may have overloaded the endogenous localization machinery and resulted in the ectopic localization of both forms of Merlin and Moesin to the plasma membrane, mimicking the condition of loss of flw expression (which caused increased membrane association of Merlin and Moesin).

Another observation was that the phenotypes resulted from overexpressing Mer transgenes were comparable to that of overexpressing Moe transgenes. This supports the view of previous studies showing that Mer also plays a role in maintaining epithelial integrity and regulating cell adhesion. Alternatively, it is possible that Merlin functions cooperatively with flw by acting as a PP1 regulatory subunit to modulate Moesin dephosphorylation, and that unregulated Merlin expression affects Moesin activity in the epithelial cells. Thus, overexpressing Merlin transgenes would lead to defective epithelial phenotypes similar to those of overexpressing Moesin transgenes.

The successful recapitulation of loss of *flw* expression by differentially expressed active Mer and Moe supports our postulation that flw regulates epithelial integrity in part by controlling dephosphorylation and the activity

of Mer and Moe. On the other hand, the partial, but not complete, recapitulation of the phenotype has two implications: (1) The phosphatase flw may have other target substrates that are regulators of epithelial organization. It has been reported that the flw phosphatases has other target proteins such as Spaghetti squash and Jun-N terminal kinase that have roles in regulating the actomyosin network in *Drosophila* wing disc (Kirchner et al, 2007; Lee & Treisman, 2004). Thus, the epithelial deformation caused by loss of *flw* expression likely represented a combinatorial effect of the dysregulation of multiple flw targets. (2) Flw may dephosphorylate Mer and Moe at serine/threonine residue(s) other than T616(Mer) and T559(Moe) which were tested in the transgenes. The differentially phosphorylated Mer and Moe by flw may participate in membrane-cytoskeleton signaling in an alternative yet more pivotal way to maintain epithelial integrity.

9. flw and Apoptosis

The epithelial defects of *loss of flw* expression appeared reduced in the adult fly stage, at which time no apparent large holes were observed on the adult wing but instead the corresponding wing area was reduced by ~25% compared to the wild type control (Figure 16A). Additionally, when overexpressing the transgenes of phospho-mutant Mer and Moe in the same *ptc*-expressing area, a small but significant decrease in the wing size was seen in overexpression of all transgenes except for the phosphomimetic, inactive Mer (Mer^{T616D}). It is thus speculated that only a small portion of the effect of

flw-knockdown on reducing the wing size was mediated by altering Mer and Moe phosphorylation, since *flw* mutants in previous studies was shown to lead to a drastic reduction in wing size and other wing defects likely by affecting the regulation of non-muscle myosin (Spaghetti squash) (Vereshchagina et al, 2004).

In the wing disc tissue where *flw* expression was knocked down, a significant increase in the numbers of apoptotic cells was also detected by staining for active Caspase 3 (Figure 17G). The elevated level of apoptosis is likely a secondary effect of the aberrant activities of Mer, Moe and other flw target proteins involved in regulating intercellular cohesion. The round epithelial cells excluded from the disc apical surface upon *flw* knockdown (Figure 13 H' and L', Figure 14 F' and I') are reminiscent of the phenotype of *l-o-f* of *sds*22, a PP1 regulatory subunit, which caused the extrusion of the affected wing epithelial cells and subsequent elimination by apoptosis. Thus, it is possible that epithelial cells in which *flw* expressed was reduced had increased migratory ability due to weakened cell adhesion, and wandered and dispersed during the tissue development, eventually became eliminated by detachment-induced apoptosis.

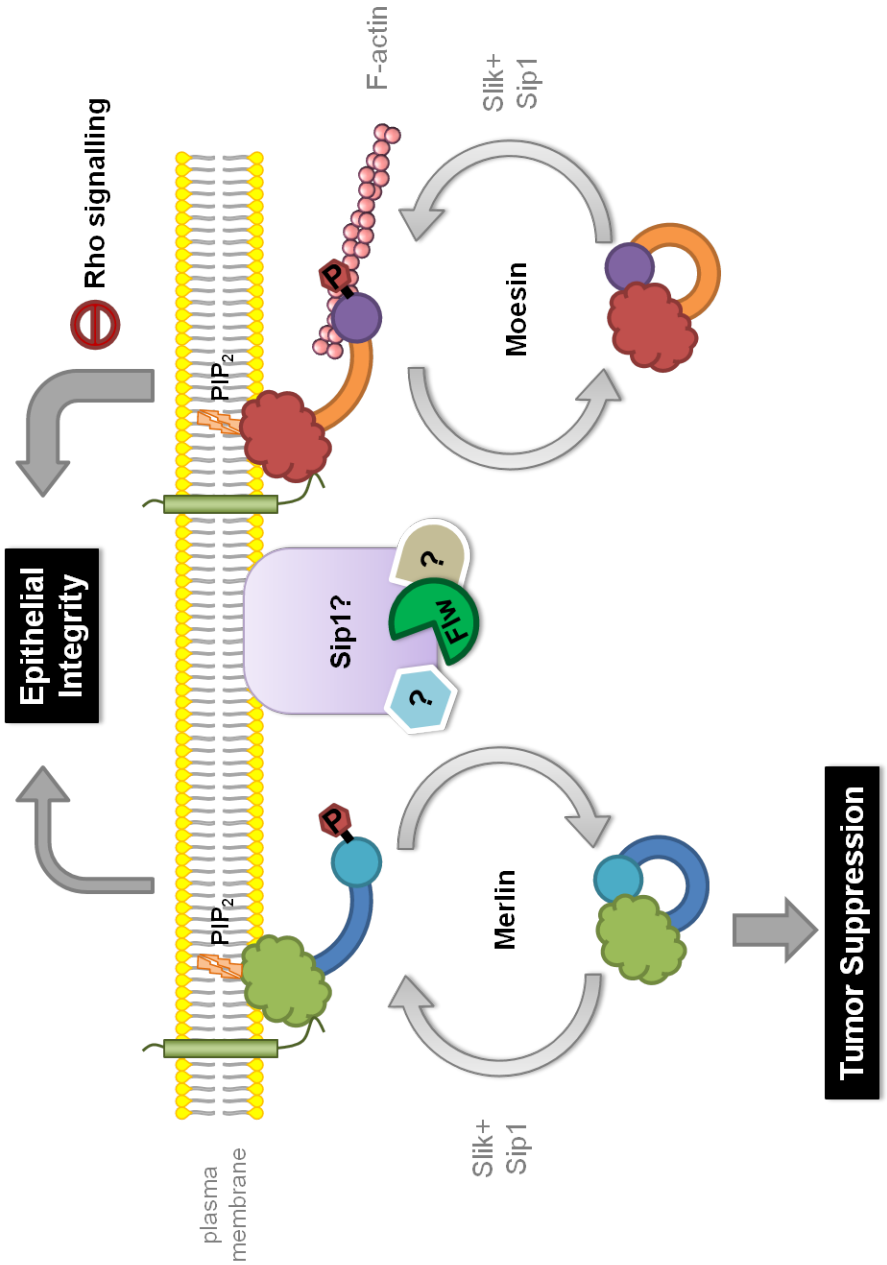
Rho signalling
Epithelial Integrity
F-actin
Slik+ Sip1
Moesin
PIP2
P
Sip1?
FlW
?
?
Merlin
Slik+ Sip1
plasma membrane
Tumor Suppression

Figure 20 | A putative model for the regulation of Merlin and Moesin activity by flw. Merlin and Moesin are coordinately dephosphorylated by the PP1 flw, which possibly utilizes the scaffolding protein Sip1 as a membrane docking site. Other regulatory proteins may be present in the Sip1-flw protein complex to modulate the signaling activity of the complex. Phosphorylation at the C-terminal domain of Mer and Moe, which may be facilitated by the PIP_2-assocation, leads to conformational switch of the protein and the change in their activities. When activated, Moesin interacts with F-actin. Both Mer and Moe participate in regulating cell adhesion and epithelial integrity, whereas Mer plays an additional role in suppressing cell proliferation. Moe exerts its function in part by negatively regulating the Rho signaling pathway. The coordinate activation-inactivation cycle of Mer and Moe is reversely regulated by the kinase Slik, upon the facilitation by Sip1.

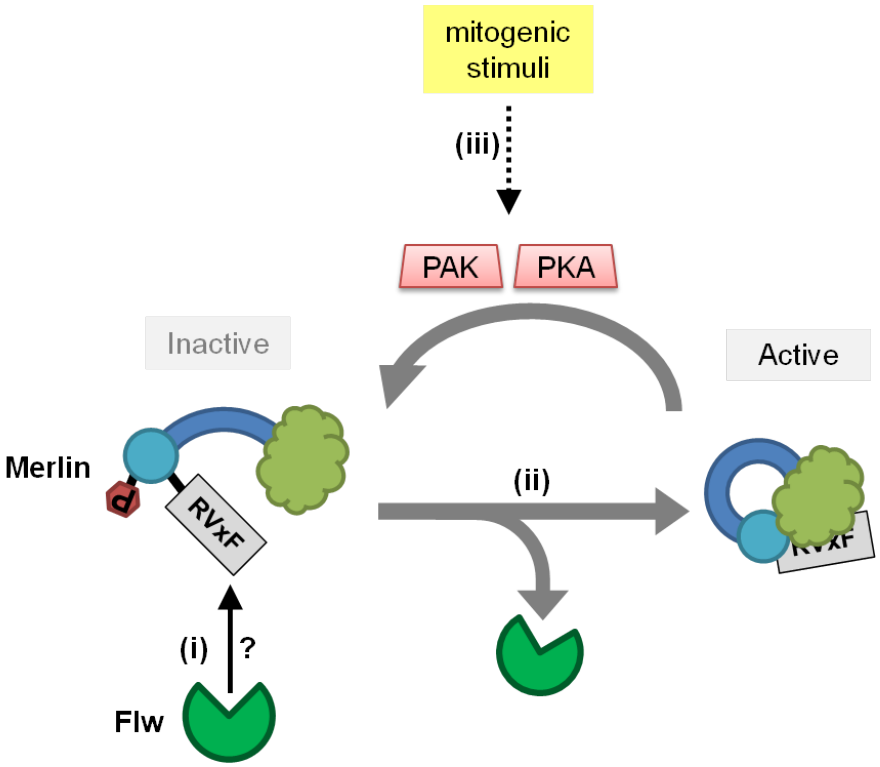

Figure 21 | A putative model of Merlin::flw interaction and their potential mutual regulation. (i) Merlin contains a PP1-binding RVxF binding motif at its C-terminus. The phosphorylated, 'open' Merlin may bind to the *Drosophila* PP1 flw via its RVxF motif, and modulates the subcellular localization of flw and/or its specificity toward other substrates. **(ii)** Merlin as a substrate of flw becomes dephosphoryated, which causes the intramolecular interaction of Merlin and activation of its tumor suppressor function. The RVxF motif is masked in the 'closed' Merlin conformer. **(iii)** Merlin is phosphorylated by PAK and PKA in response to mitogenic stimuli. Once inactivated, Merlin no longer inhibits cell proliferation, and cells switch to the growth permissive condition.

Chapter Five

Future Directions

1. Identifying Additional Components of the flw-containing Complex

In this work, flapwing the *Drosophila* PP1c-β9c is identified as the phosphatase of Merlin and Moesin. However, flw is the catalytic subunit of the PP1 holoenzyme and a regulatory subunit must interact with flw to define its substrate specificity to Mer and Moe and/or to facilitate its targeting at close proximity to the apical membrane compartment where Mer and Moe is enriched.

Previous studies have demonstrated that several regulatory (R) subunits of PP1c are involved in regulating the activity of Mer and Moe both in *Drosophila* and mammals. In particular, the conserved R subunit of PP1, MYPT-1, was demonstrated to interact with both Merlin and with ERMs, and is involved in the phosphorylation of Merlin at S518 in mammalian cells (Fukata et al, 1998; Jin et al, 2006). The *Drosophila* orthologue of MYPT-1, MYPT-75D was found to co-immunopreciptate with flw in *Drosophila* tissues overexpressing both epitope-tagged Mer and Moe (Vereshchagina et al, 2004). Moreover, overexpressing a mutant form of MYPT-75D caused oocyte polarity defects similar to, but milder than the phenotype of loss of function of *flw* (Sun et al, 2011). In addition, another PP1 regulatory subunit, Sds22, is involved in the phosphorylation of Moesin in *Drosophila*, and its mutant displayed a similar phenotype in disruption of epithelial morphology to that of *flw* (Grusche et al, 2009; Jiang et al, 2011). Therefore, MYPT-75D and Sds22 are two potential regulatory subunits of flw in regulating Mer and Moe phosphorylation. To test this, co-IP for MYPT-75D and Sds22 can be carried out using *Drosophila* S2 cells cotransfected with epitope-tagged MYPT-75D,

Sds22 and flw. The detection of MYPT-75D and/or Sds22 in association with the flw-containing complex would suggest that MYPT-75D and/or Sds22 are the regulatory subunits of the PP1 flw. Furthermore, epistatic analyses can be performed to investigate the genetic interactions between *flw* and *MYPT-75D* as well as *flw* and *Sds22*. For example, wing disc tissue in which the expression of *flw* and *MYPT-75D*/*Sds22* was reduced by using RNAi-mediated knockdown can be examined for potential defects in epithelial morphology. If the double knockdown mutant exhibits a more severe phenotype than any of the single knockdowns, it may be inferred that *flw* and the two putative PP1 regulatory subunits function in the same biochemical pathway.

2. *Determining the Role of Sip1 in flw-mediated Phosphorylation*

There are three reasons that Sip1 is a good candidate as the activity modulator of the flw-containing complex: First, Sip1 was found to bind flw in *in vitro* pulldown assay in this study (Figure 5C). Second, Sip1 is a membrane-cytoskeleton linker localized to the apical membrane of the epithelial cells with partial co-localization with apical F-actin (Fouassier et al, 2001; Hughes et al, 2010; Kreimann et al, 2007; Weinman et al, 1995). Lastly, Sip1 directly interacts with the FERM domain of ERM proteins and is required for the activating phosphorylation of Mer and Moe by the Slik kinase (Hughes et al, 2010; Morales et al, 2007; Reczek et al, 1997).

To test if Sip1 plays a role in dephosphorylation of Mer and Moe in the flw-containing complex, the first step is to determine whether Sip1 is present in the flw-containing protein complex *in vivo*. *Drosophila* S2 cells co-transfected with epitope-tagged Sip1 and HA-flw can be used for co-IP of Sip1 using the anti-HA antibody. Alternatively, co-IP of HA-flw using the anti-Sip1 antibody can be performed with the *Drosophila* wing disc tissue lysate overexpressing UAS HA-*flw* using the MS1096-Gal4 driver.

To determine whether Sip1 is required for the function of flw-containing complex in Mer and Moe phosphorylation, loss of function of *Sip1* homozygous mutant embryo tissue lysate (e.g. $Sip1^{06373}$ (Hughes et al, 2010; Spradling et al, 1999)) can be used for Mer and Moe phosphorylation analyses in which *flw* is overexpressed using a ubiquitously expressing Gal4 driver (e.g. $Sip1^{06373}$/ $Sip1^{06373}$, *Actin5c*-Gal4 UAS-*flw*). $Sip1^{06373}$ homozygosity causes lethality just before or shortly after embryo hatching, thus tissues at a later developmental stage are not available for analyses (Hughes et al, 2010). The ratio of hypo-phosphorylated Mer and Moe to the hyper-phosphoryated isoforms will be compared to that in tissue with wild type *Sip1* and overexpressed *flw* (*Actin5c*-Gal4 X UAS-*flw*), as well as the wild type control (*Actin5c*-Gal4 X w^{1118}). If Sip1 is required for flw-mediated phosphorylation, in the *Sip1* homozygous null sample, the pattern of the phospho-isoforms of Mer and Moe will be similar to the wild type control, since loss of expression of *Sip1* abrogates flw-mediated phosphorylation. On the other hand, if Sip1 is not required, the phosphorylation patterns of Mer and Moe will be more

similar to that with *flw* overexpression, since phosphorylation of Mer and Moe by flw is independent of Sip1 in this case.

3. Determine Whether Loss of flw Confers Metastatic Properties

The observation of round epithelial cells on the ventral side of the wing disc in *apt*-Gal X UAS *flw*-IR (Figure 14 D′ and G′) leads to the speculation that these cells might have originated from the dorsal epithelia and migrated across the boundary due to altered cell adhesion and enhanced motility. To confirm the origin of the cells, larval and early pupal wing disc tissue with reduced *flw* expression shall be marked by GFP-expression (e.g. *apt*-Gal4 X UAS *flw*-IR, UAS-GFP). Since the location of cells in each compartment is restricted by boundaries in normal tissues, the detection of GFP-positive cells on the ventral side of the D-V boundary would suggest the dorsal origin of the cells and their enhanced migratory potential.

The potential increase of cell invasiveness upon *flw* knockdown could be a result of the altered activity of any or all of the following three independent signaling pathways: (1) Over-phosphorylation of Merlin which impairs its activity in inhibiting cell invasion. It has been proposed that Merlin may function both as a structural component to stabilize intercellular adhesion as well as a signaling component to down-regulate Rac activation (Shaw et al, 2001). (2) Mis-localization of active Moesin which causes its aberrant activity in regulating Rho signaling (Speck et al, 2003). (3) Change in the

phosphorylation of other established and unknown flw targets and their activity in controlling cell adhesion and migration.

To determine whether flw regulates cell motility and invasiveness by affecting the signaling pathways downstream of Mer and Moe, epistatic analyses can be performed. Specifically, *flw* expression can be reduced in the disc tissues which overexpress constitutively active Rho- or Rac-GTPase, both of which are critical regulators of actin-cytoskeleton reorganization and cell motility (Bustelo, 2012; Szczepanowska, 2009). If Rho and/or Rac function downstream of flw, with Mer and/or Moe being the signaling intermediate, the phenotype of epithelial morphology and integrity upon *flw* knockdown is expected to be fully or partially rescued by overexpression of the GTPases.

Bibliography

Adams JM, Cory S (2007) Bcl-2-regulated apoptosis: mechanism and therapeutic potential. *Current opinion in immunology* **19:** 488-496

Adelstein RS, Conti MA, Anderson W, Jr. (1973) Phosphorylation of platelet myosin. *Series haematologica* **6:** 403-409

Ahn JY, Liu X, Liu Z, Pereira L, Cheng D, Peng J, Wade PA, Hamburger AW, Ye K (2006) Nuclear Akt associates with PKC-phosphorylated Ebp1, preventing DNA fragmentation by inhibition of caspase-activated DNase. *EMBO J* **25:** 2083-2095

Ahronowitz I, Xin W, Kiely R, Sims K, MacCollin M, Nunes FP (2007) Mutational spectrum of the NF2 gene: a meta-analysis of 12 years of research and diagnostic laboratory findings. *Human mutation* **28:** 1-12

Akhmametyeva EM, Mihaylova MM, Luo H, Kharzai S, Welling DB, Chang LS (2006) Regulation of the neurofibromatosis 2 gene promoter expression during embryonic development. *Developmental dynamics : an official publication of the American Association of Anatomists* **235:** 2771-2785

Alfthan K, Heiska L, Gronholm M, Renkema GH, Carpen O (2004) Cyclic AMP-dependent protein kinase phosphorylates merlin at serine 518 independently of p21-activated kinase and promotes merlin-ezrin heterodimerization. *J Biol Chem* **279:** 18559-18566

Ambach A, Saunus J, Konstandin M, Wesselborg S, Meuer SC, Samstag Y (2000) The serine phosphatases PP1 and PP2A associate with and activate the actin-binding protein cofilin in human T lymphocytes. *European journal of immunology* **30:** 3422-3431

Ammoun S, Flaiz C, Ristic N, Schuldt J, Hanemann CO (2008) Dissecting and targeting the growth factor-dependent and growth factor-independent extracellular signal-regulated kinase pathway in human schwannoma. *Cancer Res* **68:** 5236-5245

Axton JM, Dombradi V, Cohen PT, Glover DM (1990) One of the protein phosphatase 1 isoenzymes in Drosophila is essential for mitosis. *Cell* **63:** 33-46

Bai Y, Liu YJ, Wang H, Xu Y, Stamenkovic I, Yu Q (2007) Inhibition of the hyaluronan-CD44 interaction by merlin contributes to the tumor-suppressor activity of merlin. *Oncogene* **26:** 836-850

Barret C, Roy C, Montcourrier P, Mangeat P, Niggli V (2000) Mutagenesis of the phosphatidylinositol 4,5-bisphosphate (PIP(2)) binding site in the NH(2)-terminal domain of ezrin correlates with its altered cellular distribution. *J Cell Biol* **151:** 1067-1080

Barton GJ, Cohen PT, Barford D (1994) Conservation analysis and structure prediction of the protein serine/threonine phosphatases. Sequence similarity with diadenosine tetraphosphatase from Escherichia coli suggests homology to the protein phosphatases. *European journal of biochemistry / FEBS* **220:** 225-237

Baser ME, Contributors to the International NFMD (2006) The distribution of constitutional and somatic mutations in the neurofibromatosis 2 gene. *Human mutation* **27:** 297-306

Bashour AM, Meng JJ, Ip W, MacCollin M, Ratner N (2002) The neurofibromatosis type 2 gene product, merlin, reverses the F-actin cytoskeletal defects in primary human Schwannoma cells. *Mol Cell Biol* **22:** 1150-1157

Baumgartner R, Poernbacher I, Buser N, Hafen E, Stocker H (2010) The WW domain protein Kibra acts upstream of Hippo in Drosophila. *Dev Cell* **18:** 309-316

Bhat MA, Izaddoost S, Lu Y, Cho KO, Choi KW, Bellen HJ (1999) Discs Lost, a novel multi-PDZ domain protein, establishes and maintains epithelial polarity. *Cell* **96:** 833-845

Bianchi AB, Hara T, Ramesh V, Gao J, Klein-Szanto AJ, Morin F, Menon AG, Trofatter JA, Gusella JF, Seizinger BR, et al. (1994) Mutations in transcript isoforms of the neurofibromatosis 2 gene in multiple human tumour types. *Nat Genet* **6:** 185-192

Bilder D, Li M, Perrimon N (2000) Cooperative regulation of cell polarity and growth by Drosophila tumor suppressors. *Science* **289:** 113-116

Bollen M (2001) Combinatorial control of protein phosphatase-1. *Trends in biochemical sciences* **26:** 426-431

Bollen M, Peti W, Ragusa MJ, Beullens M (2010) The extended PP1 toolkit: designed to create specificity. *Trends in biochemical sciences* **35:** 450-458

Brand AH, Perrimon N (1993) Targeted gene expression as a means of altering cell fates and generating dominant phenotypes. *Development* **118:** 401-415

Brault E, Gautreau A, Lamarine M, Callebaut I, Thomas G, Goutebroze L (2001) Normal membrane localization and actin association of the NF2 tumor

suppressor protein are dependent on folding of its N-terminal domain. *J Cell Sci* **114:** 1901-1912

Bretscher A, Edwards K, Fehon RG (2002) ERM proteins and merlin: integrators at the cell cortex. *Nat Rev Mol Cell Biol* **3:** 586-599

Bustelo XR (2012) Intratumoral stages of metastatic cells: a synthesis of ontogeny, Rho/Rac GTPases, epithelial-mesenchymal transitions, and more. *Bioessays* **34:** 748-759

Canals D, Roddy P, Hannun YA (2012) Protein phosphatase 1alpha mediates ceramide-induced ERM protein dephosphorylation: a novel mechanism independent of phosphatidylinositol 4, 5-biphosphate (PIP2) and myosin/ERM phosphatase. *J Biol Chem* **287:** 10145-10155

Carreno S, Kouranti I, Glusman ES, Fuller MT, Echard A, Payre F (2008) Moesin and its activating kinase Slik are required for cortical stability and microtubule organization in mitotic cells. *J Cell Biol* **180:** 739-746

Chacko S, Conti MA, Adelstein RS (1977) Effect of phosphorylation of smooth muscle myosin on actin activation and Ca2+ regulation. *Proc Natl Acad Sci U S A* **74:** 129-133

Cho E, Feng Y, Rauskolb C, Maitra S, Fehon R, Irvine KD (2006) Delineation of a Fat tumor suppressor pathway. *Nat Genet* **38:** 1142-1150

Clift D, Bizzari F, Marston AL (2009) Shugoshin prevents cohesin cleavage by PP2A(Cdc55)-dependent inhibition of separase. *Genes Dev* **23:** 766-780

Cohen PT (1988) Two isoforms of protein phosphatase 1 may be produced from the same gene. *FEBS Lett* **232:** 17-23

Cohen PT (1997) Novel protein serine/threonine phosphatases: variety is the spice of life. *Trends in biochemical sciences* **22:** 245-251

Cole BK, Curto M, Chan AW, McClatchey AI (2008) Localization to the cortical cytoskeleton is necessary for Nf2/merlin-dependent epidermal growth factor receptor silencing. *Mol Cell Biol* **28:** 1274-1284

Cox RT, Kirkpatrick C, Peifer M (1996) Armadillo is required for adherens junction assembly, cell polarity, and morphogenesis during Drosophila embryogenesis. *J Cell Biol* **134:** 133-148

Curto M, Cole BK, Lallemand D, Liu CH, McClatchey AI (2007) Contact-dependent inhibition of EGFR signaling by Nf2/Merlin. *J Cell Biol* **177:** 893-903

Curto M, McClatchey AI (2008) Nf2/Merlin: a coordinator of receptor signalling and intercellular contact. *Br J Cancer* **98:** 256-262

Deak, II (1977) Mutations of Drosophila melanogaster that affect muscles. *Journal of embryology and experimental morphology* **40:** 35-63

del Peso L, Gonzalez-Garcia M, Page C, Herrera R, Nunez G (1997) Interleukin-3-induced phosphorylation of BAD through the protein kinase Akt. *Science* **278:** 687-689

Dessauge F, Cayla X, Albar JP, Fleischer A, Ghadiri A, Duhamel M, Rebollo A (2006) Identification of PP1alpha as a caspase-9 regulator in IL-2 deprivation-induced apoptosis. *Journal of immunology* **177:** 2441-2451

Di Guglielmo GM, Le Roy C, Goodfellow AF, Wrana JL (2003) Distinct endocytic pathways regulate TGF-beta receptor signalling and turnover. *Nat Cell Biol* **5:** 410-421

Doi Y, Itoh M, Yonemura S, Ishihara S, Takano H, Noda T, Tsukita S (1999) Normal development of mice and unimpaired cell adhesion/cell motility/actin-based cytoskeleton without compensatory up-regulation of ezrin or radixin in moesin gene knockout. *J Biol Chem* **274:** 2315-2321

Dombradi V, Axton JM, Brewis ND, da Cruz e Silva EF, Alphey L, Cohen PT (1990) Drosophila contains three genes that encode distinct isoforms of protein phosphatase 1. *European journal of biochemistry / FEBS* **194:** 739-745

Dombradi V, Cohen PT (1992) Protein phosphorylation is involved in the regulation of chromatin condensation during interphase. *FEBS Lett* **312:** 21-26

Duffy JB (2002) GAL4 system in Drosophila: a fly geneticist's Swiss army knife. *Genesis* **34:** 1-15

Edgar BA (2006) From cell structure to transcription: Hippo forges a new path. *Cell* **124:** 267-273

Egloff MP, Johnson DF, Moorhead G, Cohen PT, Cohen P, Barford D (1997) Structural basis for the recognition of regulatory subunits by the catalytic subunit of protein phosphatase 1. *EMBO J* **16:** 1876-1887

Emanuele MJ, Lan W, Jwa M, Miller SA, Chan CS, Stukenberg PT (2008) Aurora B kinase and protein phosphatase 1 have opposing roles in modulating kinetochore assembly. *J Cell Biol* **181:** 241-254

Endo S, Zhou X, Connor J, Wang B, Shenolikar S (1996) Multiple structural elements define the specificity of recombinant human inhibitor-1 as a protein phosphatase-1 inhibitor. *Biochemistry* **35:** 5220-5228

Eto M, Kitazawa T, Yazawa M, Mukai H, Ono Y, Brautigan DL (2001) Histamine-induced vasoconstriction involves phosphorylation of a specific

inhibitor protein for myosin phosphatase by protein kinase C alpha and delta isoforms. *J Biol Chem* **276:** 29072-29078

Evans DG, Huson SM, Donnai D, Neary W, Blair V, Newton V, Harris R (1992a) A clinical study of type 2 neurofibromatosis. *The Quarterly journal of medicine* **84:** 603-618

Evans DG, Huson SM, Donnai D, Neary W, Blair V, Newton V, Strachan T, Harris R (1992b) A genetic study of type 2 neurofibromatosis in the United Kingdom. II. Guidelines for genetic counselling. *J Med Genet* **29:** 847-852

Evans DG, Moran A, King A, Saeed S, Gurusinghe N, Ramsden R (2005) Incidence of vestibular schwannoma and neurofibromatosis 2 in the North West of England over a 10-year period: higher incidence than previously thought. *Otology & neurotology : official publication of the American Otological Society, American Neurotology Society [and] European Academy of Otology and Neurotology* **26:** 93-97

Feng J, Ito M, Ichikawa K, Isaka N, Nishikawa M, Hartshorne DJ, Nakano T (1999) Inhibitory phosphorylation site for Rho-associated kinase on smooth muscle myosin phosphatase. *J Biol Chem* **274:** 37385-37390

Fouassier L, Duan CY, Feranchak AP, Yun CH, Sutherland E, Simon F, Fitz JG, Doctor RB (2001) Ezrin-radixin-moesin-binding phosphoprotein 50 is expressed at the apical membrane of rat liver epithelia. *Hepatology* **33:** 166-176

Freeman MR, Doherty J (2006) Glial cell biology in Drosophila and vertebrates. *Trends in neurosciences* **29:** 82-90

Fukata Y, Kimura K, Oshiro N, Saya H, Matsuura Y, Kaibuchi K (1998) Association of the myosin-binding subunit of myosin phosphatase and moesin: dual regulation of moesin phosphorylation by Rho-associated kinase and myosin phosphatase. *J Cell Biol* **141:** 409-418

Gary R, Bretscher A (1995) Ezrin self-association involves binding of an N-terminal domain to a normally masked C-terminal domain that includes the F-actin binding site. *Molecular biology of the cell* **6:** 1061-1075

Genevet A, Wehr MC, Brain R, Thompson BJ, Tapon N (2010) Kibra is a regulator of the Salvador/Warts/Hippo signaling network. *Dev Cell* **18:** 300-308

Gibbons JA, Kozubowski L, Tatchell K, Shenolikar S (2007) Expression of human protein phosphatase-1 in Saccharomyces cerevisiae highlights the role of phosphatase isoforms in regulating eukaryotic functions. *J Biol Chem* **282:** 21838-21847

Giono LE, Manfredi JJ (2006) The p53 tumor suppressor participates in multiple cell cycle checkpoints. *J Cell Physiol* **209:** 13-20

Giovannini M, Robanus-Maandag E, Niwa-Kawakita M, van der Valk M, Woodruff JM, Goutebroze L, Merel P, Berns A, Thomas G (1999) Schwann cell hyperplasia and tumors in transgenic mice expressing a naturally occurring mutant NF2 protein. *Genes Dev* **13:** 978-986

Gogvadze V, Orrenius S, Zhivotovsky B (2006) Multiple pathways of cytochrome c release from mitochondria in apoptosis. *Biochim Biophys Acta* **1757:** 639-647

Golovnina K, Blinov A, Akhmametyeva EM, Omelyanchuk LV, Chang LS (2005) Evolution and origin of merlin, the product of the Neurofibromatosis type 2 (NF2) tumor-suppressor gene. *BMC Evol Biol* **5:** 69

Gonzalez-Agosti C, Xu L, Pinney D, Beauchamp R, Hobbs W, Gusella J, Ramesh V (1996) The merlin tumor suppressor localizes preferentially in membrane ruffles. *Oncogene* **13:** 1239-1247

Goulev Y, Fauny JD, Gonzalez-Marti B, Flagiello D, Silber J, Zider A (2008) SCALLOPED interacts with YORKIE, the nuclear effector of the hippo tumor-suppressor pathway in Drosophila. *Curr Biol* **18:** 435-441

Grusche FA, Hidalgo C, Fletcher G, Sung HH, Sahai E, Thompson BJ (2009) Sds22, a PP1 phosphatase regulatory subunit, regulates epithelial cell polarity and shape [Sds22 in epithelial morphology]. *BMC developmental biology* **9:** 14

Gusella JF, Ramesh V, MacCollin M, Jacoby LB (1996) Neurofibromatosis 2: loss of merlin's protective spell. *Curr Opin Genet Dev* **6:** 87-92

Gusella JF, Ramesh V, MacCollin M, Jacoby LB (1999) Merlin: the neurofibromatosis 2 tumor suppressor. *Biochim Biophys Acta* **1423:** M29-36

Gutmann DH, Haipek CA, Hoang Lu K (1999) Neurofibromatosis 2 tumor suppressor protein, merlin, forms two functionally important intramolecular associations. *Journal of neuroscience research* **58:** 706-716

Hagting A, Den Elzen N, Vodermaier HC, Waizenegger IC, Peters JM, Pines J (2002) Human securin proteolysis is controlled by the spindle checkpoint and reveals when the APC/C switches from activation by Cdc20 to Cdh1. *J Cell Biol* **157:** 1125-1137

Hamaratoglu F, Willecke M, Kango-Singh M, Nolo R, Hyun E, Tao C, Jafar-Nejad H, Halder G (2006) The tumour-suppressor genes NF2/Merlin and Expanded act through Hippo signalling to regulate cell proliferation and apoptosis. *Nat Cell Biol* **8:** 27-36

Hanahan D, Weinberg RA (2000) The hallmarks of cancer. *Cell* **100:** 57-70

Hao JJ, Liu Y, Kruhlak M, Debell KE, Rellahan BL, Shaw S (2009) Phospholipase C-mediated hydrolysis of PIP2 releases ERM proteins from lymphocyte membrane. *J Cell Biol* **184:** 451-462

Harada H, Becknell B, Wilm M, Mann M, Huang LJ, Taylor SS, Scott JD, Korsmeyer SJ (1999) Phosphorylation and inactivation of BAD by mitochondria-anchored protein kinase A. *Molecular cell* **3:** 413-422

Harrisingh MC, Lloyd AC (2004) Ras/Raf/ERK signalling and NF1. *Cell cycle* **3:** 1255-1258

Hartshorne DJ (1998) Myosin phosphatase: subunits and interactions. *Acta physiologica Scandinavica* **164:** 483-493

Hergovich A, Hemmings BA (2009) Mammalian NDR/LATS protein kinases in hippo tumor suppressor signaling. *BioFactors* **35:** 338-345

Heroes E, Lesage B, Gornemann J, Beullens M, Van Meervelt L, Bollen M (2013) The PP1 binding code: a molecular-lego strategy that governs specificity. *The FEBS journal* **280:** 584-595

Herzog F, Primorac I, Dube P, Lenart P, Sander B, Mechtler K, Stark H, Peters JM (2009) Structure of the anaphase-promoting complex/cyclosome interacting with a mitotic checkpoint complex. *Science* **323:** 1477-1481

Hipfner DR, Keller N, Cohen SM (2004) Slik Sterile-20 kinase regulates Moesin activity to promote epithelial integrity during tissue growth. *Genes Dev* **18:** 2243-2248

Hosoya T, Takizawa K, Nitta K, Hotta Y (1995) glial cells missing: a binary switch between neuronal and glial determination in Drosophila. *Cell* **82:** 1025-1036

Hsu JY, Sun ZW, Li X, Reuben M, Tatchell K, Bishop DK, Grushcow JM, Brame CJ, Caldwell JA, Hunt DF, Lin R, Smith MM, Allis CD (2000) Mitotic phosphorylation of histone H3 is governed by Ipl1/aurora kinase and Glc7/PP1 phosphatase in budding yeast and nematodes. *Cell* **102:** 279-291

Huang J, Wu S, Barrera J, Matthews K, Pan D (2005) The Hippo signaling pathway coordinately regulates cell proliferation and apoptosis by inactivating Yorkie, the Drosophila Homolog of YAP. *Cell* **122:** 421-434

Hughes SC, Fehon RG (2006) Phosphorylation and activity of the tumor suppressor Merlin and the ERM protein Moesin are coordinately regulated by the Slik kinase. *J Cell Biol* **175:** 305-313

Hughes SC, Formstecher E, Fehon RG (2010) Sip1, the Drosophila orthologue of EBP50/NHERF1, functions with the sterile 20 family kinase Slik to regulate Moesin activity. *J Cell Sci* **123:** 1099-1107

Ikebe M, Hartshorne DJ, Elzinga M (1986) Identification, phosphorylation, and dephosphorylation of a second site for myosin light chain kinase on the 20,000-dalton light chain of smooth muscle myosin. *J Biol Chem* **261:** 36-39

Ito M, Nakano T, Erdodi F, Hartshorne DJ (2004) Myosin phosphatase: structure, regulation and function. *Molecular and cellular biochemistry* **259:** 197-209

Jiang Y, Scott KL, Kwak SJ, Chen R, Mardon G (2011) Sds22/PP1 links epithelial integrity and tumor suppression via regulation of myosin II and JNK signaling. *Oncogene* **30:** 3248-3260

Jin H, Sperka T, Herrlich P, Morrison H (2006) Tumorigenic transformation by CPI-17 through inhibition of a merlin phosphatase. *Nature* **442:** 576-579

Jones BW, Fetter RD, Tear G, Goodman CS (1995) glial cells missing: a genetic switch that controls glial versus neuronal fate. *Cell* **82:** 1013-1023

Kaempchen K, Mielke K, Utermark T, Langmesser S, Hanemann CO (2003) Upregulation of the Rac1/JNK signaling pathway in primary human schwannoma cells. *Human molecular genetics* **12:** 1211-1221

Katayose Y, Li M, Al-Murrani SW, Shenolikar S, Damuni Z (2000) Protein phosphatase 2A inhibitors, I(1)(PP2A) and I(2)(PP2A), associate with and modify the substrate specificity of protein phosphatase 1. *J Biol Chem* **275:** 9209-9214

Kim J, Jones BW, Zock C, Chen Z, Wang H, Goodman CS, Anderson DJ (1998) Isolation and characterization of mammalian homologs of the Drosophila gene glial cells missing. *Proc Natl Acad Sci U S A* **95:** 12364-12369

Kim Y, Holland AJ, Lan W, Cleveland DW (2010) Aurora kinases and protein phosphatase 1 mediate chromosome congression through regulation of CENP-E. *Cell* **142:** 444-455

Kirchner J, Gross S, Bennett D, Alphey L (2007) The nonmuscle myosin phosphatase PP1beta (flapwing) negatively regulates Jun N-terminal kinase in wing imaginal discs of Drosophila. *Genetics* **175:** 1741-1749

Kissil JL, Johnson KC, Eckman MS, Jacks T (2002) Merlin phosphorylation by p21-activated kinase 2 and effects of phosphorylation on merlin localization. *J Biol Chem* **277:** 10394-10399

Kissil JL, Wilker EW, Johnson KC, Eckman MS, Yaffe MB, Jacks T (2003) Merlin, the product of the Nf2 tumor suppressor gene, is an inhibitor of the p21-activated kinase, Pak1. *Molecular cell* **12:** 841-849

Kley N, Seizinger BR (1995) The neurofibromatosis 2 (NF2) tumour suppressor gene: implications beyond the hereditary tumour syndrome? *Cancer surveys* **25:** 207-218

Knust E, Bossinger O (2002) Composition and formation of intercellular junctions in epithelial cells. *Science* **298:** 1955-1959

Koyama M, Ito M, Feng J, Seko T, Shiraki K, Takase K, Hartshorne DJ, Nakano T (2000) Phosphorylation of CPI-17, an inhibitory phosphoprotein of smooth muscle myosin phosphatase, by Rho-kinase. *FEBS Lett* **475:** 197-200

Kreimann EL, Morales FC, de Orbeta-Cruz J, Takahashi Y, Adams H, Liu TJ, McCrea PD, Georgescu MM (2007) Cortical stabilization of beta-catenin contributes to NHERF1/EBP50 tumor suppressor function. *Oncogene* **26:** 5290-5299

Kulukian A, Han JS, Cleveland DW (2009) Unattached kinetochores catalyze production of an anaphase inhibitor that requires a Mad2 template to prime Cdc20 for BubR1 binding. *Dev Cell* **16:** 105-117

Kunda P, Rodrigues NT, Moeendarbary E, Liu T, Ivetic A, Charras G, Baum B (2012) PP1-mediated moesin dephosphorylation couples polar relaxation to mitotic exit. *Curr Biol* **22:** 231-236

Kwon YG, Huang HB, Desdouits F, Girault JA, Greengard P, Nairn AC (1997) Characterization of the interaction between DARPP-32 and protein phosphatase 1 (PP-1): DARPP-32 peptides antagonize the interaction of PP-1 with binding proteins. *Proc Natl Acad Sci U S A* **94:** 3536-3541

Lai ZC, Wei X, Shimizu T, Ramos E, Rohrbaugh M, Nikolaidis N, Ho LL, Li Y (2005) Control of cell proliferation and apoptosis by mob as tumor suppressor, mats. *Cell* **120:** 675-685

LaJeunesse DR, McCartney BM, Fehon RG (1998) Structural analysis of Drosophila merlin reveals functional domains important for growth control and subcellular localization. *J Cell Biol* **141:** 1589-1599

LaJeunesse DR, McCartney BM, Fehon RG (2001) A systematic screen for dominant second-site modifiers of Merlin/NF2 phenotypes reveals an interaction with blistered/DSRF and scribbler. *Genetics* **158:** 667-679

Lallemand D, Curto M, Saotome I, Giovannini M, McClatchey AI (2003) NF2 deficiency promotes tumorigenesis and metastasis by destabilizing adherens junctions. *Genes Dev* **17:** 1090-1100

Lamb RS, Ward RE, Schweizer L, Fehon RG (1998) Drosophila coracle, a member of the protein 4.1 superfamily, has essential structural functions in the septate junctions and developmental functions in embryonic and adult epithelial cells. *Molecular biology of the cell* **9:** 3505-3519

Lasota J, Fetsch JF, Wozniak A, Wasag B, Sciot R, Miettinen M (2001) The neurofibromatosis type 2 gene is mutated in perineurial cell tumors: a molecular genetic study of eight cases. *The American journal of pathology* **158:** 1223-1229

Lau YK, Murray LB, Houshmandi SS, Xu Y, Gutmann DH, Yu Q (2008) Merlin is a potent inhibitor of glioma growth. *Cancer Res* **68:** 5733-5742

Laulajainen M, Muranen T, Nyman TA, Carpen O, Gronholm M (2011) Multistep phosphorylation by oncogenic kinases enhances the degradation of the NF2 tumor suppressor merlin. *Neoplasia* **13:** 643-652

Le Roy C, Wrana JL (2005) Clathrin- and non-clathrin-mediated endocytic regulation of cell signalling. *Nat Rev Mol Cell Biol* **6:** 112-126

Lecuit T, Wieschaus E (2002) Junctions as organizing centers in epithelial cells? A fly perspective. *Traffic* **3:** 92-97

Lee A, Treisman JE (2004) Excessive Myosin activity in mbs mutants causes photoreceptor movement out of the Drosophila eye disc epithelium. *Molecular biology of the cell* **15:** 3285-3295

Lee J, Zhou P (2007) DCAFs, the missing link of the CUL4-DDB1 ubiquitin ligase. *Molecular cell* **26:** 775-780

Leiserson WM, Harkins EW, Keshishian H (2000) Fray, a Drosophila serine/threonine kinase homologous to mammalian PASK, is required for axonal ensheathment. *Neuron* **28:** 793-806

Li Q, Gao H, Xu H, Wang X, Pan Y, Hao F, Qiu X, Stoecker M, Wang E, Wang E (2012a) Expression of ezrin correlates with malignant phenotype of lung cancer, and in vitro knockdown of ezrin reverses the aggressive biological behavior of lung cancer cells. *Tumour biology : the journal of the International Society for Oncodevelopmental Biology and Medicine* **33:** 1493-1504

Li W, Cooper J, Karajannis MA, Giancotti FG (2012b) Merlin: a tumour suppressor with functions at the cell cortex and in the nucleus. *EMBO reports*

Li W, You L, Cooper J, Schiavon G, Pepe-Caprio A, Zhou L, Ishii R, Giovannini M, Hanemann CO, Long SB, Erdjument-Bromage H, Zhou P, Tempst P, Giancotti FG (2010) Merlin/NF2 suppresses tumorigenesis by inhibiting the E3 ubiquitin ligase CRL4(DCAF1) in the nucleus. *Cell* **140:** 477-490

Lin Q, Buckler ESt, Muse SV, Walker JC (1999) Molecular evolution of type 1 serine/threonine protein phosphatases. *Molecular phylogenetics and evolution* **12:** 57-66

Liu D, Vleugel M, Backer CB, Hori T, Fukagawa T, Cheeseman IM, Lampson MA (2010) Regulated targeting of protein phosphatase 1 to the outer kinetochore by KNL1 opposes Aurora B kinase. *J Cell Biol* **188:** 809-820

Liu J, Brautigan DL (2000) Glycogen synthase association with the striated muscle glycogen-targeting subunit of protein phosphatase-1. Synthase activation involves scaffolding regulated by beta-adrenergic signaling. *J Biol Chem* **275:** 26074-26081

Lloyd TE, Atkinson R, Wu MN, Zhou Y, Pennetta G, Bellen HJ (2002) Hrs regulates endosome membrane invagination and tyrosine kinase receptor signaling in Drosophila. *Cell* **108:** 261-269

Lomas J, Bello MJ, Arjona D, Alonso ME, Martinez-Glez V, Lopez-Marin I, Aminoso C, de Campos JM, Isla A, Vaquero J, Rey JA (2005) Genetic and epigenetic alteration of the NF2 gene in sporadic meningiomas. *Genes Chromosomes Cancer* **42:** 314-319

Lutchman M, Rouleau GA (1995) The neurofibromatosis type 2 gene product, schwannomin, suppresses growth of NIH 3T3 cells. *Cancer Res* **55:** 2270-2274

Mack NA, Whalley HJ, Castillo-Lluva S, Malliri A (2011) The diverse roles of Rac signaling in tumorigenesis. *Cell cycle* **10:** 1571-1581

Magendantz M, Henry MD, Lander A, Solomon F (1995) Interdomain interactions of radixin in vitro. *J Biol Chem* **270:** 25324-25327

Maitra S, Kulikauskas RM, Gavilan H, Fehon RG (2006) The tumor suppressors Merlin and Expanded function cooperatively to modulate receptor endocytosis and signaling. *Curr Biol* **16:** 702-709

Mani T, Hennigan RF, Foster LA, Conrady DG, Herr AB, Ip W (2011) FERM domain phosphoinositide binding targets merlin to the membrane and is essential for its growth-suppressive function. *Mol Cell Biol* **31:** 1983-1996

Martuza RL, Eldridge R (1988) Neurofibromatosis 2 (bilateral acoustic neurofibromatosis). *The New England journal of medicine* **318:** 684-688

Matsui T, Maeda M, Doi Y, Yonemura S, Amano M, Kaibuchi K, Tsukita S, Tsukita S (1998) Rho-kinase phosphorylates COOH-terminal threonines of ezrin/radixin/moesin (ERM) proteins and regulates their head-to-tail association. *J Cell Biol* **140:** 647-657

Mautner VF, Lindenau M, Baser ME, Hazim W, Tatagiba M, Haase W, Samii M, Wais R, Pulst SM (1996) The neuroimaging and clinical spectrum of neurofibromatosis 2. *Neurosurgery* **38:** 880-885; discussion 885-886

McCartney BM, Fehon RG (1996) Distinct cellular and subcellular patterns of expression imply distinct functions for the Drosophila homologues of moesin and the neurofibromatosis 2 tumor suppressor, merlin. *J Cell Biol* **133:** 843-852

McCartney BM, Kulikauskas RM, LaJeunesse DR, Fehon RG (2000) The neurofibromatosis-2 homologue, Merlin, and the tumor suppressor expanded function together in Drosophila to regulate cell proliferation and differentiation. *Development* **127:** 1315-1324

McClatchey AI, Fehon RG (2009) Merlin and the ERM proteins--regulators of receptor distribution and signaling at the cell cortex. *Trends Cell Biol* **19:** 198-206

McClatchey AI, Giovannini M (2005) Membrane organization and tumorigenesis--the NF2 tumor suppressor, Merlin. *Genes Dev* **19:** 2265-2277

McClatchey AI, Saotome I, Mercer K, Crowley D, Gusella JF, Bronson RT, Jacks T (1998) Mice heterozygous for a mutation at the Nf2 tumor suppressor locus develop a range of highly metastatic tumors. *Genes Dev* **12:** 1121-1133

McClatchey AI, Saotome I, Ramesh V, Gusella JF, Jacks T (1997) The Nf2 tumor suppressor gene product is essential for extraembryonic development immediately prior to gastrulation. *Genes Dev* **11:** 1253-1265

McLaughlin ME, Kruger GM, Slocum KL, Crowley D, Michaud NA, Huang J, Magendantz M, Jacks T (2007) The Nf2 tumor suppressor regulates cell-cell adhesion during tissue fusion. *Proc Natl Acad Sci U S A* **104:** 3261-3266

Medina E, Williams J, Klipfell E, Zarnescu D, Thomas G, Le Bivic A (2002) Crumbs interacts with moesin and beta(Heavy)-spectrin in the apical membrane skeleton of Drosophila. *J Cell Biol* **158:** 941-951

Mercer WE (1992) Cell cycle regulation and the p53 tumor suppressor protein. *Critical reviews in eukaryotic gene expression* **2:** 251-263

Morales FC, Takahashi Y, Kreimann EL, Georgescu MM (2004) Ezrin-radixin-moesin (ERM)-binding phosphoprotein 50 organizes ERM proteins at the apical membrane of polarized epithelia. *Proc Natl Acad Sci U S A* **101:** 17705-17710

Morales FC, Takahashi Y, Momin S, Adams H, Chen X, Georgescu MM (2007) NHERF1/EBP50 head-to-tail intramolecular interaction masks association with PDZ domain ligands. *Mol Cell Biol* **27:** 2527-2537

Morrison DK, Murakami MS, Cleghon V (2000) Protein kinases and phosphatases in the Drosophila genome. *J Cell Biol* **150:** F57-62

Morrison H, Sherman LS, Legg J, Banine F, Isacke C, Haipek CA, Gutmann DH, Ponta H, Herrlich P (2001) The NF2 tumor suppressor gene product,

merlin, mediates contact inhibition of growth through interactions with CD44. *Genes Dev* **15:** 968-980

Morrison H, Sperka T, Manent J, Giovannini M, Ponta H, Herrlich P (2007) Merlin/neurofibromatosis type 2 suppresses growth by inhibiting the activation of Ras and Rac. *Cancer Res* **67:** 520-527

Muller HA, Wieschaus E (1996) armadillo, bazooka, and stardust are critical for early stages in formation of the zonula adherens and maintenance of the polarized blastoderm epithelium in Drosophila. *J Cell Biol* **134:** 149-163

Musacchio A, Salmon ED (2007) The spindle-assembly checkpoint in space and time. *Nat Rev Mol Cell Biol* **8:** 379-393

Nakamura F, Huang L, Pestonjamasp K, Luna EJ, Furthmayr H (1999) Regulation of F-actin binding to platelet moesin in vitro by both phosphorylation of threonine 558 and polyphosphatidylinositides. *Molecular biology of the cell* **10:** 2669-2685

Ng T, Parsons M, Hughes WE, Monypenny J, Zicha D, Gautreau A, Arpin M, Gschmeissner S, Verveer PJ, Bastiaens PI, Parker PJ (2001) Ezrin is a downstream effector of trafficking PKC-integrin complexes involved in the control of cell motility. *EMBO J* **20:** 2723-2741

Nilsson J, Yekezare M, Minshull J, Pines J (2008) The APC/C maintains the spindle assembly checkpoint by targeting Cdc20 for destruction. *Nat Cell Biol* **10:** 1411-1420

O'Connell BC, Harper JW (2007) Ubiquitin proteasome system (UPS): what can chromatin do for you? *Current opinion in cell biology* **19:** 206-214

Oh H, Reddy BV, Irvine KD (2009) Phosphorylation-independent repression of Yorkie in Fat-Hippo signaling. *Dev Biol* **335:** 188-197

Ohno S (2001) Intercellular junctions and cellular polarity: the PAR-aPKC complex, a conserved core cassette playing fundamental roles in cell polarity. *Current opinion in cell biology* **13:** 641-648

Okada T, Lopez-Lago M, Giancotti FG (2005) Merlin/NF-2 mediates contact inhibition of growth by suppressing recruitment of Rac to the plasma membrane. *J Cell Biol* **171:** 361-371

Oleinik NV, Krupenko NI, Krupenko SA (2010) ALDH1L1 inhibits cell motility via dephosphorylation of cofilin by PP1 and PP2A. *Oncogene* **29:** 6233-6244

Olsen JV, Blagoev B, Gnad F, Macek B, Kumar C, Mortensen P, Mann M (2006) Global, in vivo, and site-specific phosphorylation dynamics in signaling networks. *Cell* **127:** 635-648

Olsen JV, Vermeulen M, Santamaria A, Kumar C, Miller ML, Jensen LJ, Gnad F, Cox J, Jensen TS, Nigg EA, Brunak S, Mann M (2010) Quantitative phosphoproteomics reveals widespread full phosphorylation site occupancy during mitosis. *Science signaling* **3:** ra3

Ou-Yang M, Liu HR, Zhang Y, Zhu X, Yang Q (2011) ERM stable knockdown by siRNA reduced in vitro migration and invasion of human SGC-7901 cells. *Biochimie* **93:** 954-961

Pan J, Chen RH (2004) Spindle checkpoint regulates Cdc20p stability in Saccharomyces cerevisiae. *Genes Dev* **18:** 1439-1451

Pantalacci S, Tapon N, Leopold P (2003) The Salvador partner Hippo promotes apoptosis and cell-cycle exit in Drosophila. *Nat Cell Biol* **5:** 921-927

Parry DM, Eldridge R, Kaiser-Kupfer MI, Bouzas EA, Pikus A, Patronas N (1994) Neurofibromatosis 2 (NF2): clinical characteristics of 63 affected individuals and clinical evidence for heterogeneity. *Am J Med Genet* **52:** 450-461

Pellock BJ, Buff E, White K, Hariharan IK (2007) The Drosophila tumor suppressors Expanded and Merlin differentially regulate cell cycle exit, apoptosis, and Wingless signaling. *Dev Biol* **304:** 102-115

Pelton PD, Sherman LS, Rizvi TA, Marchionni MA, Wood P, Friedman RA, Ratner N (1998) Ruffling membrane, stress fiber, cell spreading and proliferation abnormalities in human Schwannoma cells. *Oncogene* **17:** 2195-2209

Peti W, Nairn AC, Page R (2013) Structural basis for protein phosphatase 1 regulation and specificity. *The FEBS journal* **280:** 596-611

Pietromonaco SF, Simons PC, Altman A, Elias L (1998) Protein kinase C-theta phosphorylation of moesin in the actin-binding sequence. *J Biol Chem* **273:** 7594-7603

Pineau P, Marchio A, Nagamori S, Seki S, Tiollais P, Dejean A (2003) Homozygous deletion scanning in hepatobiliary tumor cell lines reveals alternative pathways for liver carcinogenesis. *Hepatology* **37:** 852-861

Pinsky BA, Kotwaliwale CV, Tatsutani SY, Breed CA, Biggins S (2006) Glc7/protein phosphatase 1 regulatory subunits can oppose the Ipl1/aurora protein kinase by redistributing Glc7. *Mol Cell Biol* **26:** 2648-2660

Polesello C, Delon I, Valenti P, Ferrer P, Payre F (2002) Dmoesin controls actin-based cell shape and polarity during Drosophila melanogaster oogenesis. *Nat Cell Biol* **4:** 782-789

Posch M, Khoudoli GA, Swift S, King EM, Deluca JG, Swedlow JR (2010) Sds22 regulates aurora B activity and microtubule-kinetochore interactions at mitosis. *J Cell Biol* **191:** 61-74

Poulikakos PI, Xiao GH, Gallagher R, Jablonski S, Jhanwar SC, Testa JR (2006) Re-expression of the tumor suppressor NF2/merlin inhibits invasiveness in mesothelioma cells and negatively regulates FAK. *Oncogene* **25:** 5960-5968

Raghavan S, Williams I, Aslam H, Thomas D, Szoor B, Morgan G, Gross S, Turner J, Fernandes J, VijayRaghavan K, Alphey L (2000) Protein phosphatase 1beta is required for the maintenance of muscle attachments. *Curr Biol* **10:** 269-272

Rebay I, Fehon RG (2009) Preparation of insoluble GST fusion proteins. *Cold Spring Harbor protocols* **2009:** pdb prot4997

Reczek D, Berryman M, Bretscher A (1997) Identification of EBP50: A PDZ-containing phosphoprotein that associates with members of the ezrin-radixin-moesin family. *J Cell Biol* **139:** 169-179

Reddy BV, Irvine KD (2011) Regulation of Drosophila glial cell proliferation by Merlin-Hippo signaling. *Development* **138:** 5201-5212

Ren L, Hong SH, Cassavaugh J, Osborne T, Chou AJ, Kim SY, Gorlick R, Hewitt SM, Khanna C (2009) The actin-cytoskeleton linker protein ezrin is regulated during osteosarcoma metastasis by PKC. *Oncogene* **28:** 792-802

Robanus-Maandag E, Giovannini M, van der Valk M, Niwa-Kawakita M, Abramowski V, Antonescu C, Thomas G, Berns A (2004) Synergy of Nf2 and p53 mutations in development of malignant tumours of neural crest origin. *Oncogene* **23:** 6541-6547

Roch F, Polesello C, Roubinet C, Martin M, Roy C, Valenti P, Carreno S, Mangeat P, Payre F (2010) Differential roles of PtdIns(4,5)P2 and phosphorylation in moesin activation during Drosophila development. *J Cell Sci* **123:** 2058-2067

Rong R, Surace EI, Haipek CA, Gutmann DH, Ye K (2004) Serine 518 phosphorylation modulates merlin intramolecular association and binding to critical effectors important for NF2 growth suppression. *Oncogene* **23:** 8447-8454

Rottner K, Stradal TE (2011) Actin dynamics and turnover in cell motility. *Current opinion in cell biology* **23:** 569-578

Roubinet C, Decelle B, Chicanne G, Dorn JF, Payrastre B, Payre F, Carreno S (2011) Molecular networks linked by Moesin drive remodeling of the cell cortex during mitosis. *J Cell Biol* **195:** 99-112

Rouleau GA, Merel P, Lutchman M, Sanson M, Zucman J, Marineau C, Hoang-Xuan K, Demczuk S, Desmaze C, Plougastel B, et al. (1993) Alteration in a new gene encoding a putative membrane-organizing protein causes neuro-fibromatosis type 2. *Nature* **363:** 515-521

Ruttledge MH, Sarrazin J, Rangaratnam S, Phelan CM, Twist E, Merel P, Delattre O, Thomas G, Nordenskjold M, Collins VP, et al. (1994) Evidence for the complete inactivation of the NF2 gene in the majority of sporadic meningiomas. *Nat Genet* **6:** 180-184

Sahara S, Aoto M, Eguchi Y, Imamoto N, Yoneda Y, Tsujimoto Y (1999) Acinus is a caspase-3-activated protein required for apoptotic chromatin condensation. *Nature* **401:** 168-173

Sainio M, Zhao F, Heiska L, Turunen O, den Bakker M, Zwarthoff E, Lutchman M, Rouleau GA, Jaaskelainen J, Vaheri A, Carpen O (1997) Neurofibromatosis 2 tumor suppressor protein colocalizes with ezrin and CD44 and associates with actin-containing cytoskeleton. *J Cell Sci* **110 (Pt 18):** 2249-2260

Salimian KJ, Ballister ER, Smoak EM, Wood S, Panchenko T, Lampson MA, Black BE (2011) Feedback control in sensing chromosome biorientation by the Aurora B kinase. *Curr Biol* **21:** 1158-1165

Salzer JL (2003) Polarized domains of myelinated axons. *Neuron* **40:** 297-318

Sasaki K, Shima H, Kitagawa Y, Irino S, Sugimura T, Nagao M (1990) Identification of members of the protein phosphatase 1 gene family in the rat and enhanced expression of protein phosphatase 1 alpha gene in rat hepatocellular carcinomas. *Japanese journal of cancer research : Gann* **81:** 1272-1280

Schulze KM, Hanemann CO, Muller HW, Hanenberg H (2002) Transduction of wild-type merlin into human schwannoma cells decreases schwannoma cell growth and induces apoptosis. *Human molecular genetics* **11:** 69-76

Scoles DR, Huynh DP, Chen MS, Burke SP, Gutmann DH, Pulst SM (2000) The neurofibromatosis 2 tumor suppressor protein interacts with hepatocyte growth factor-regulated tyrosine kinase substrate. *Human molecular genetics* **9:** 1567-1574

Shang X, Wang Y, Zhao Q, Wu K, Li X, Ji X, He R, Zhang W (2012) siRNAs target sites selection of ezrin and the influence of RNA interference on ezrin expression and biological characters of osteosarcoma cells. *Molecular and cellular biochemistry* **364:** 363-371

Shaw PH (1996) The role of p53 in cell cycle regulation. *Pathology, research and practice* **192:** 669-675

Shaw RJ, McClatchey AI, Jacks T (1998) Regulation of the neurofibromatosis type 2 tumor suppressor protein, merlin, by adhesion and growth arrest stimuli. *J Biol Chem* **273:** 7757-7764

Shaw RJ, Paez JG, Curto M, Yaktine A, Pruitt WM, Saotome I, O'Bryan JP, Gupta V, Ratner N, Der CJ, Jacks T, McClatchey AI (2001) The Nf2 tumor suppressor, merlin, functions in Rac-dependent signaling. *Dev Cell* **1:** 63-72

Sheikh HA, Tometsko M, Niehouse L, Aldeeb D, Swalsky P, Finkelstein S, Barnes EL, Hunt JL (2004) Molecular genotyping of medullary thyroid carcinoma can predict tumor recurrence. *The American journal of surgical pathology* **28:** 101-106

Sher I, Hanemann CO, Karplus PA, Bretscher A (2012) The tumor suppressor merlin controls growth in its open state, and phosphorylation converts it to a less-active more-closed state. *Dev Cell* **22:** 703-705

Sherman L, Xu HM, Geist RT, Saporito-Irwin S, Howells N, Ponta H, Herrlich P, Gutmann DH (1997) Interdomain binding mediates tumor growth suppression by the NF2 gene product. *Oncogene* **15:** 2505-2509

Shi Y (2009) Serine/threonine phosphatases: mechanism through structure. *Cell* **139:** 468-484

Shimizu T, Seto A, Maita N, Hamada K, Tsukita S, Tsukita S, Hakoshima T (2002) Structural basis for neurofibromatosis type 2. Crystal structure of the merlin FERM domain. *J Biol Chem* **277:** 10332-10336

Sigismund S, Argenzio E, Tosoni D, Cavallaro E, Polo S, Di Fiore PP (2008) Clathrin-mediated internalization is essential for sustained EGFR signaling but dispensable for degradation. *Dev Cell* **15:** 209-219

Skoufias DA, Indorato RL, Lacroix F, Panopoulos A, Margolis RL (2007) Mitosis persists in the absence of Cdk1 activity when proteolysis or protein phosphatase activity is suppressed. *J Cell Biol* **179:** 671-685

Song Z, Steller H (1999) Death by design: mechanism and control of apoptosis. *Trends Cell Biol* **9:** M49-52

Speck O, Hughes SC, Noren NK, Kulikauskas RM, Fehon RG (2003) Moesin functions antagonistically to the Rho pathway to maintain epithelial integrity. *Nature* **421:** 83-87

Spradling AC, Stern D, Beaton A, Rhem EJ, Laverty T, Mozden N, Misra S, Rubin GM (1999) The Berkeley Drosophila Genome Project gene disruption project: Single P-element insertions mutating 25% of vital Drosophila genes. *Genetics* **153:** 135-177

Stamenkovic I, Yu Q (2009) Shedding light on proteolytic cleavage of CD44: the responsible sheddase and functional significance of shedding. *The Journal of investigative dermatology* **129:** 1321-1324

Stark MJ (1996) Yeast protein serine/threonine phosphatases: multiple roles and diverse regulation. *Yeast* **12:** 1647-1675

Stemmer-Rachamimov AO, Xu L, Gonzalez-Agosti C, Burwick JA, Pinney D, Beauchamp R, Jacoby LB, Gusella JF, Ramesh V, Louis DN (1997) Universal absence of merlin, but not other ERM family members, in schwannomas. *The American journal of pathology* **151:** 1649-1654

Stickney JT, Bacon WC, Rojas M, Ratner N, Ip W (2004) Activation of the tumor suppressor merlin modulates its interaction with lipid rafts. *Cancer Res* **64:** 2717-2724

Striedinger K, VandenBerg SR, Baia GS, McDermott MW, Gutmann DH, Lal A (2008) The neurofibromatosis 2 tumor suppressor gene product, merlin, regulates human meningioma cell growth by signaling through YAP. *Neoplasia* **10:** 1204-1212

Sughrue ME, Yeung AH, Rutkowski MJ, Cheung SW, Parsa AT (2011) Molecular biology of familial and sporadic vestibular schwannomas: implications for novel therapeutics. *Journal of neurosurgery* **114:** 359-366

Sun CX, Haipek C, Scoles DR, Pulst SM, Giovannini M, Komada M, Gutmann DH (2002) Functional analysis of the relationship between the neurofibromatosis 2 tumor suppressor and its binding partner, hepatocyte growth factor-regulated tyrosine kinase substrate. *Human molecular genetics* **11:** 3167-3178

Sun Y, Yan Y, Denef N, Schupbach T (2011) Regulation of somatic myosin activity by protein phosphatase 1beta controls Drosophila oocyte polarization. *Development* **138:** 1991-2001

Szczepanowska J (2009) Involvement of Rac/Cdc42/PAK pathway in cytoskeletal rearrangements. *Acta biochimica Polonica* **56:** 225-234

Takeuchi K, Sato N, Kasahara H, Funayama N, Nagafuchi A, Yonemura S, Tsukita S, Tsukita S (1994) Perturbation of cell adhesion and microvilli formation by antisense oligonucleotides to ERM family members. *J Cell Biol* **125:** 1371-1384

Takizawa N, Koga Y, Ikebe M (2002) Phosphorylation of CPI17 and myosin binding subunit of type 1 protein phosphatase by p21-activated kinase. *Biochemical and biophysical research communications* **297:** 773-778

Tamrakar S, Ludlow JW (2000) The carboxyl-terminal region of the retinoblastoma protein binds non-competitively to protein phosphatase type 1alpha and inhibits catalytic activity. *J Biol Chem* **275:** 27784-27789

Tanaka J, Ito M, Feng J, Ichikawa K, Hamaguchi T, Nakamura M, Hartshorne DJ, Nakano T (1998) Interaction of myosin phosphatase target subunit 1 with the catalytic subunit of type 1 protein phosphatase. *Biochemistry* **37:** 16697-16703

Tanentzapf G, Tepass U (2003) Interactions between the crumbs, lethal giant larvae and bazooka pathways in epithelial polarization. *Nat Cell Biol* **5:** 46-52

Tang X, Jang SW, Wang X, Liu Z, Bahr SM, Sun SY, Brat D, Gutmann DH, Ye K (2007) Akt phosphorylation regulates the tumour-suppressor merlin through ubiquitination and degradation. *Nat Cell Biol* **9:** 1199-1207

Thaxton C, Bott M, Walker B, Sparrow NA, Lambert S, Fernandez-Valle C (2011) Schwannomin/merlin promotes Schwann cell elongation and influences myelin segment length. *Molecular and cellular neurosciences* **47:** 1-9

Thornton BR, Toczyski DP (2003) Securin and B-cyclin/CDK are the only essential targets of the APC. *Nat Cell Biol* **5:** 1090-1094

Tikoo A, Varga M, Ramesh V, Gusella J, Maruta H (1994) An anti-Ras function of neurofibromatosis type 2 gene product (NF2/Merlin). *J Biol Chem* **269:** 23387-23390

Toth A, Kiss E, Herberg FW, Gergely P, Hartshorne DJ, Erdodi F (2000) Study of the subunit interactions in myosin phosphatase by surface plasmon resonance. *European journal of biochemistry / FEBS* **267:** 1687-1697

Trofatter JA, MacCollin MM, Rutter JL, Murrell JR, Duyao MP, Parry DM, Eldridge R, Kley N, Menon AG, Pulaski K, et al. (1993) A novel moesin-, ezrin-, radixin-like gene is a candidate for the neurofibromatosis 2 tumor suppressor. *Cell* **75:** 826

Tsukada M, Prokscha A, Eichele G (2006) Neurabin II mediates doublecortin-dephosphorylation on actin filaments. *Biochemical and biophysical research communications* **343:** 839-847

Turunen O, Wahlstrom T, Vaheri A (1994) Ezrin has a COOH-terminal actin-binding site that is conserved in the ezrin protein family. *J Cell Biol* **126:** 1445-1453

Ueki K, Wen-Bin C, Narita Y, Asai A, Kirino T (1999) Tight association of loss of merlin expression with loss of heterozygosity at chromosome 22q in sporadic meningiomas. *Cancer Res* **59:** 5995-5998

Vanoosthuyse V, Hardwick KG (2009) A novel protein phosphatase 1-dependent spindle checkpoint silencing mechanism. *Curr Biol* **19:** 1176-1181

Vereshchagina N, Bennett D, Szoor B, Kirchner J, Gross S, Vissi E, White-Cooper H, Alphey L (2004) The essential role of PP1beta in Drosophila is to regulate nonmuscle myosin. *Molecular biology of the cell* **15:** 4395-4405

Vincent S, Vonesch JL, Giangrande A (1996) Glide directs glial fate commitment and cell fate switch between neurones and glia. *Development* **122:** 131-139

Viswanatha R, Ohouo PY, Smolka MB, Bretscher A (2012) Local phosphocycling mediated by LOK/SLK restricts ezrin function to the apical aspect of epithelial cells. *J Cell Biol* **199:** 969-984

Weinman EJ, Steplock D, Wang Y, Shenolikar S (1995) Characterization of a protein cofactor that mediates protein kinase A regulation of the renal brush border membrane Na(+)-H+ exchanger. *The Journal of clinical investigation* **95:** 2143-2149

Weiss B, Bollag G, Shannon K (1999) Hyperactive Ras as a therapeutic target in neurofibromatosis type 1. *Am J Med Genet* **89:** 14-22

Wodarz A, Ramrath A, Grimm A, Knust E (2000) Drosophila atypical protein kinase C associates with Bazooka and controls polarity of epithelia and neuroblasts. *J Cell Biol* **150:** 1361-1374

Xiao GH, Beeser A, Chernoff J, Testa JR (2002) p21-activated kinase links Rac/Cdc42 signaling to merlin. *J Biol Chem* **277:** 883-886

Xiao L, Gong LL, Yuan D, Deng M, Zeng XM, Chen LL, Zhang L, Yan Q, Liu JP, Hu XH, Sun SM, Liu J, Ma HL, Zheng CB, Fu H, Chen PC, Zhao JQ, Xie SS, Zou LJ, Xiao YM, Liu WB, Zhang J, Liu Y, Li DW (2010) Protein phosphatase-1 regulates Akt1 signal transduction pathway to control gene expression, cell survival and differentiation. *Cell Death Differ* **17:** 1448-1462

Xu HM, Gutmann DH (1998) Merlin differentially associates with the microtubule and actin cytoskeleton. *Journal of neuroscience research* **51:** 403-415

Yamashiro S, Yamakita Y, Totsukawa G, Goto H, Kaibuchi K, Ito M, Hartshorne DJ, Matsumura F (2008) Myosin phosphatase-targeting subunit 1 regulates mitosis by antagonizing polo-like kinase 1. *Dev Cell* **14:** 787-797

Yang J, Hurley TD, DePaoli-Roach AA (2000) Interaction of inhibitor-2 with the catalytic subunit of type 1 protein phosphatase. Identification of a sequence analogous to the consensus type 1 protein phosphatase-binding motif. *J Biol Chem* **275:** 22635-22644

Yogesha SD, Sharff AJ, Giovannini M, Bricogne G, Izard T (2011) Unfurling of the band 4.1, ezrin, radixin, moesin (FERM) domain of the merlin tumor suppressor. *Protein science : a publication of the Protein Society* **20:** 2113-2120

Zhang J, Smolen GA, Haber DA (2008) Negative regulation of YAP by LATS1 underscores evolutionary conservation of the Drosophila Hippo pathway. *Cancer Res* **68:** 2789-2794

Zhang N, Bai H, David KK, Dong J, Zheng Y, Cai J, Giovannini M, Liu P, Anders RA, Pan D (2010) The Merlin/NF2 tumor suppressor functions through the YAP oncoprotein to regulate tissue homeostasis in mammals. *Dev Cell* **19:** 27-38

Zhao B, Wei X, Li W, Udan RS, Yang Q, Kim J, Xie J, Ikenoue T, Yu J, Li L, Zheng P, Ye K, Chinnaiyan A, Halder G, Lai ZC, Guan KL (2007) Inactivation of YAP oncoprotein by the Hippo pathway is involved in cell contact inhibition and tissue growth control. *Genes Dev* **21:** 2747-2761

Zhao S, Lee EY (1997) A protein phosphatase-1-binding motif identified by the panning of a random peptide display library. *J Biol Chem* **272:** 28368-28372

Zhou L, Hanemann CO (2012) Merlin, a multi-suppressor from cell membrane to the nucleus. *FEBS Lett* **586:** 1403-1408

Zich J, Hardwick KG (2010) Getting down to the phosphorylated 'nuts and bolts' of spindle checkpoint signalling. *Trends in biochemical sciences* **35:** 18-27